

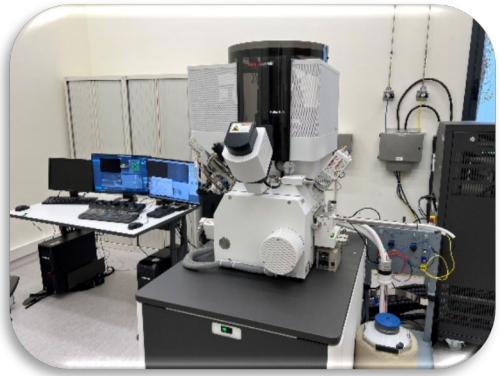
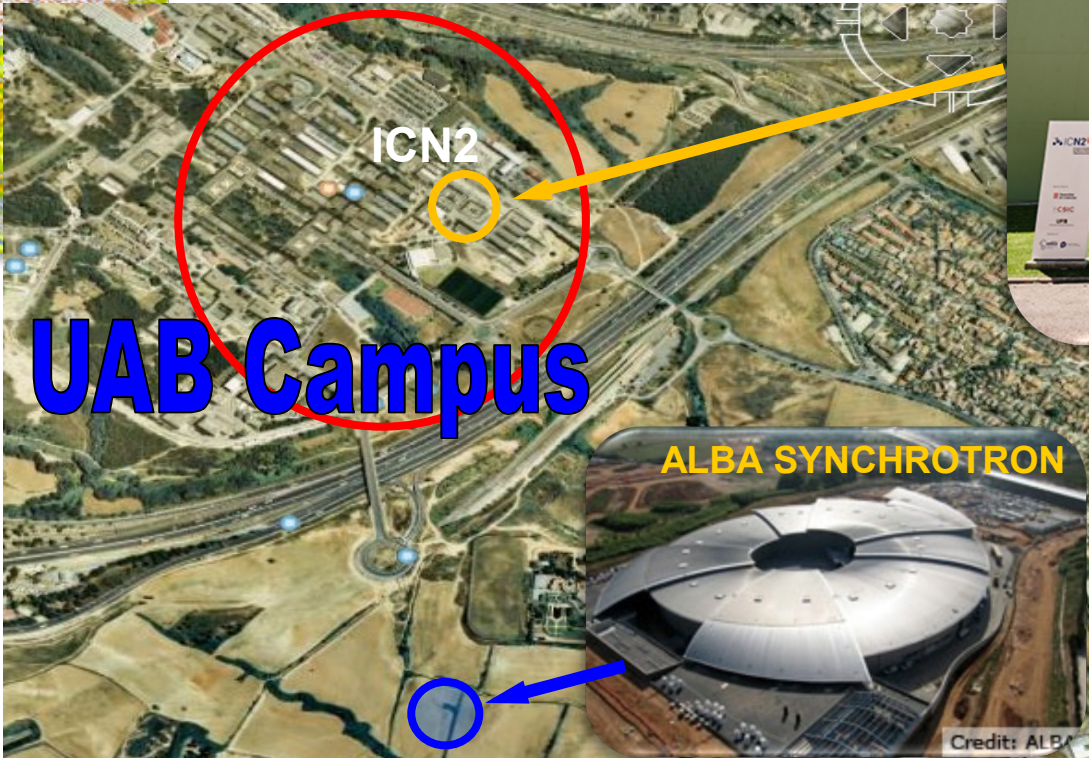
In-situ STEM for energy and catalysis nanomaterials

Jordi Arbiol

*ICREA & Catalan Institute of Nanoscience and Nanotechnology – ICN2
CSIC & BIST*

Contact e-mail : arbiol@icrea.cat

URL: www.gaen.cat

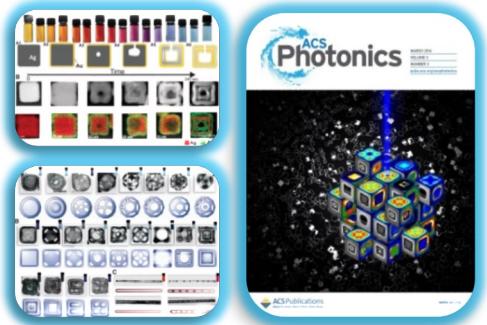


- ❑ ICN2 (CSIC & BIST)
- ❑ ALBA-CELLS


Unió Europea
Fons Europeu
de Desenvolupament Regional

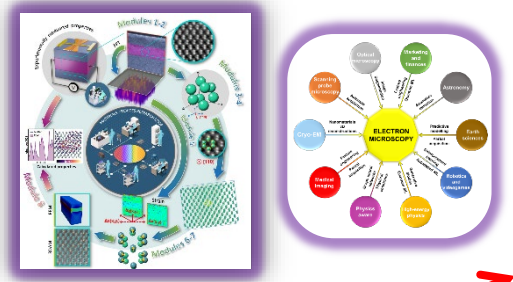

Generalitat de Catalunya
Departament de Recerca i Universitats

Research Lines



AI Data Analysis & Modelling

Nanoscale Horiz., **7**, 1427 (2022)
Adv. Intel. Syst., **7**, 2400986 (2025)
Adv. Mater., 10.1002/adma.202506785 (2026)
Adv. Intel. Syst., 10.1002/aisy.202501077 (2026)

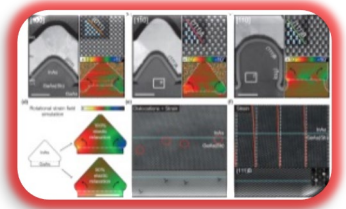
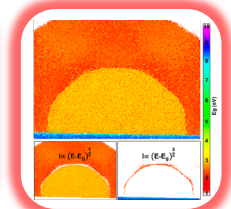
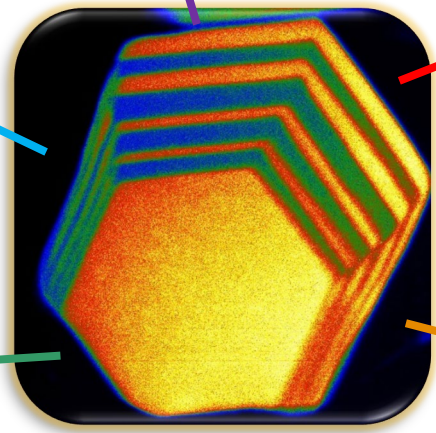


Nanowires, 2DEG & Quantum

Nature Mater., **20**, 1106 (2021)
Nature Commun., **13**, 4089 (2022)
Nature, **612**, 442 (2022)
Nature Commun., **14**, 7738 (2023)
npj Quantum Information, **10**, 32 (2024)
Nature Commun., **16**, 2103 (2025)
Adv. Funct. Mater., **35**, 2423734 (2025)

Metal NPs Bio & Photonics

Science, **334**, 1377 (2011)
Nanophoton., **6**, 193 (2017)
Nature Nanotech., **19**, 514 (2024)



Nanostructures for Energy & Catalysis

Nature Catalysis, **5**, 212 (2022)
Adv. Mater., **35**, 2306447 (2023)
Nature Rev. Chem., **8**, 159 (2024)
Adv. Mater., **36**, 2400810 (2024)
Adv. Mater., **36**, 2400572 (2024)
Science, **384**, 1373 (2024)
ACS Ener. Lett., **9**, 6178 (2024)
The Innovation, **6**, 100810 (2025)
Matter, **8**, 102139 (2025)
Adv. Mater., **38**, e11345(2026)

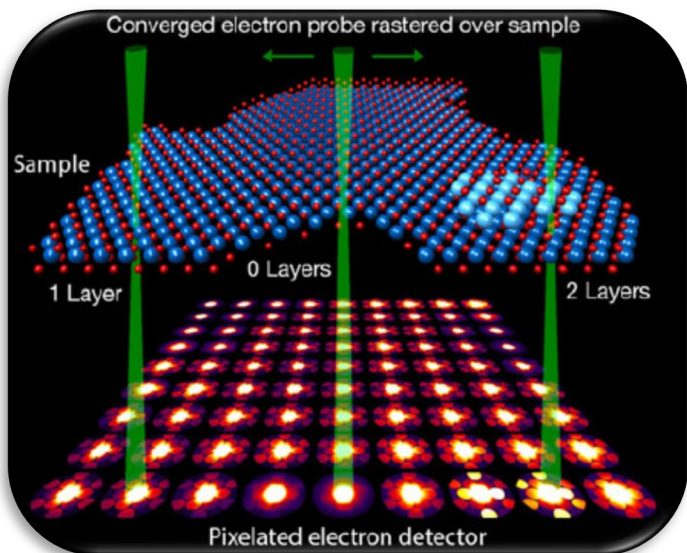
Oxides & Spintronics

Nature Mater., **11**, 329 (2012)
Adv. Mater., **31**, 1905288 (2019)
PRL, **130**, 21680 (2023)
Nature Mater., **24**, 1359 (2025)

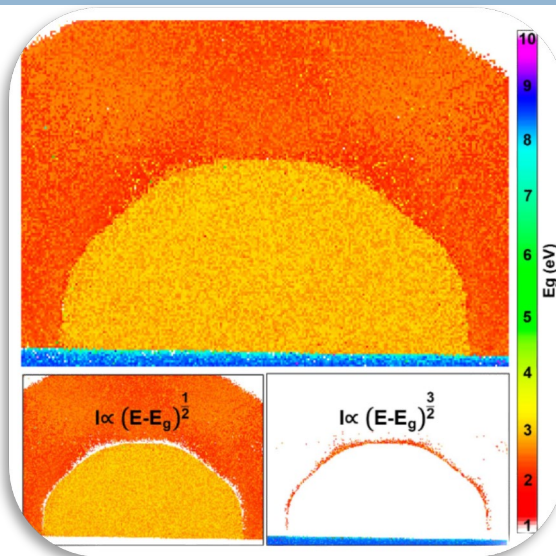


HR imaging, spectroscopy & diffraction

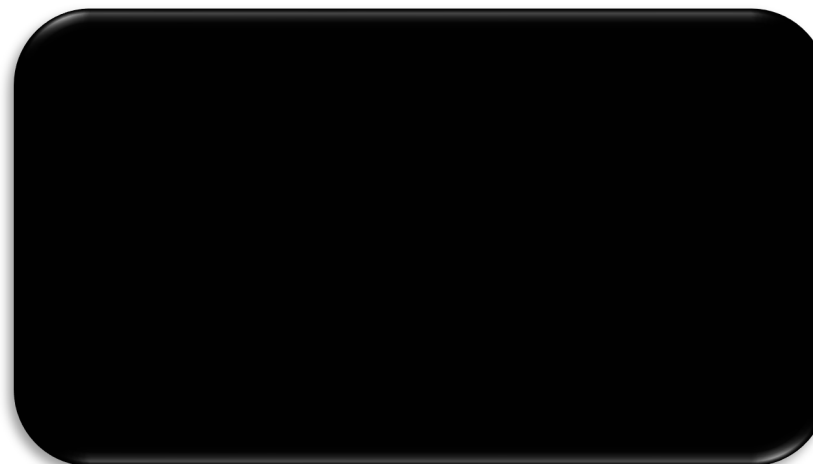
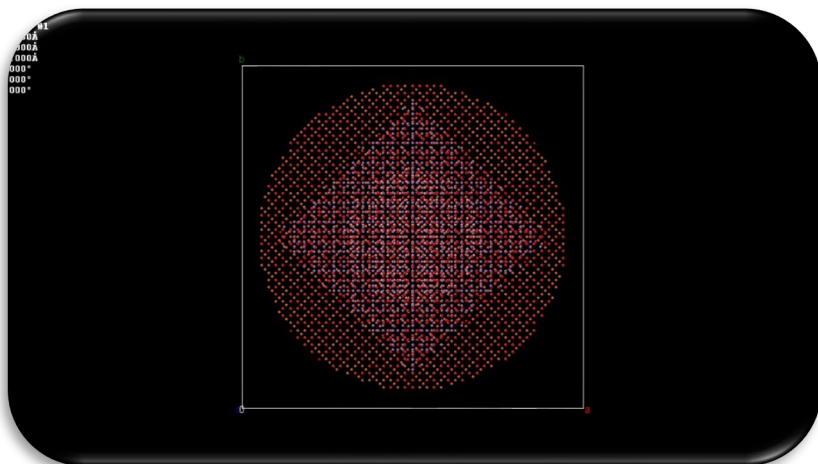
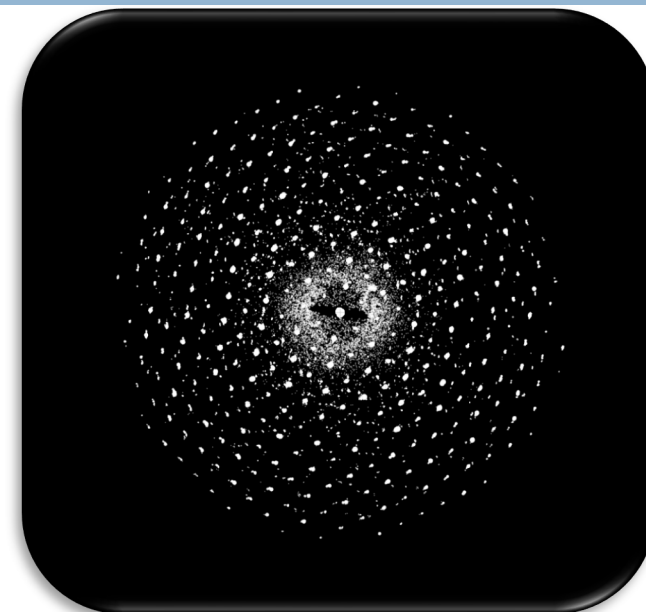
4



Microscopy & Microanal., **25**, 563 (2019)



Nature Commun., **13**, 4089 (2022)

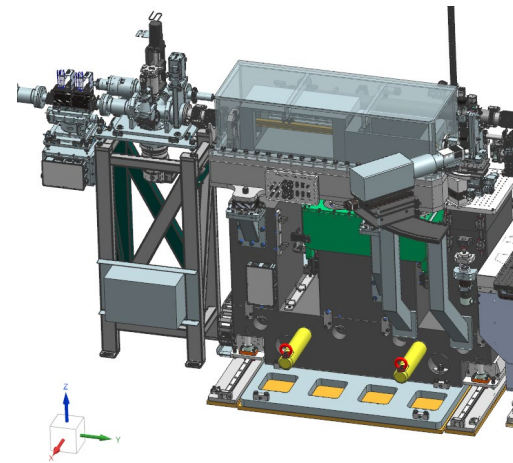
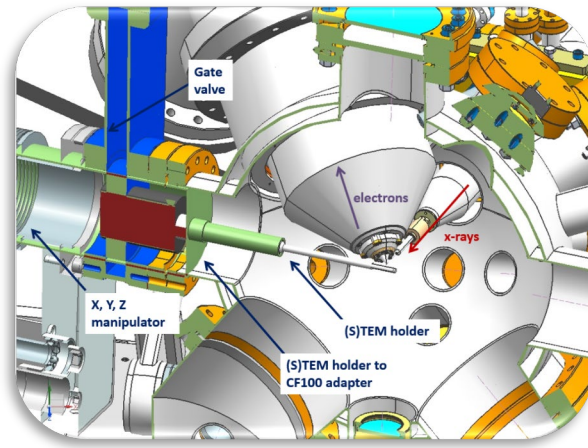


ACS Nano, **8**, 2290 (2014)



In-CAEM has developed a **singular infrastructure** for research in **advanced energy materials** in order to address the scientific challenges of the European Green Deal:

<p>Multi-modal Multi-lengthscale Correlative</p>	}	<p>in situ/operando experiments, combining</p>	{	<p>(Scanning) transmission electron microscopy Scanning probe microscopies Synchrotron X-rays (spectroscopy, diffraction,...) Advanced data analytics (HPC, deep learning, AI,...)</p>
---	---	--	---	--



In-situ (S)TEM

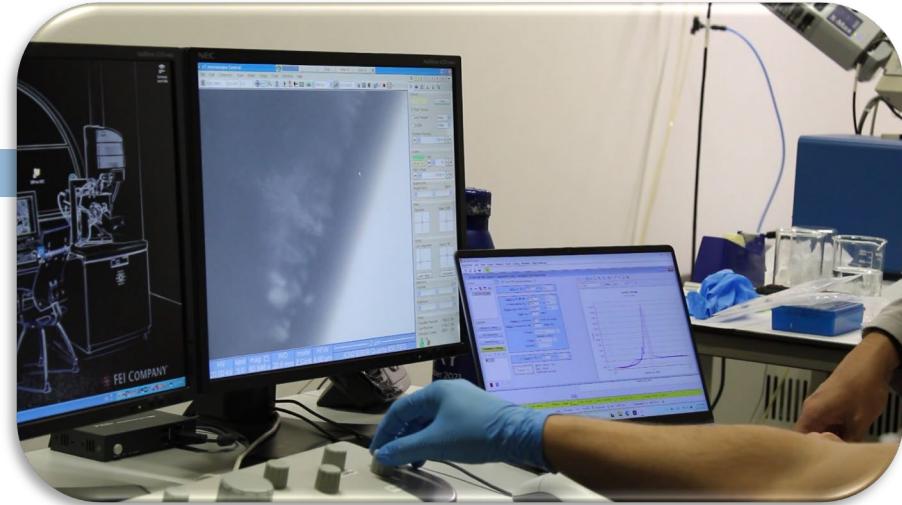
8

- TFS Spectra 300 & ULTRA
- (AC)² & Monochromated (S)TEM:
 - 4D STEM (Empad & K3)
 - Super X & ULTRA EDX
 - Continuum K3 & ILIAD
- Catalysis sample holder system
 - Controlled gas mixing and flow
 - Controlled T + bias
 - RGA
- Electrochemistry sample holder system
 - Liquid Flow
 - In-situ electrodes
 - Potentionstat
 - SEM echem cell
- Liquid nitrogen cooling/heating/bias sample holder

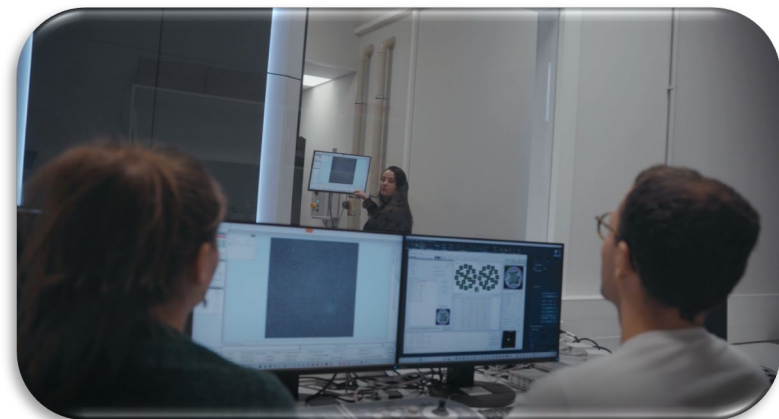
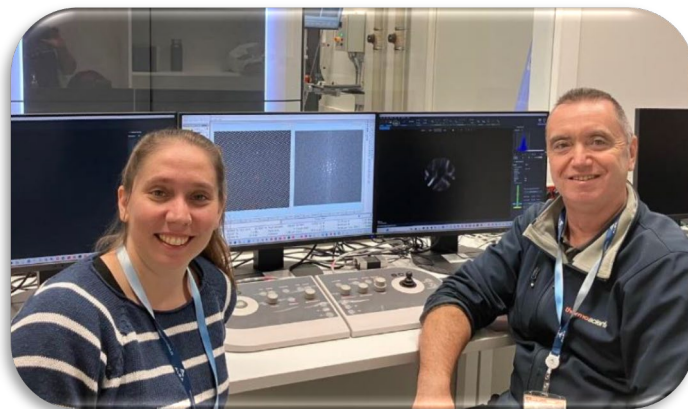
Climate Infinity TEM holder

Stream Infinity TEM holder

Lighting Arctic TEM holder

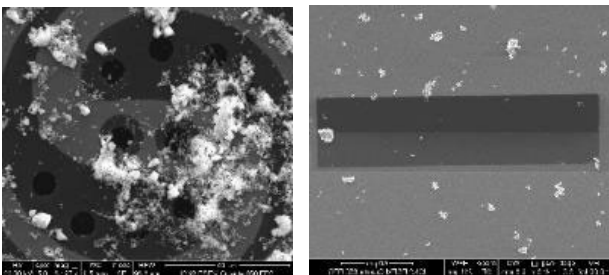
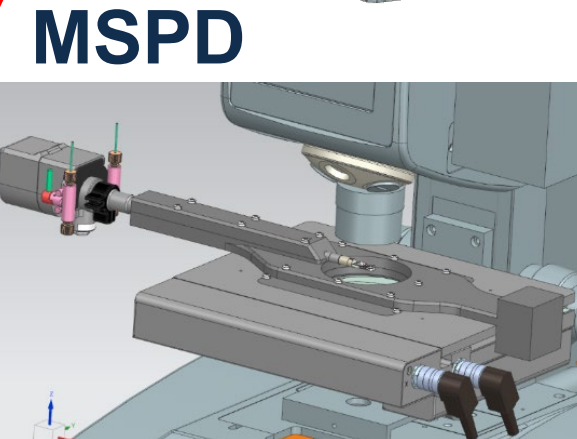
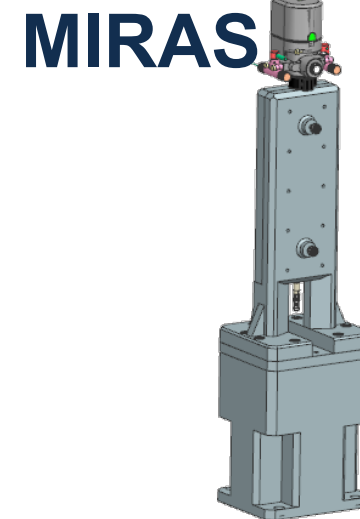
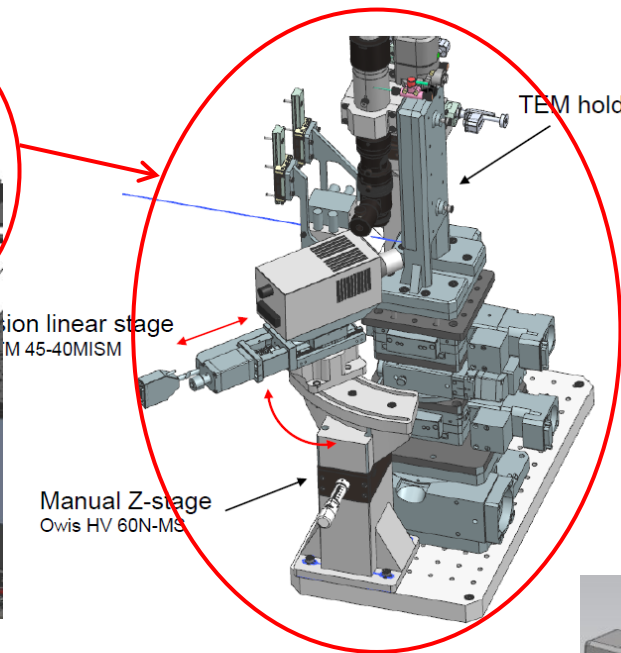
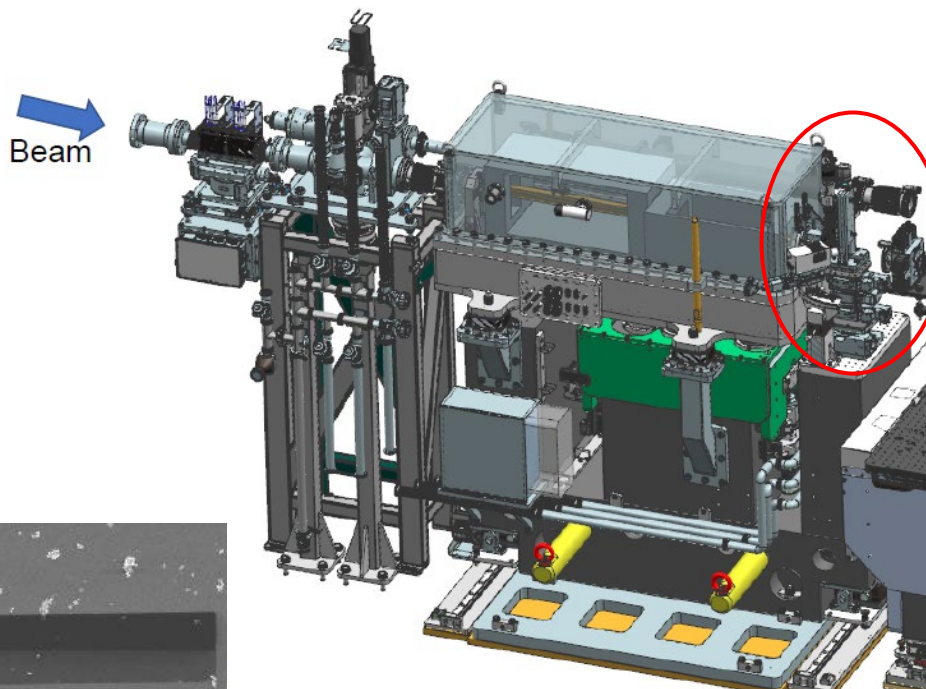
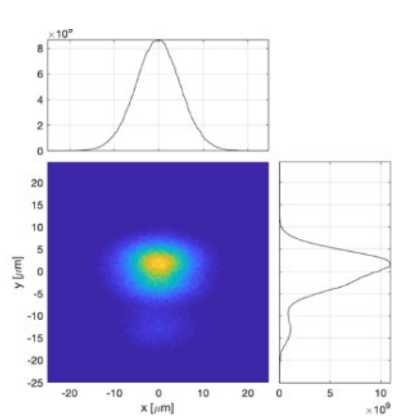


Cu(II) ↔ Cu (0) in-situ redox



□ **μNOTOS: microspot XAS experimental station**

X-Rays ↔ (S)TEM



Finançat per:



BL adaptations for correlative experiments

Automapping optical microscope
PEEM visualization system
BOREAS visualization system
Sample platelets
Platelet adapter AFMs
UHV suitcase
Laminar flow cabin
Metal sputtering system
Electropolishing system
Ar suitcase
Mistral TXM tip adapters

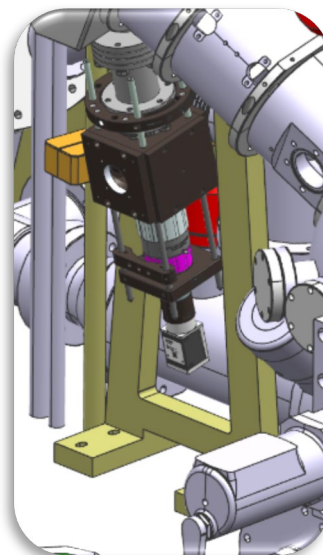
MISTRAL Transmission X-ray Microscope



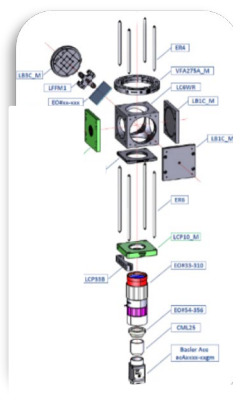
Arctic chips



Climate & Stream nanoreactors



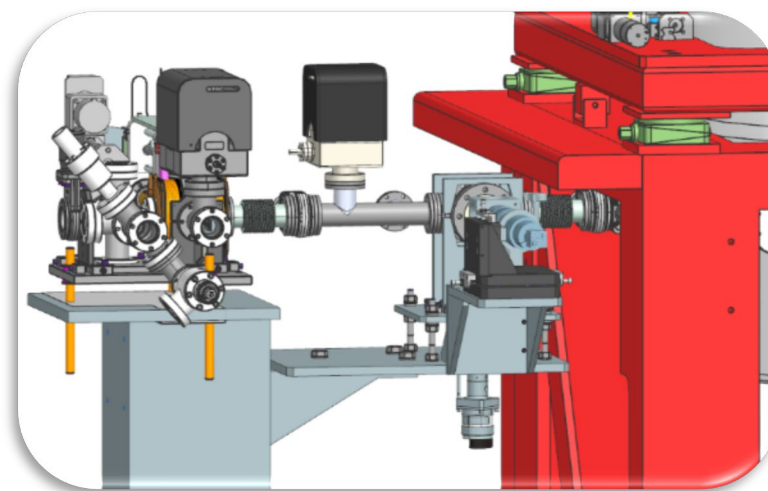
PEEM



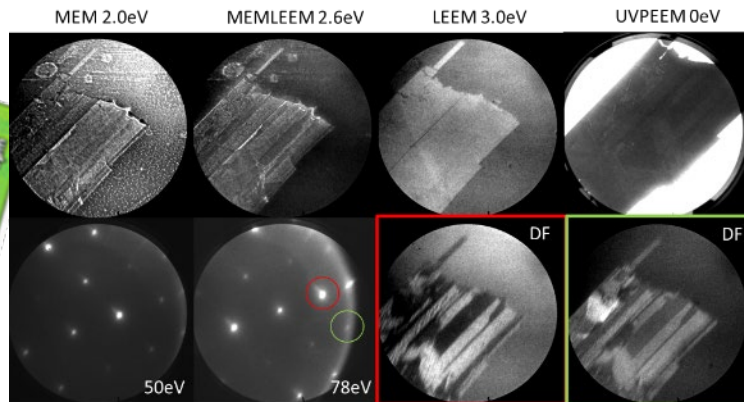
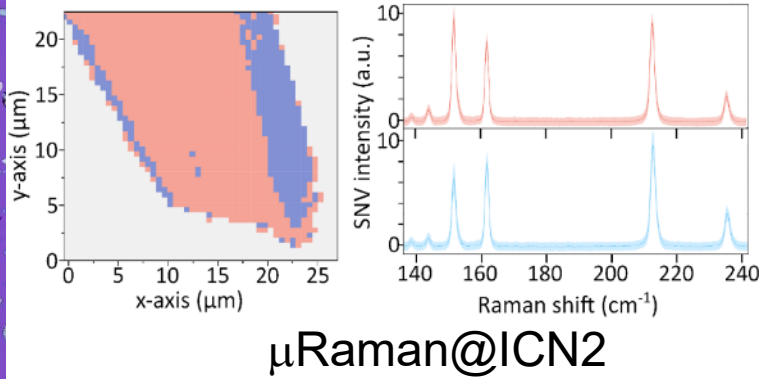
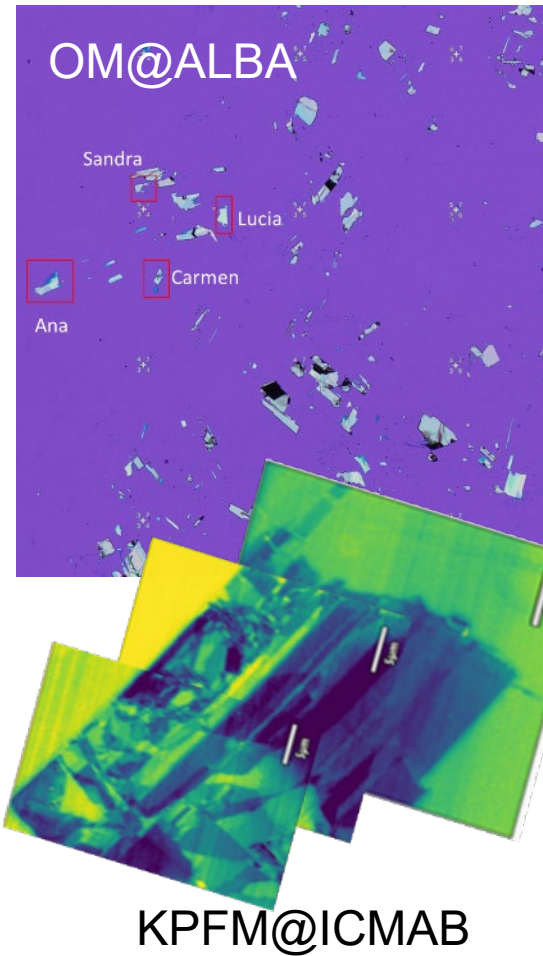
UHV suitcase



BOREAS

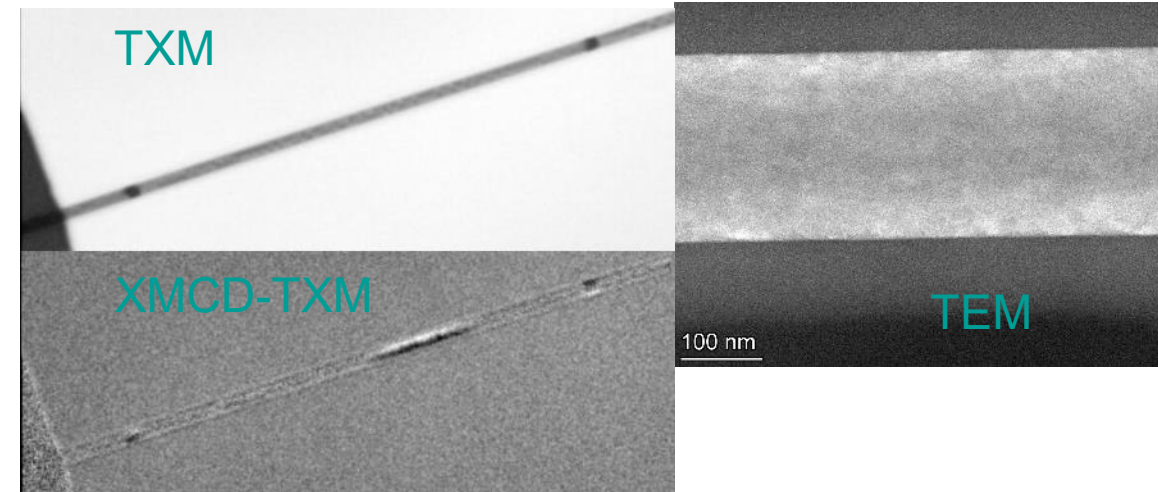
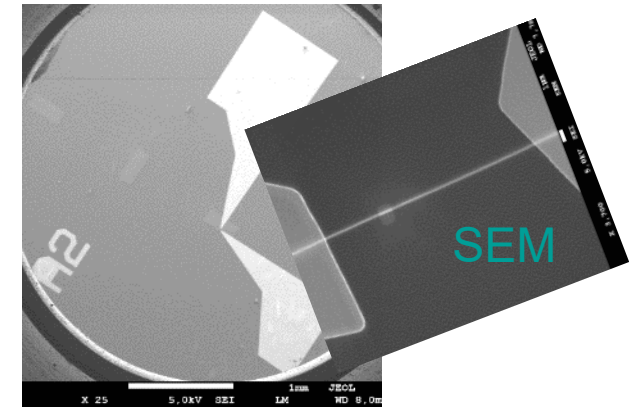


2D: ReS₂ flakes

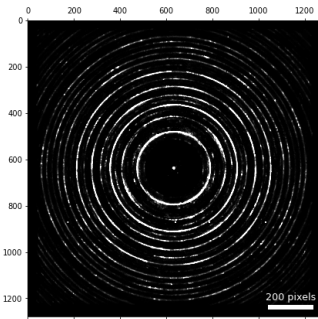
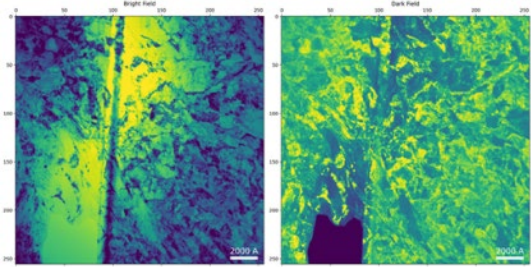


LEEM, UVPEEM & μLEED @ALBA

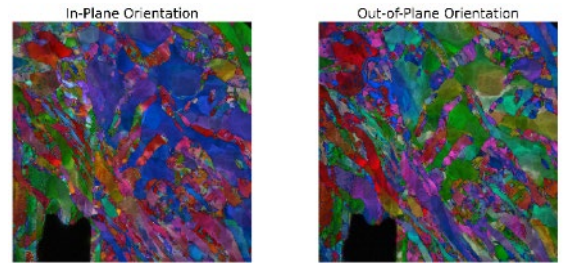
3D: Magnetic NWs



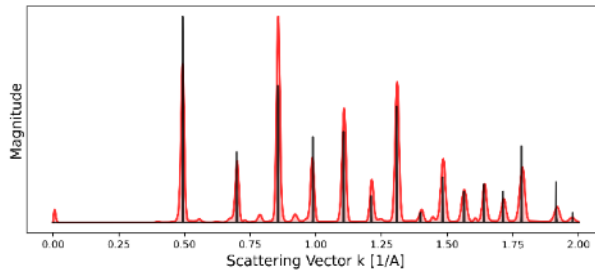
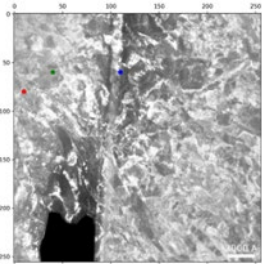
2-D histogram of e-diffraction spots coordinates, generate virtual diffraction pattern of overall region



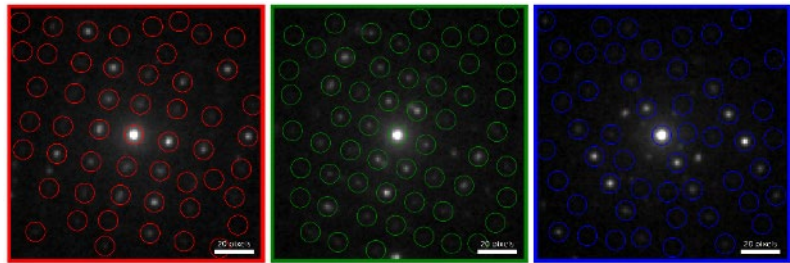
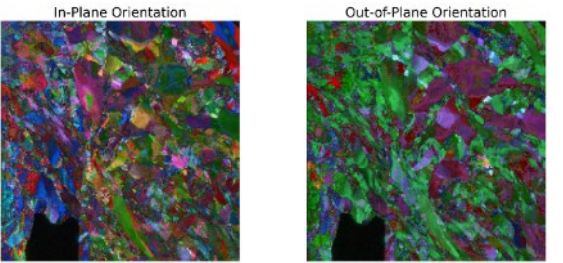
Orientation-map for BCC



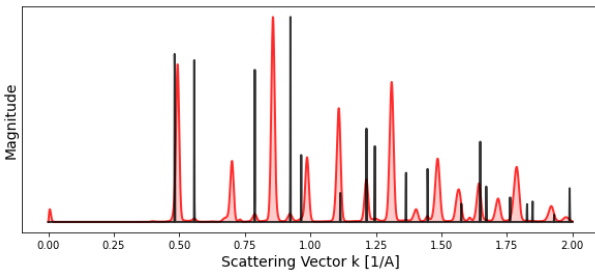
(MM1000)



Orientation-map for FCC



Data: N. Bagués @METCAM

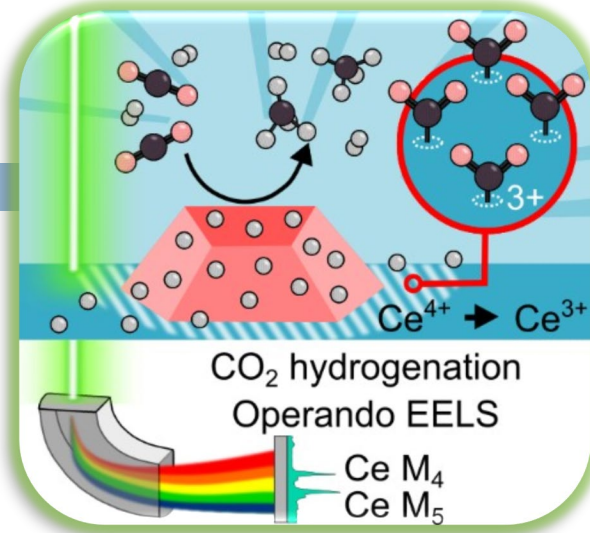


Azimuthal integration of the scattering electron diffraction pattern of whole scanned region overlaid on BCC theoretical peaks

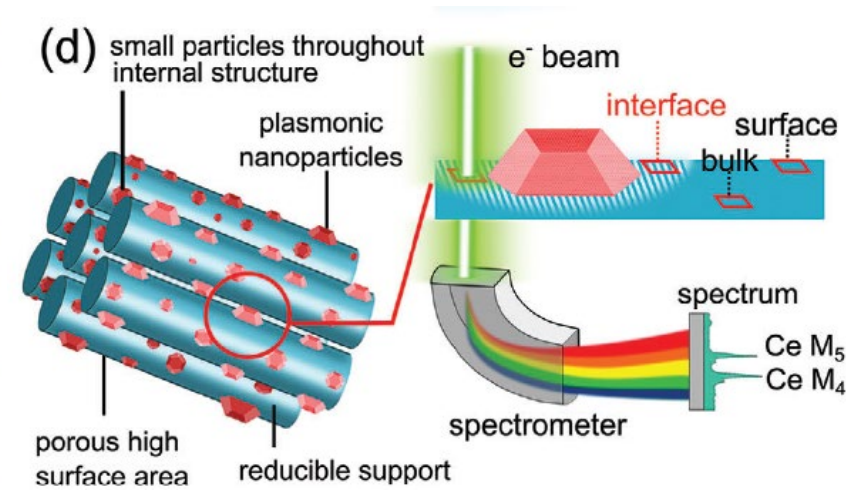
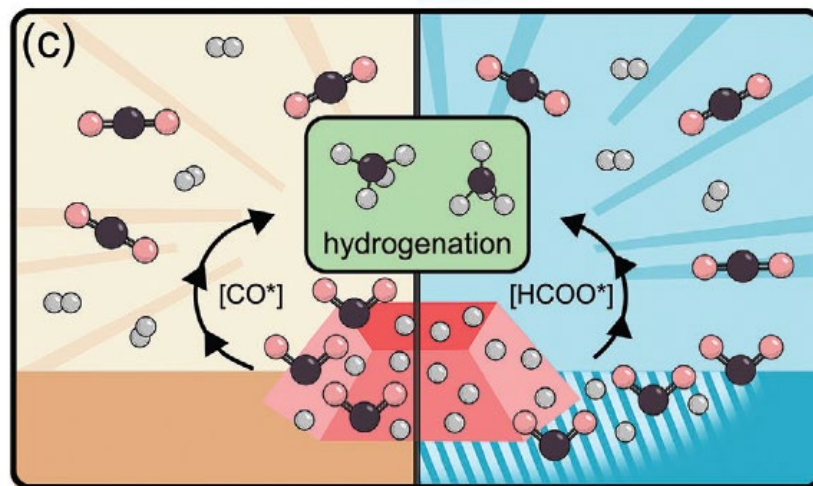
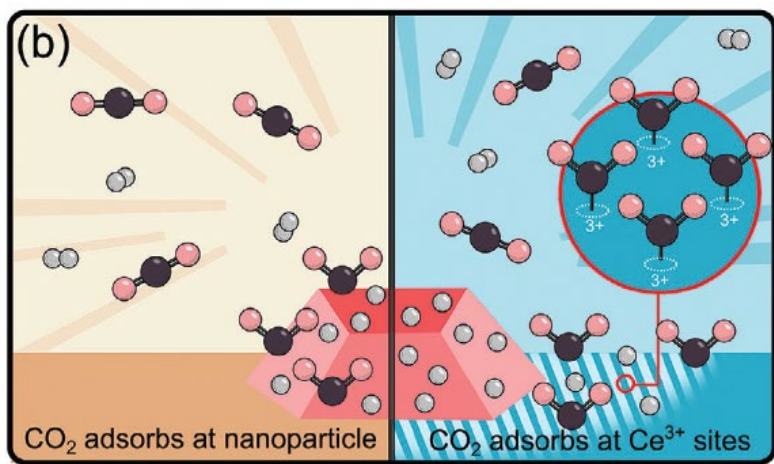
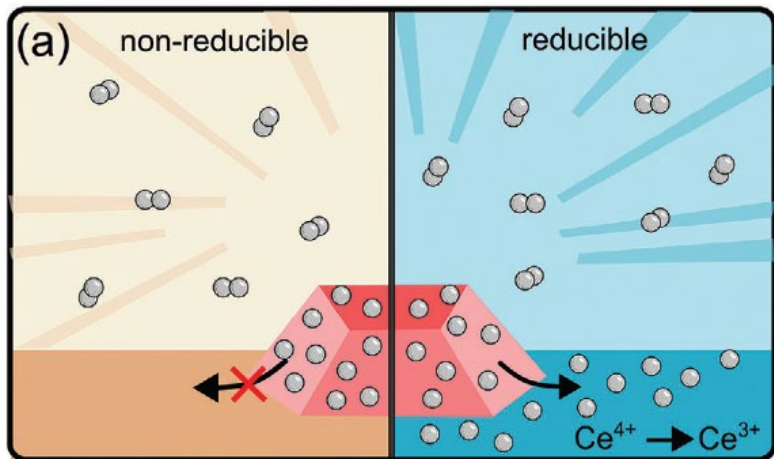
Finançat per:

CO₂ in-situ methanation

13



Thermally driven CO₂ methanation using Ni/CeO₂-based catalyst.



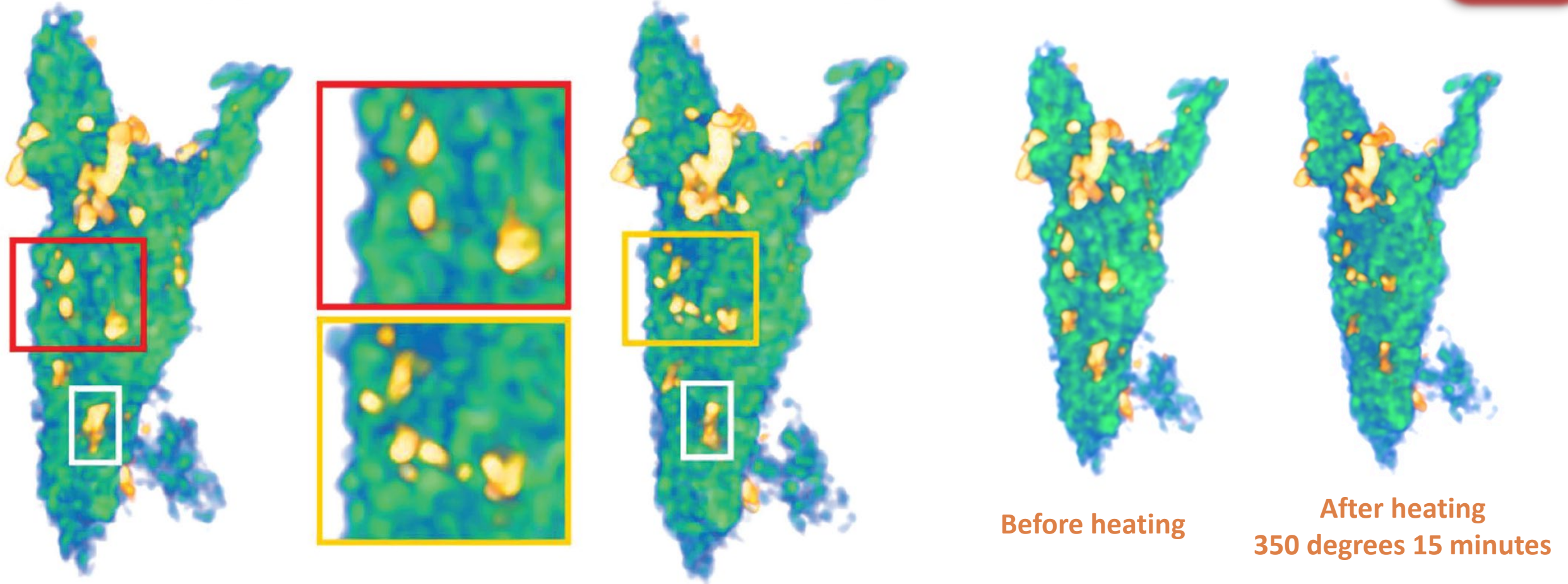
With: Universiteit Antwerpen
 IREC[®]
 Institut de Recerca en Energia de Catalunya
 Catalonia Institute for Energy Research

Appl. Catal. B, **291**, 120038 (2021)

Adv. Mater., **35**, 2306447 (2023)



In Situ Heating Tomography on a DENSsolutions Wildfire heating holder



There is a variation in volume of Ni NPs on the surface after heating.
Positions of individual nanoparticles do not change.

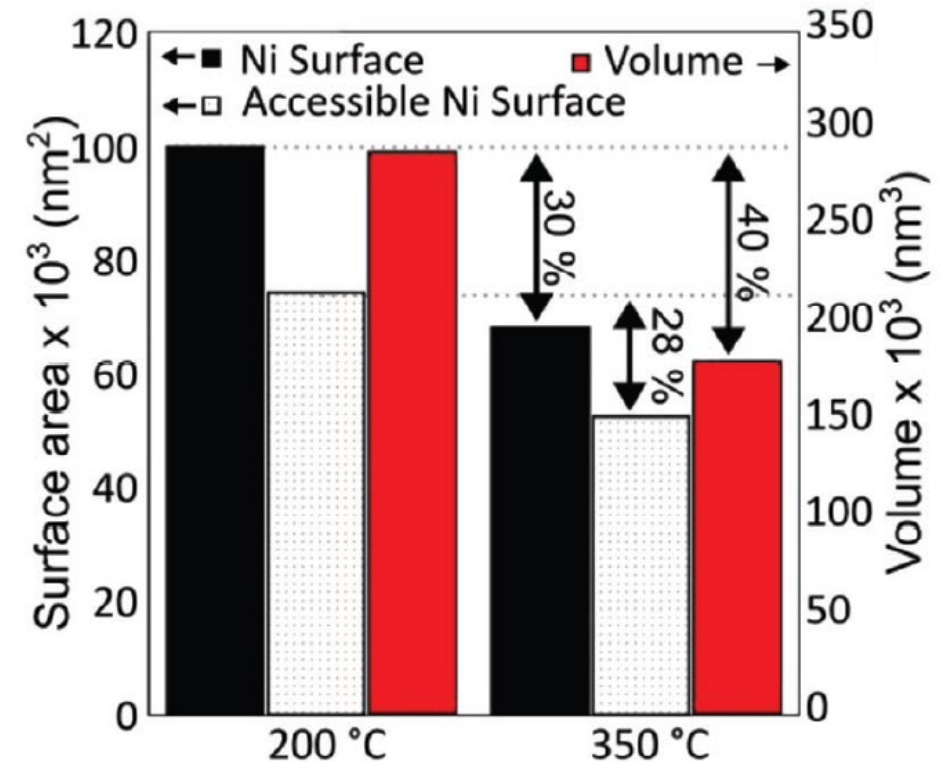
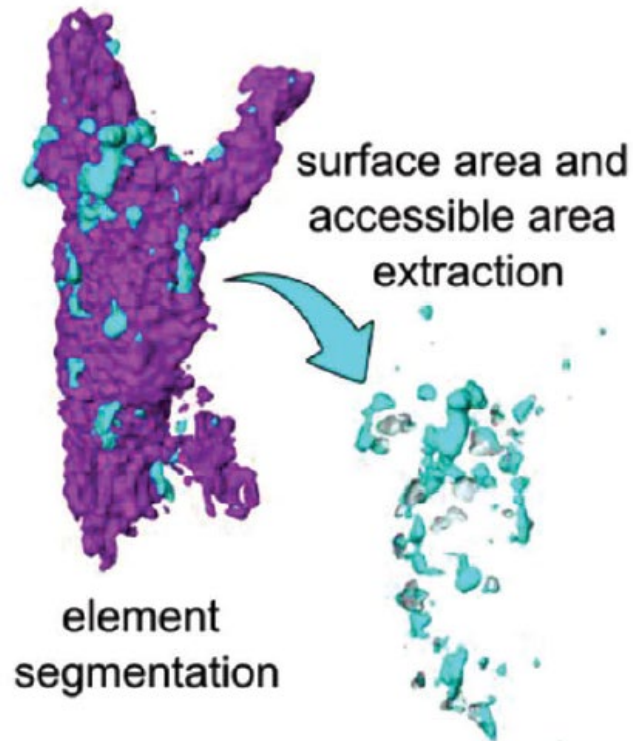
Adv. Mater., **35**, 2306447 (2023)

Volume Change Upon Heating



15

In Situ Heating Tomography on a DENSsolutions Wildfire heating holder



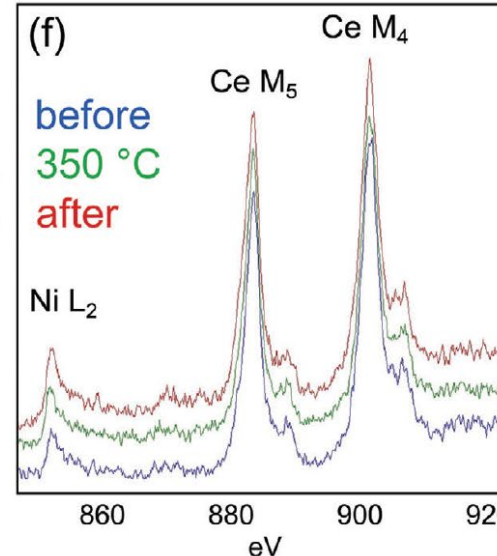
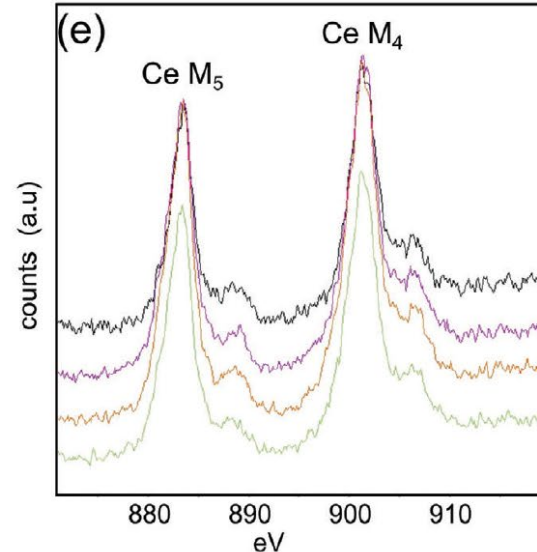
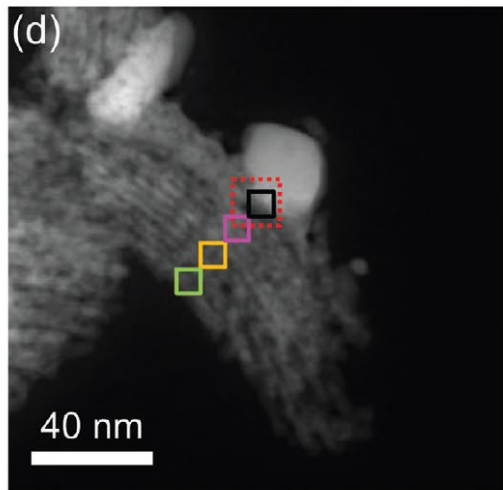
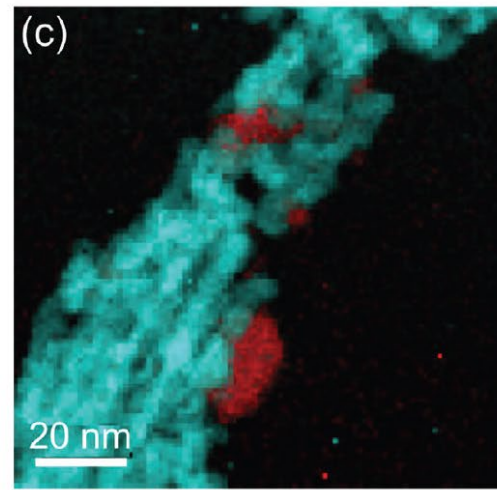
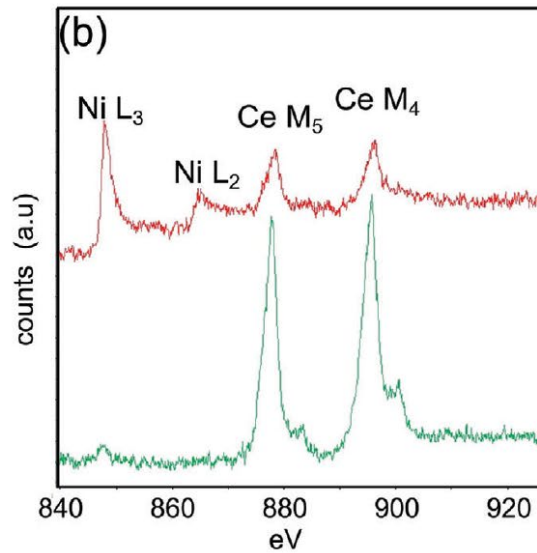
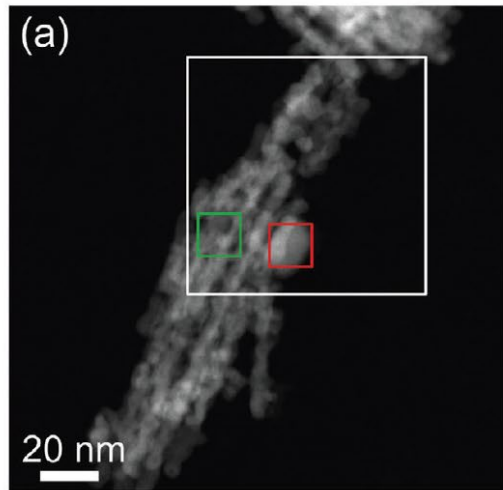
Volume lost after heating

Adv. Mater., **35**, 2306447 (2023)

Ceria oxidation state during heating



16



In situ heating EELS analyses

EEL spectra compared from the near and far regions with respect to the Ni NP reveal no variation in Ce oxidation state based on proximity to Ni NPs. During this acquisition, the catalyst was heated to 120 °C to minimize carbon contamination.

Ce³⁺ abundance does not increase at elevated temperatures and still remains independent to Ni proximity at 400 °C.

Appl. Catal. B, **291**, 120038 (2021)

Adv. Mater., **35**, 2306447 (2023)

CO₂ in-situ methanation



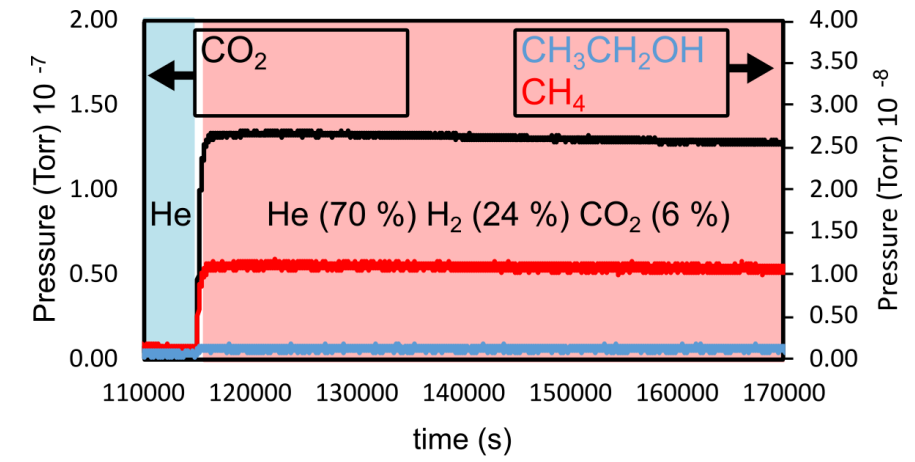
17



Operando electron energy loss spectroscopy (EELS) of Ni/MP-CeO₂ under hydrogenation conditions.

In a DENSolutions Climate G+ with a nanocell reactor.

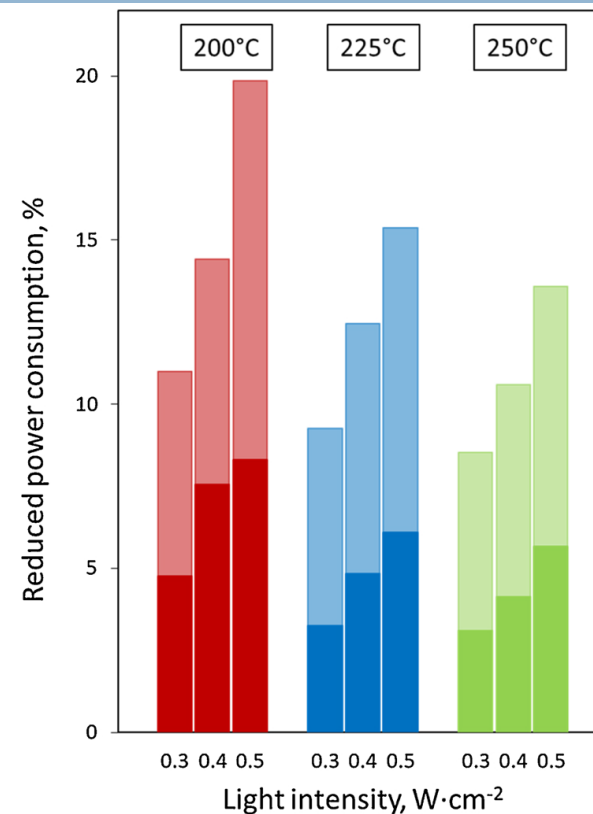
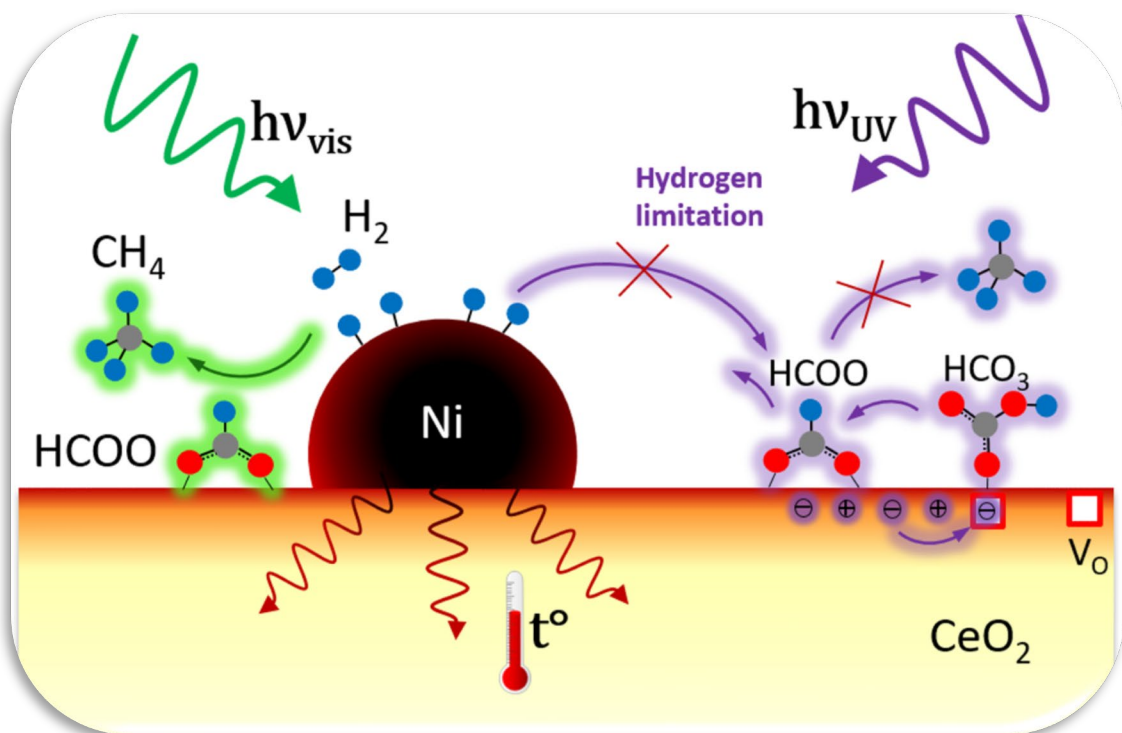
Sample at 350°C under CO₂:H₂:He atmosphere. Oxidation state maps suggest an increase in Ce³⁺ close the Ni nanoparticle



Adv. Mater., **35**, 2306447 (2023)



Next Steps: Effects of solar irradiation on thermally driven CO₂ methanation using Ni/CeO₂-based catalyst.



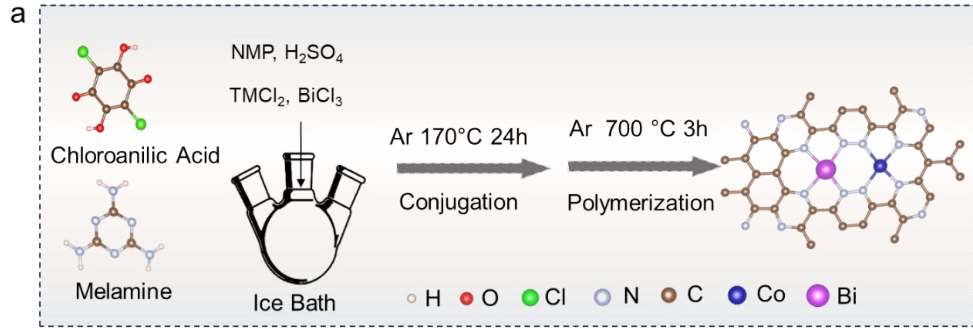
Plasmonic Activated Ni/CeO₂ Nanoreactors x2.4 activity under Sunlight

With: Universiteit Antwerpen

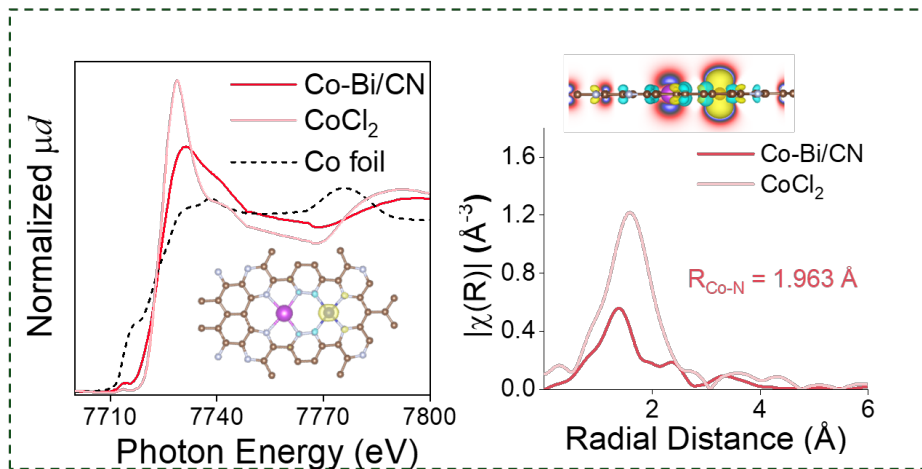
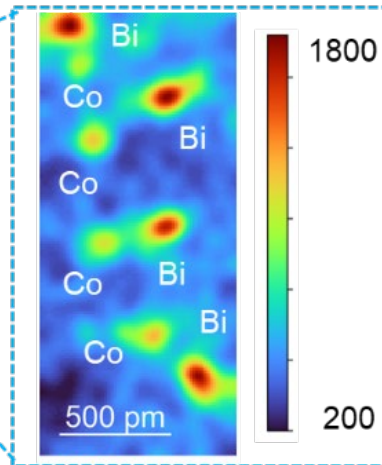
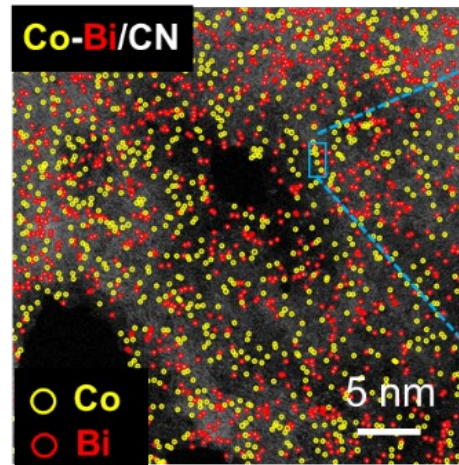
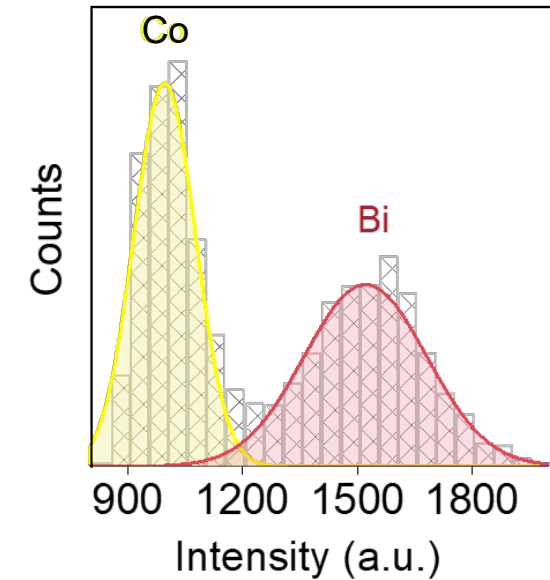
IREC[®]
 Institut de Recerca en Energia de Catalunya
 Catalonia Institute for Energy Research

Appl. Catal. B, **291**, 120038 (2021)

Adv. Mater., **35**, 2306447 (2023)



Promoting Electrochemical Reactions with Dual-Atom Catalysts for High-Rate Lithium-Sulfur Batteries



Physicochemical characterization of TM-Bi/CN DACs using a Laplacian of Gaussian algorithm

- 32% coupled Co-Bi pairs
- 31% either Bi-Bi or Co-Co pairs
- 37% existed as isolated Co or Bi atoms

Adv. Mater., **38**, e11345 (2026)

Why Dual-Atom Catalysts (DACs)?



21

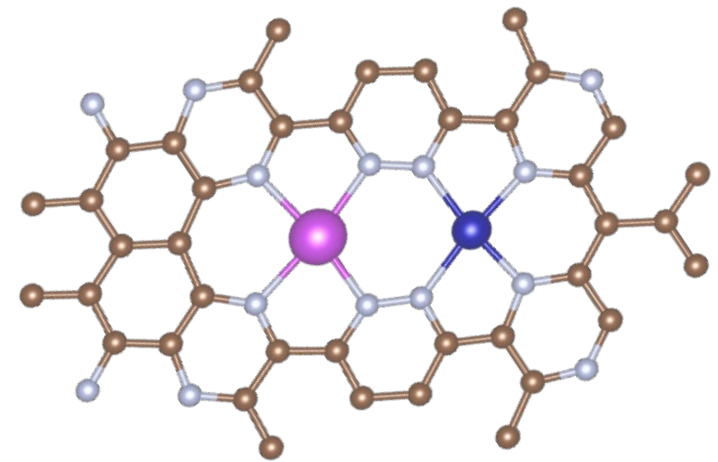
SACs

- Maximized atomic utilization efficiency
- Unique electronic structures
- Superior activity and selectivity

DACs

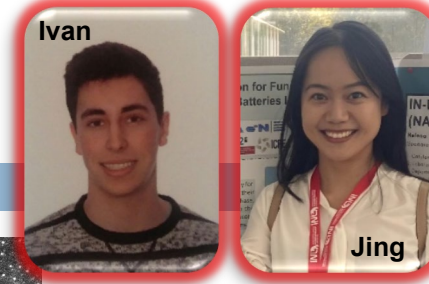
- Better tunability
- Inherent asymmetry
- Broader compositional flexibility
- The potential synergistic effects

1+1>2?

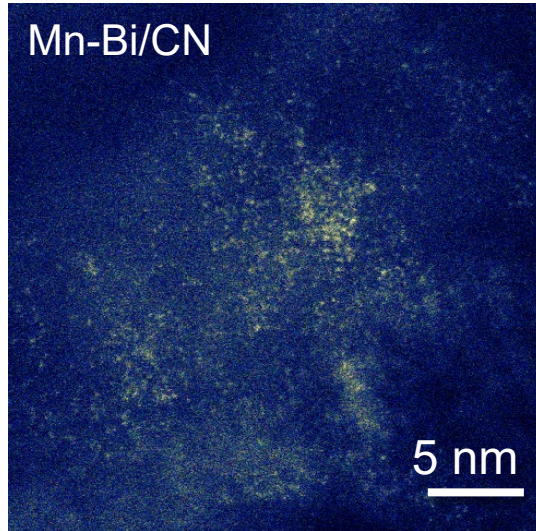


- Dual-atoms catalysts additive design;
- Promoted SRRs;
- Metal utilization—0.2%

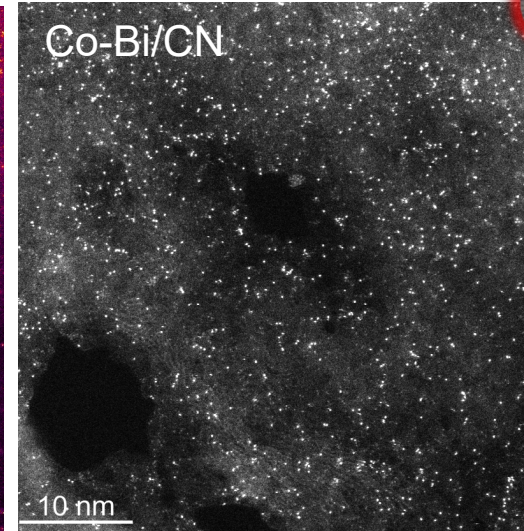
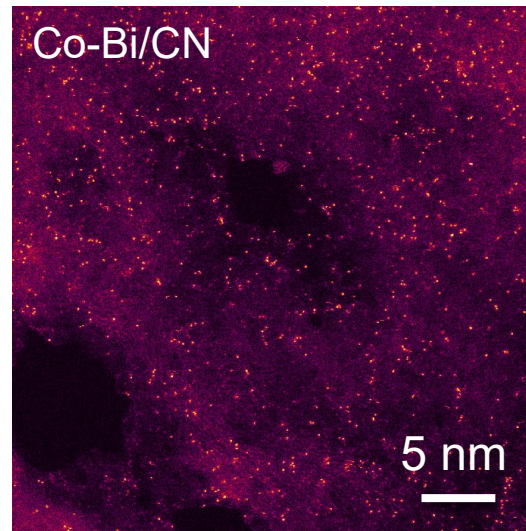
Adv. Mater., **38**, e11345 (2026)



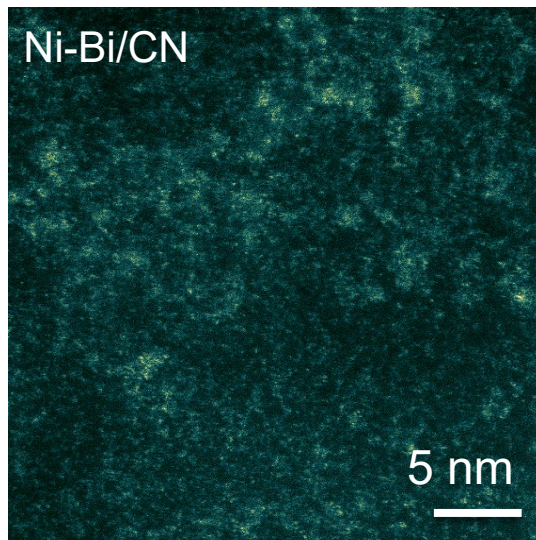
a



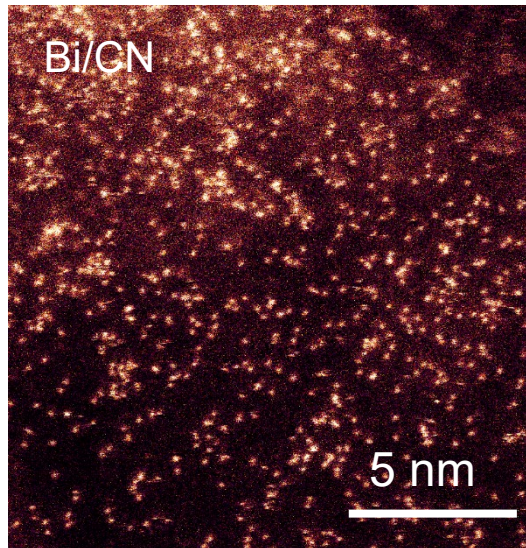
b



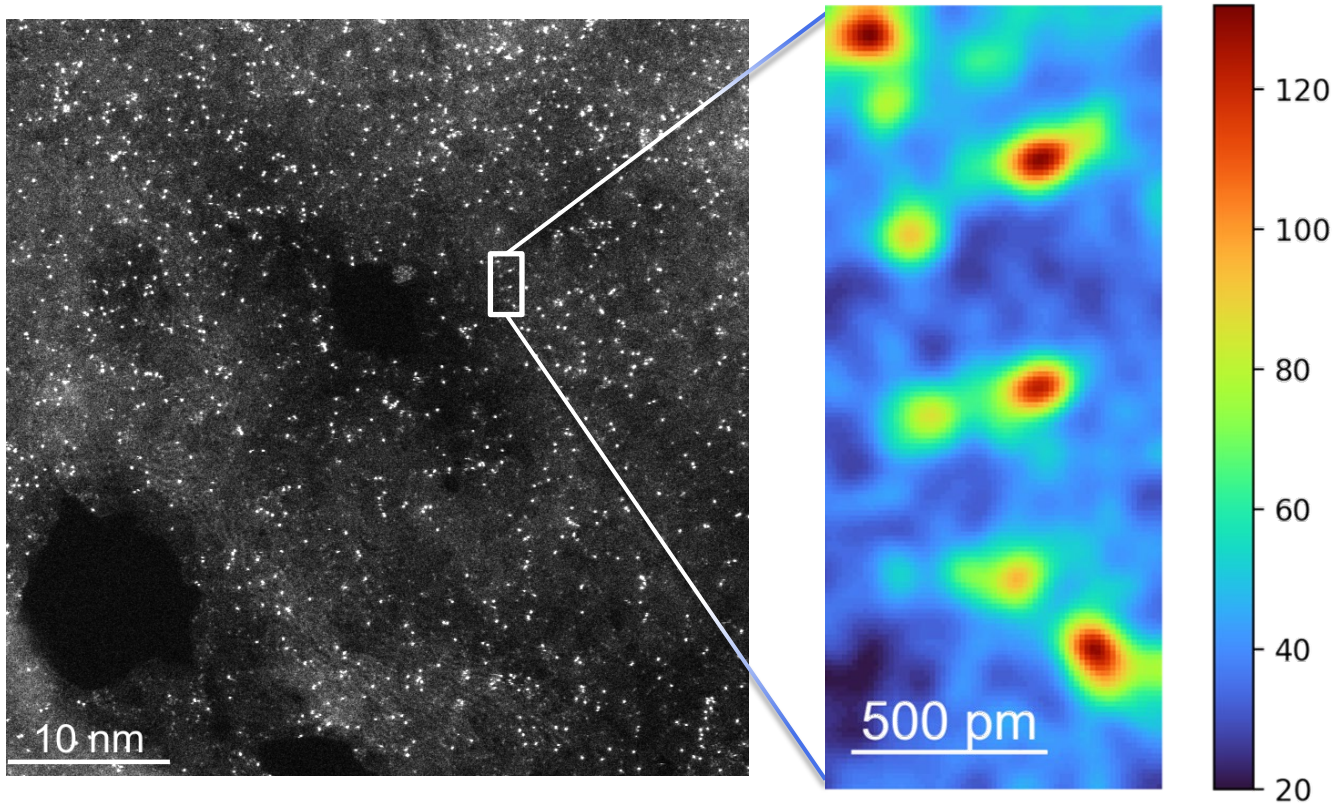
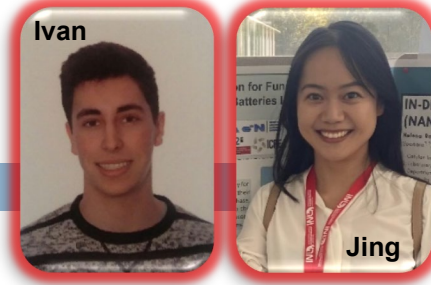
c



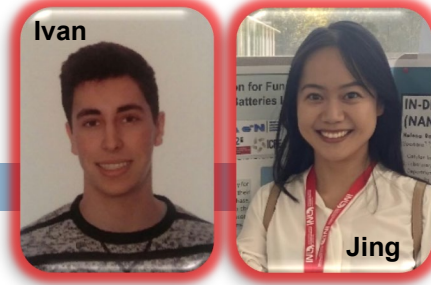
d



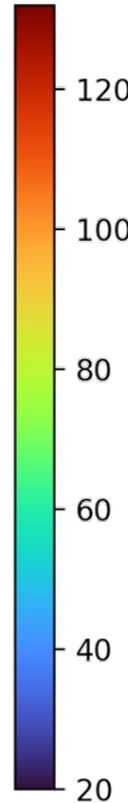
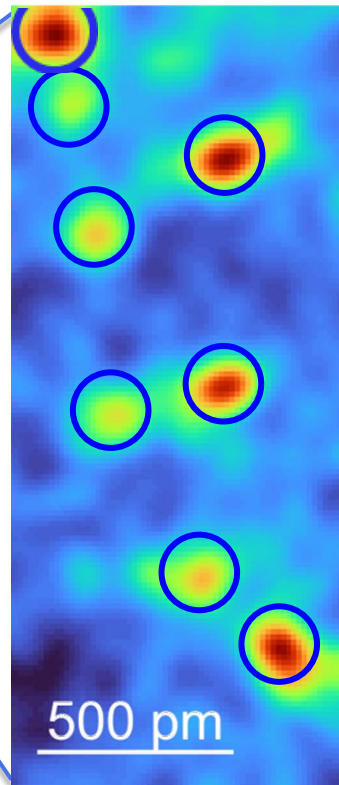
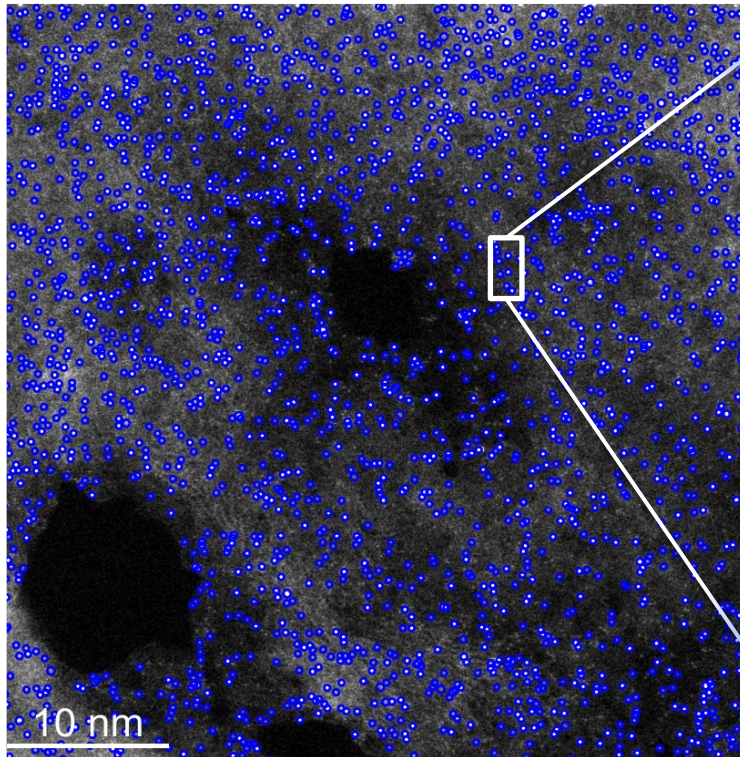
Adv. Mater., **38**, e11345 (2026)



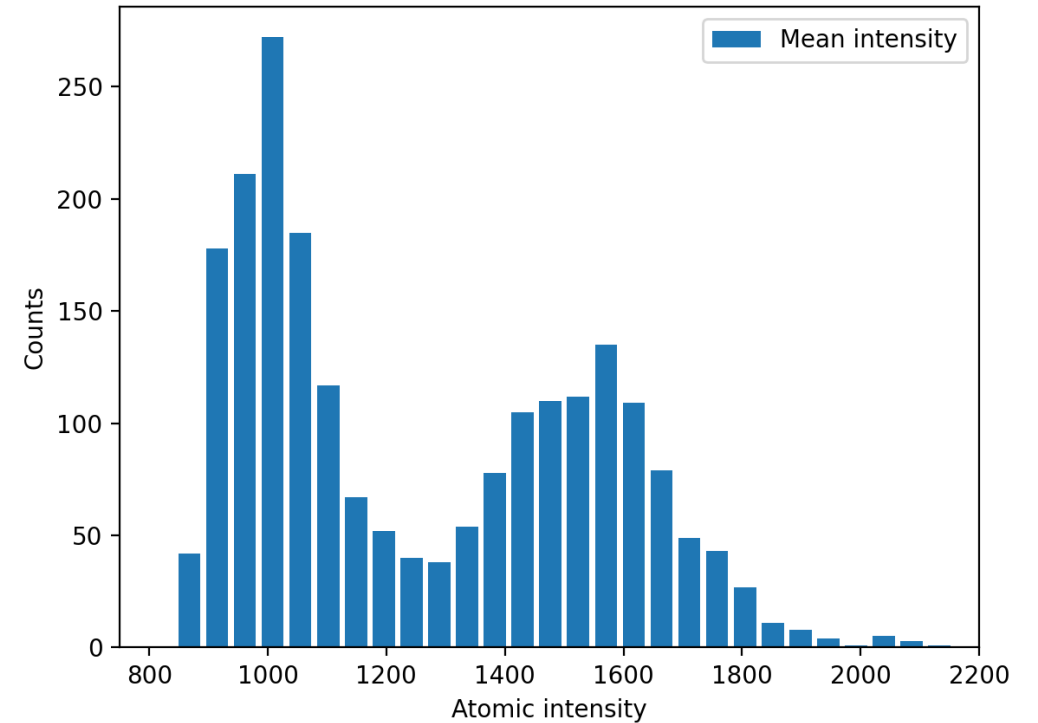
Adv. Mater., **38**, e11345 (2026)

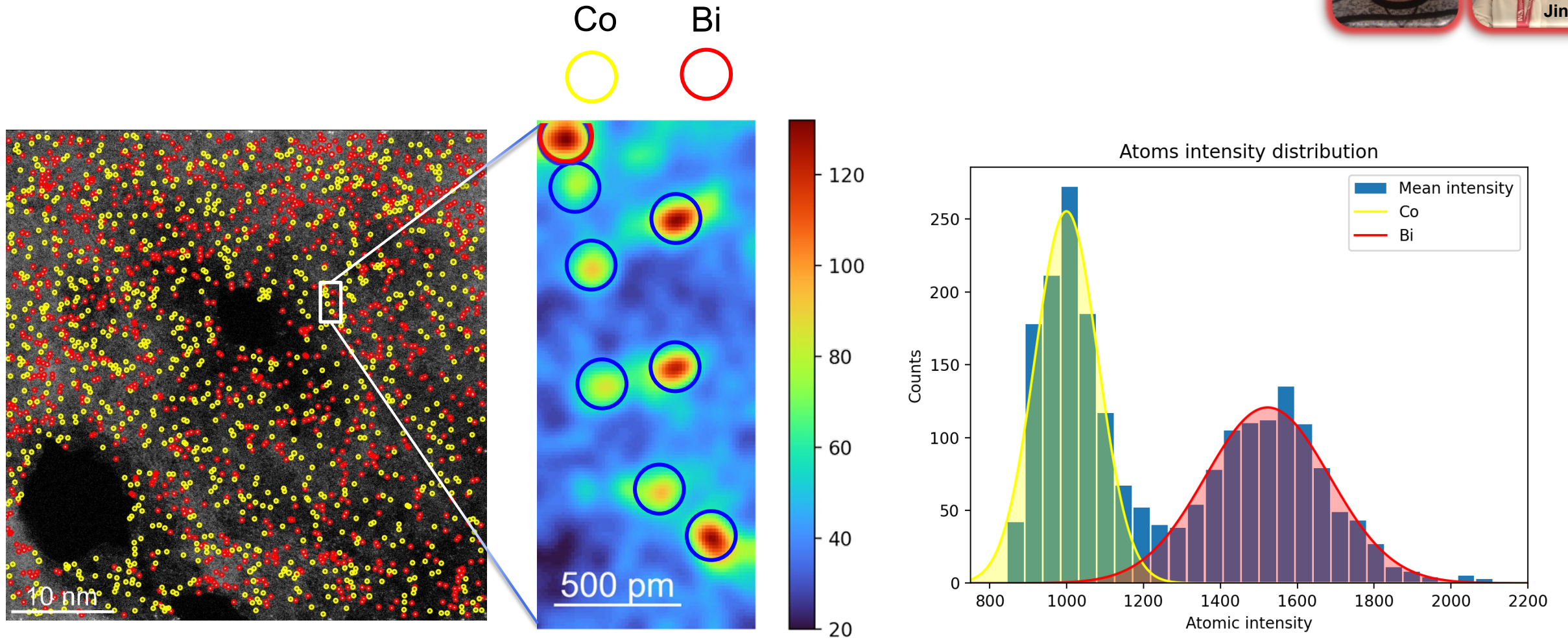


Atomic position

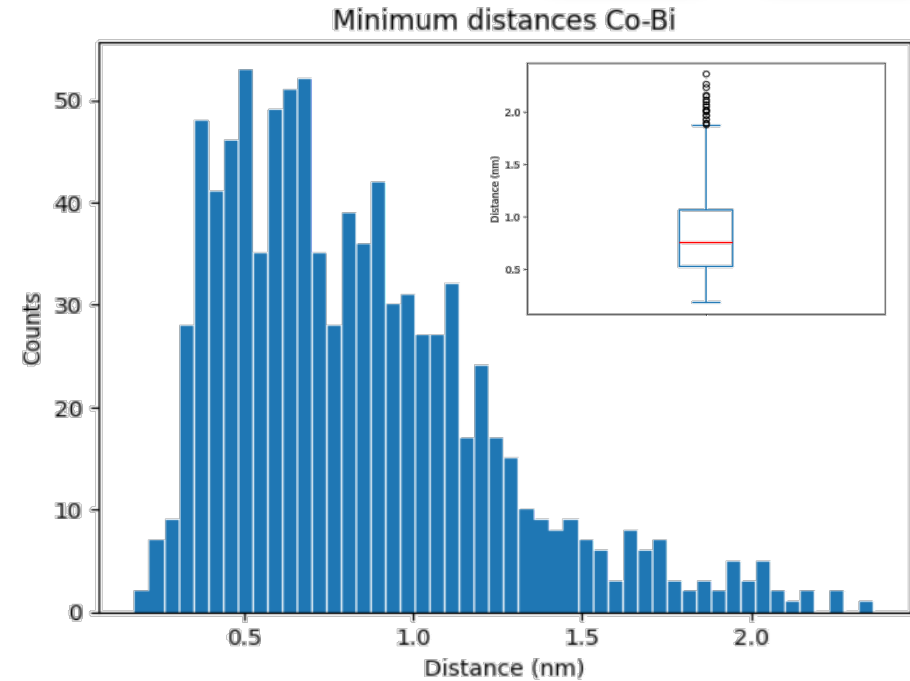
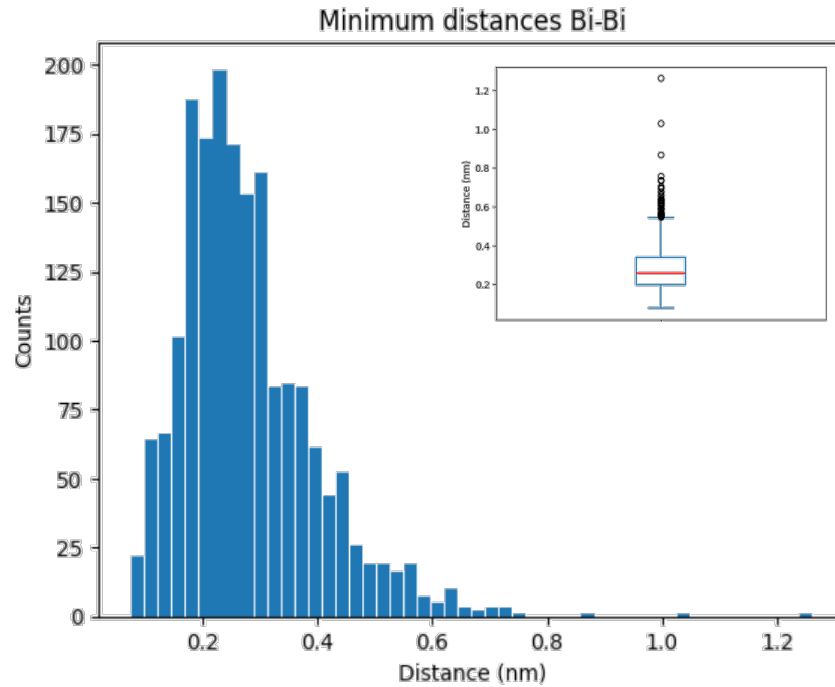
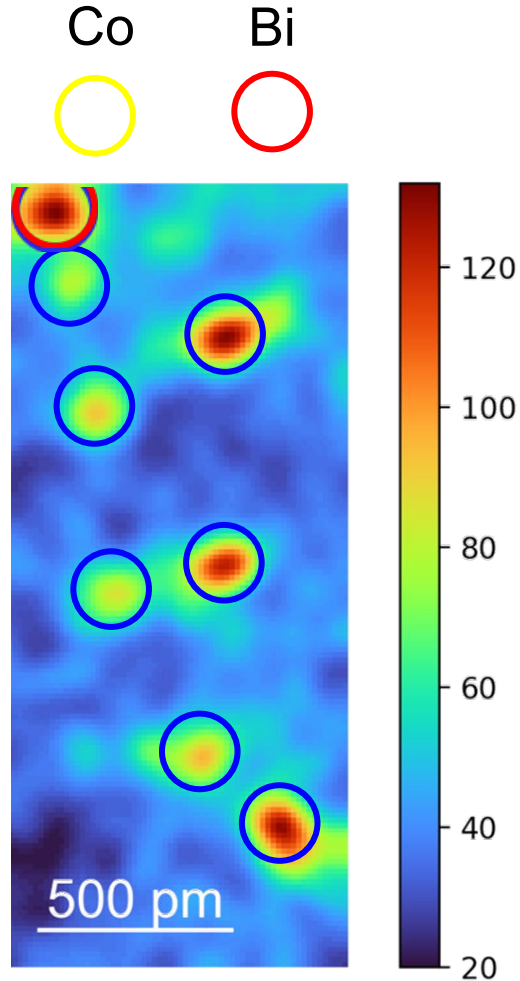


Atoms intensity distribution





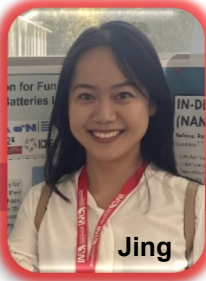
Adv. Mater., **38**, e11345 (2026)



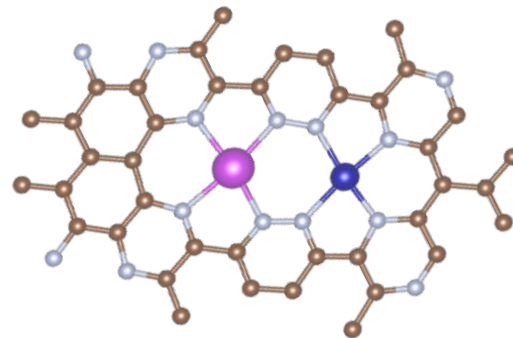
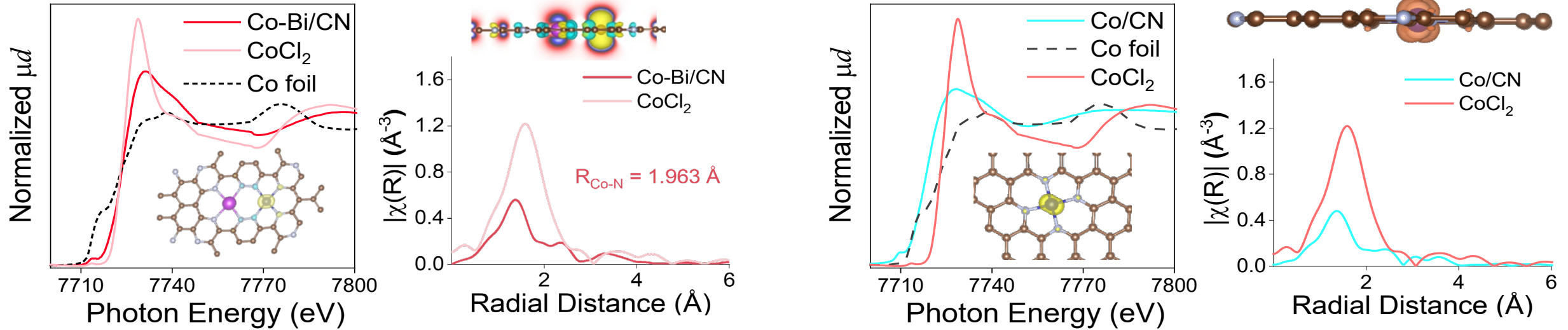
Histograms of the minimum distance's distribution from Co and Bi atoms within Co-Bi/CN

- ≈32% of the metal atoms form coupled Co-Bi pairs**
- ≈31% were organized as either Bi-Bi or Co-Co pairs**
- ≈37% existed as isolated Co or Bi atoms.**

Adv. Mater., **38**, e11345 (2026)



TM K-edge XANES spectra (left) and FT of the EXAF spectra (right)

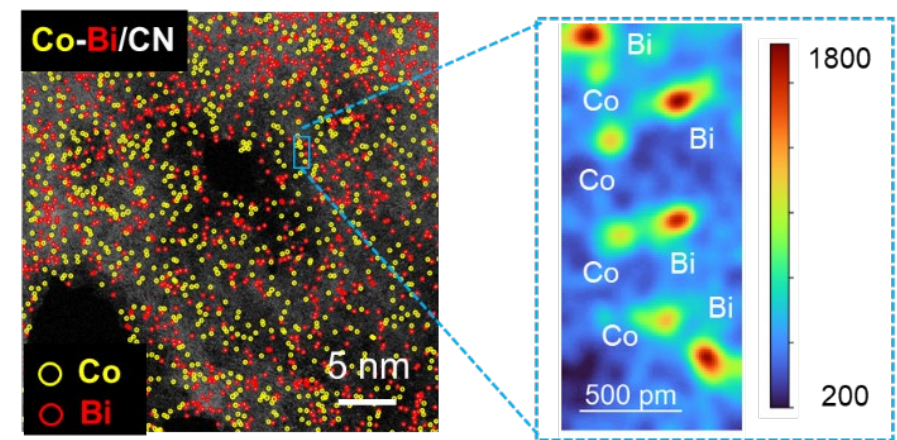
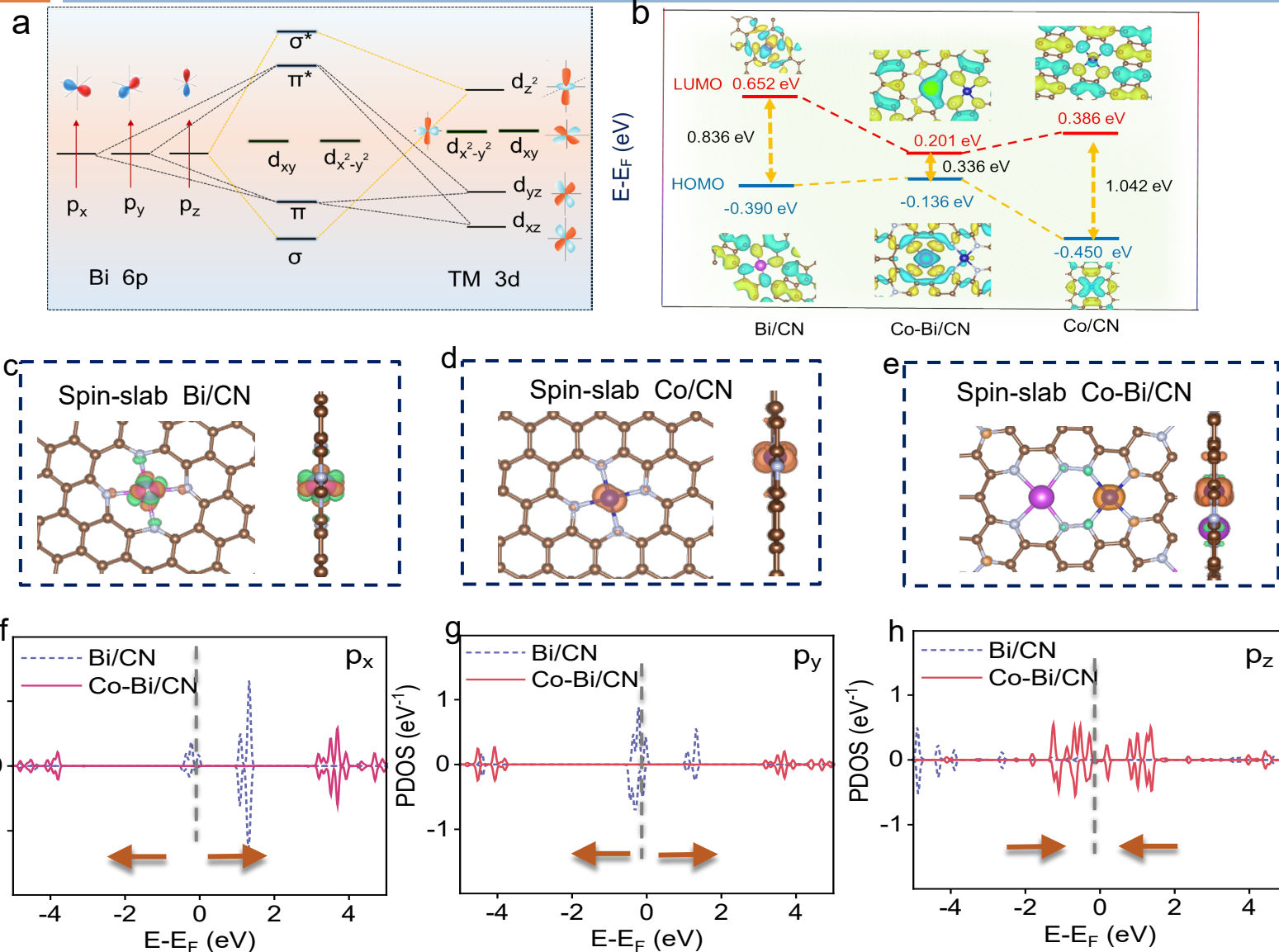


Adv. Mater., **38**, e11345 (2026)

Mechanistic Insights: Synergistic Catalysis



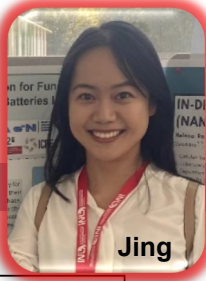
29



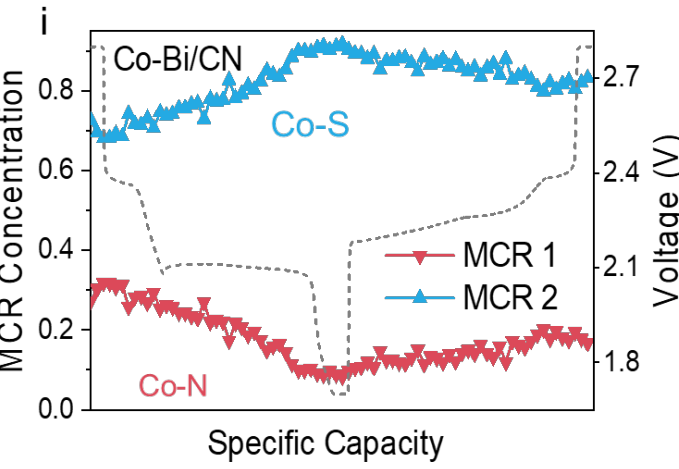
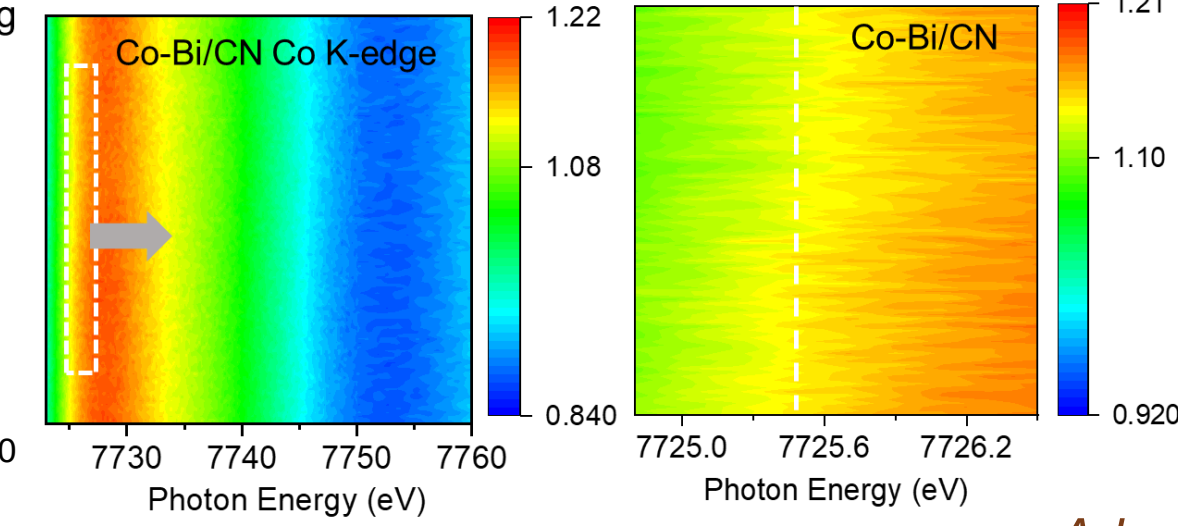
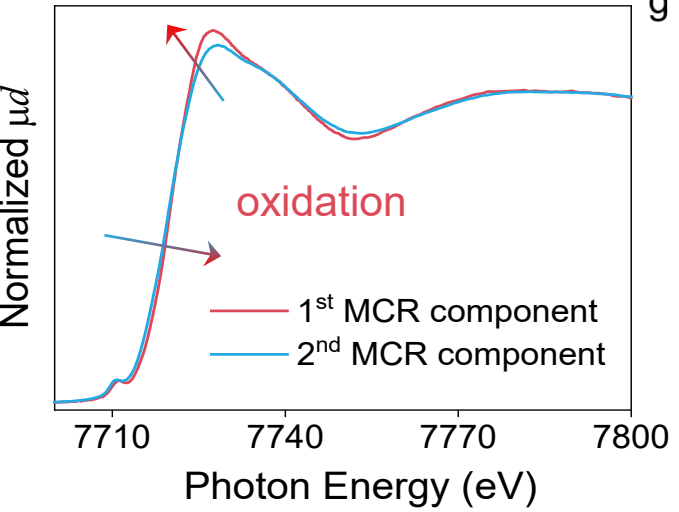
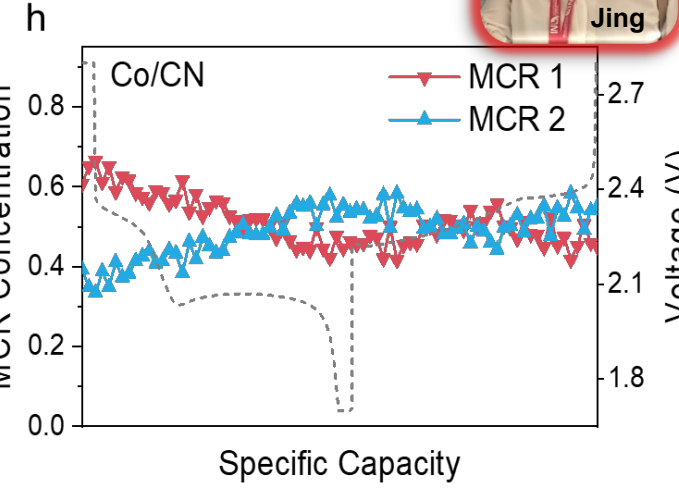
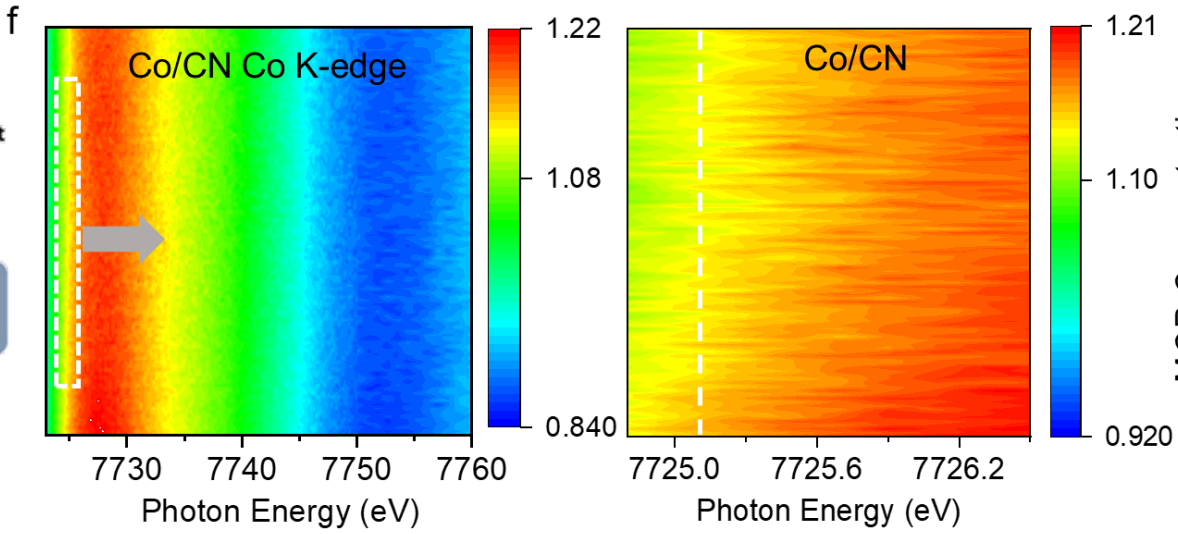
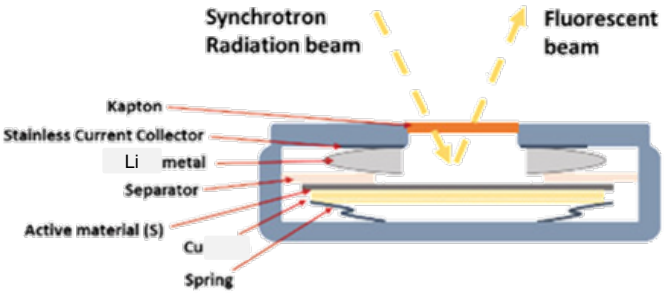
32% coupled Co-Bi pairs
 31% either Bi-Bi or Co-Co pairs
 37% existed as isolated Co or Bi atoms

Adv. Mater., **38**, e11345 (2026)

Mechanistic Insights: Synergistic Catalysis



30



Adv. Mater., **38**, e11345 (2026)

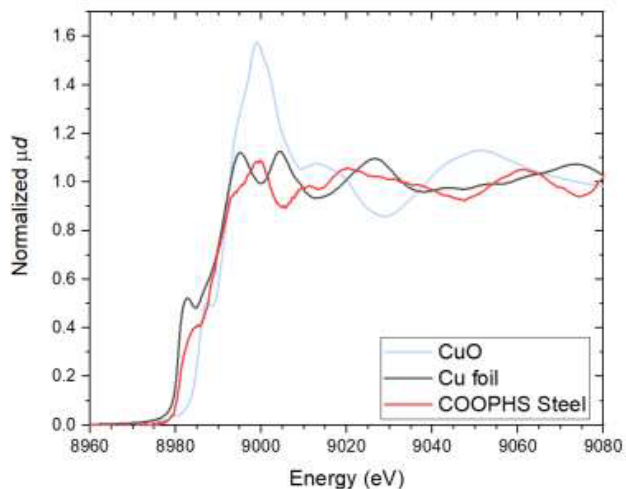


Figure 1. XANES Cu K-edge spectra of Cu agglomerations in 22MnB5 steel, shown alongside CuO and Cu foil standards for comparison. Taken from Kino's report on WP5

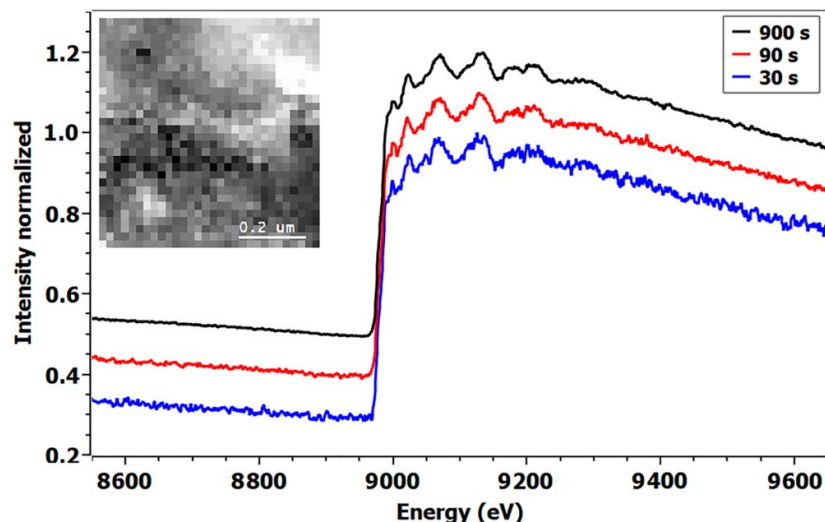


Figure 2. Inset: 30x30 spectrum image (SI) scan map of metallic Cu. XEELS spectra at the Cu K-edge

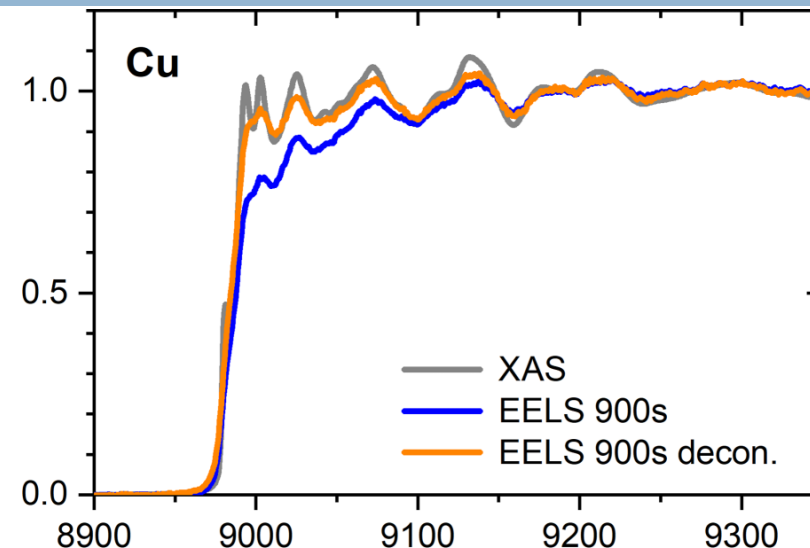
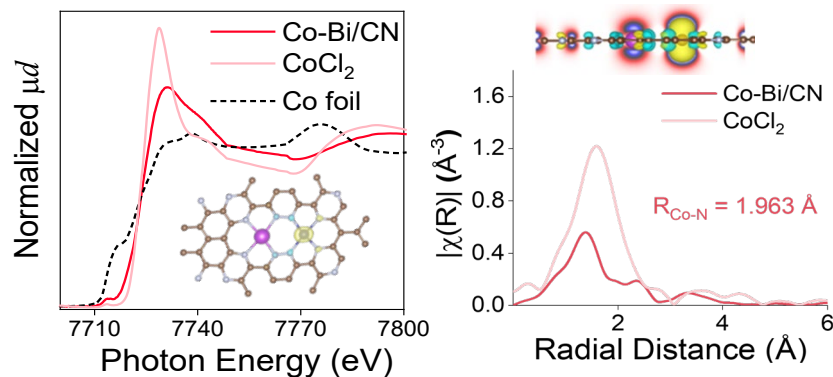


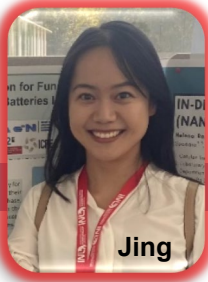
Figure 3. EELS (900 s, without and with low-loss deconvolution) and the XAS data measured for metallic Cu at the Cu K-edge after background subtraction, normalization, and flattening (DESY).



Adv. Mater., **38**, e11345 (2026)

DOI: 10.1103/PhysRevApplied.23.054095

*Combine with EXAFS + XEELS simulations



$$1+1>2!$$

- **Superior Catalysts Identified:** Among the synthesized TM–Bi/CN dual-atom catalysts, **Co–Bi/CN/S** and **Ni–Bi/CN/S** exhibit the fastest sulfur redox kinetics, highest first discharge plateau, balanced Q_2/Q_1 ratios, and excellent rate performance.
- **Limiting Factors Clarified:** **Mn–Bi/CN/S**, **Co/CN/S**, and **Bi/CN/S** show inefficient $S_8 \rightarrow Li_2S_8$ conversion, premature Li_2S_2 formation, and extended Li_2S nucleation times, which lead to active material loss, poor rate capability, and reduced cycling stability.
- **Mechanistic Insights Provided:** DFT calculations reveal that the **asymmetric Co–Bi coordination** enhances local electron density, strengthens Co–S interactions, and improves electron transfer, thereby boosting the catalytic activity of Co–Bi/CN.
- **Design Principles Established:** The combined electrochemical and theoretical results establish a **rational platform for designing optimized dual-atom catalysts**, with strong implications for high-performance Li–S cathodes and other conversion-type electrocatalytic systems.

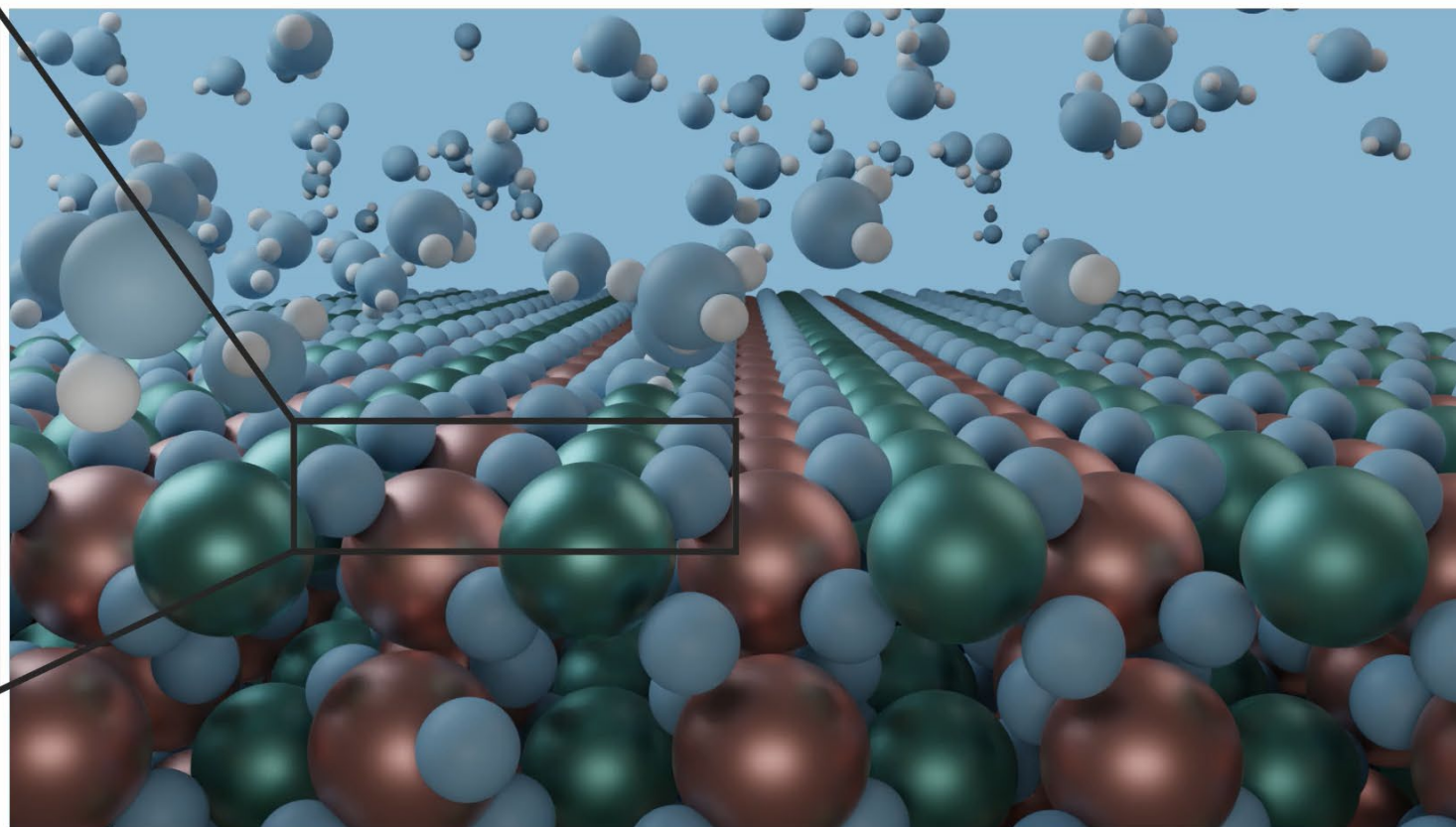
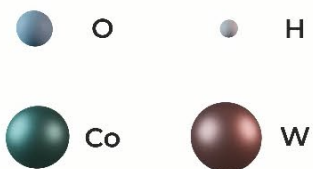
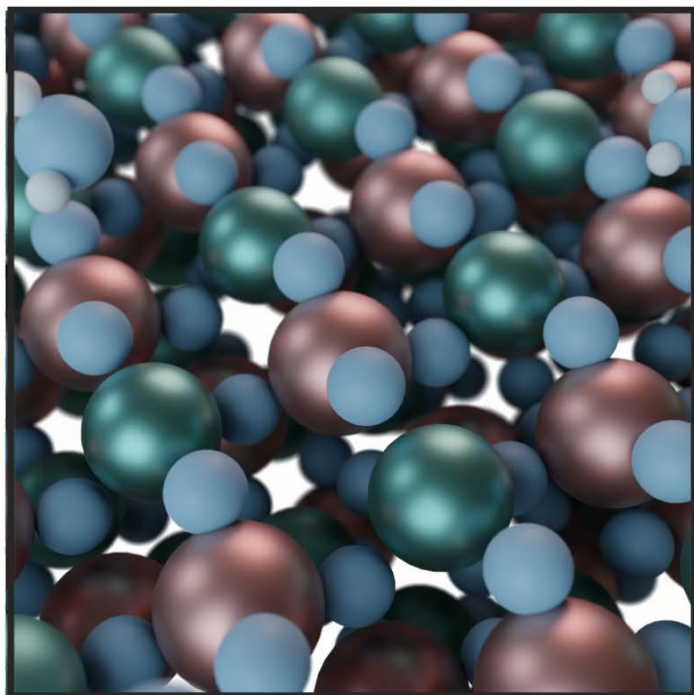
Adv. Mater., **38**, e11345 (2026)

Activation of CoWO₄ for OER



Delamination process

The activation mechanism involves introducing **high-valence sacrificial elements** like W that during activation, a **water/hydroxide – WO₄²⁻ anion exchange process** creates a defective lattice that can trap hydroxide and water species

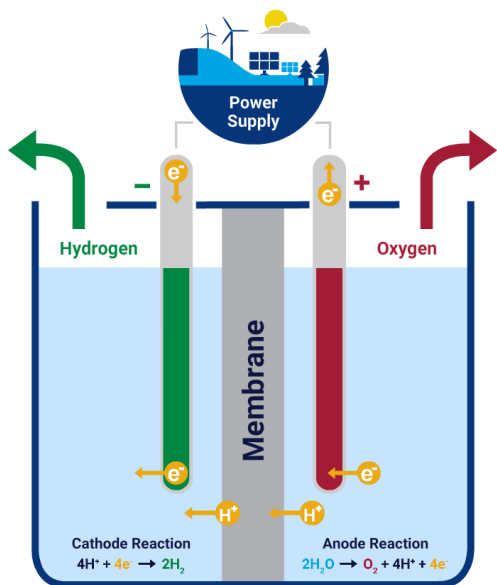


Science, **384**, 1373 (2024)

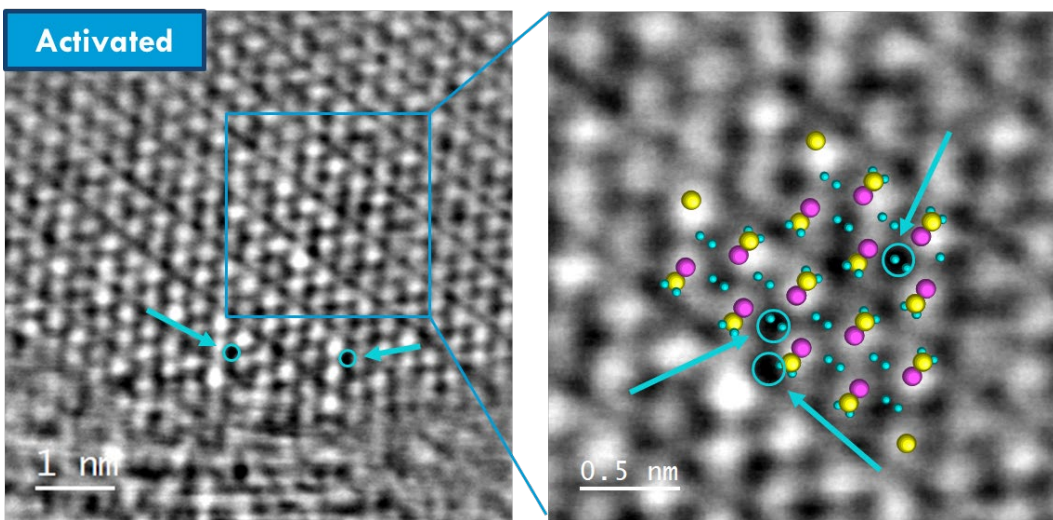
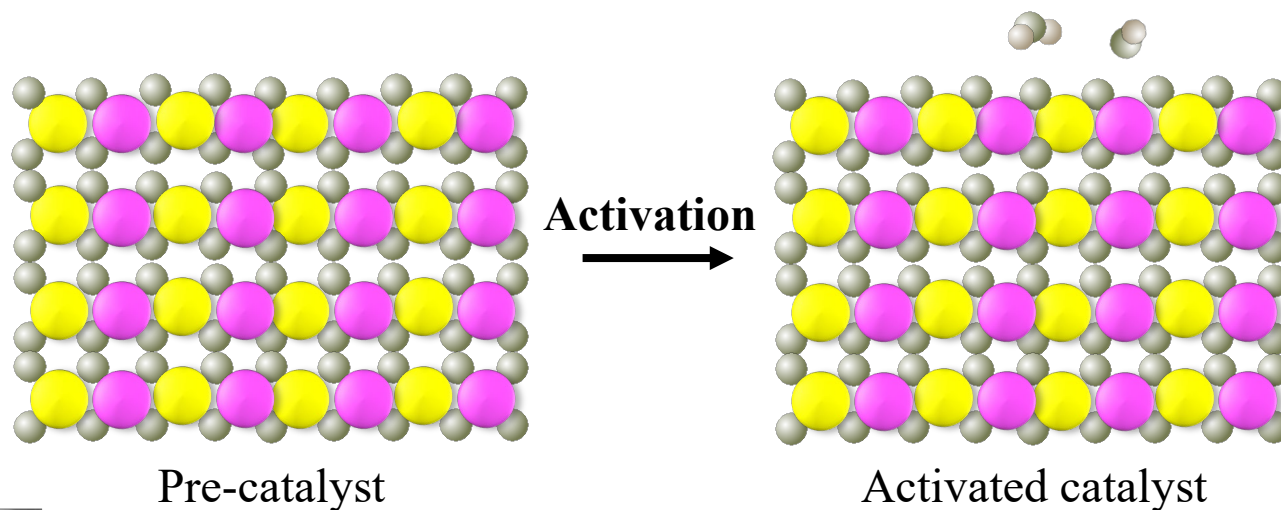
Activation of CoWO₄ for OER



38

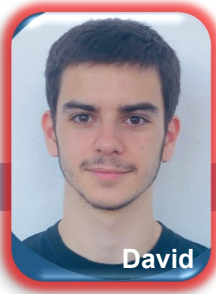


- Cobalt
- Tungsten
- Oxygen
- Hydrogen



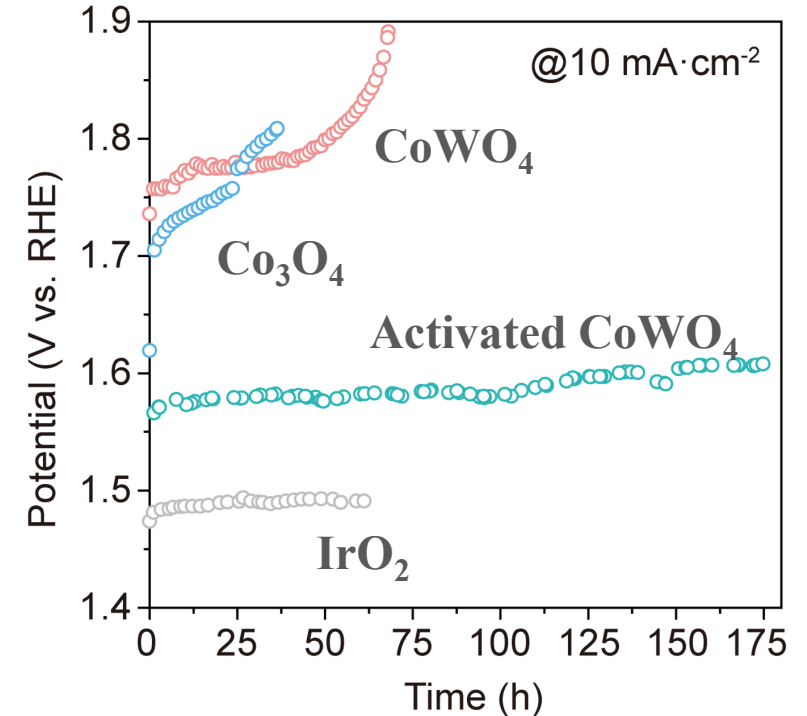
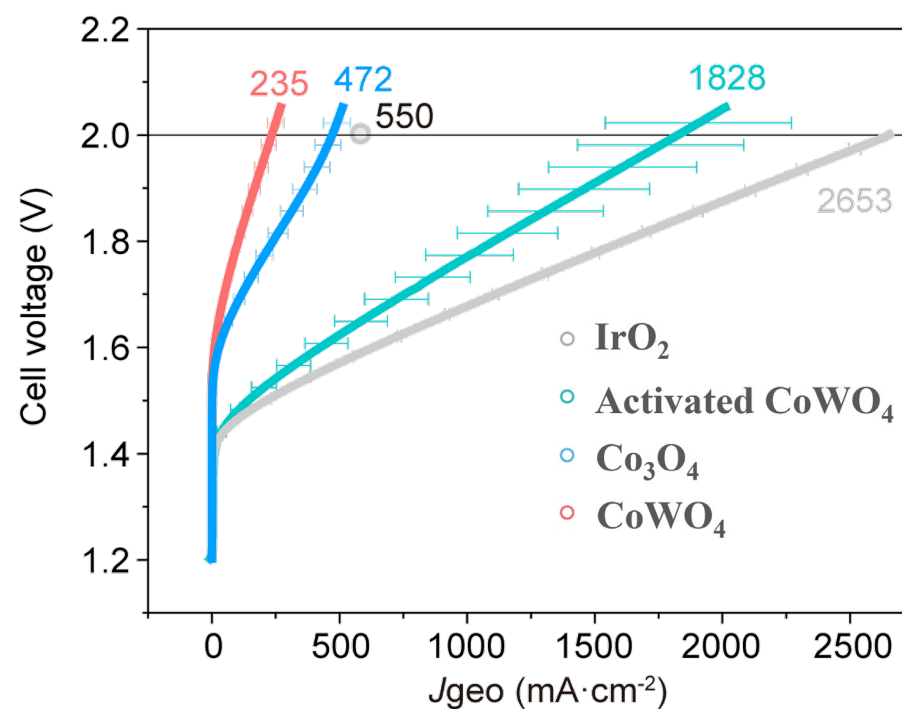
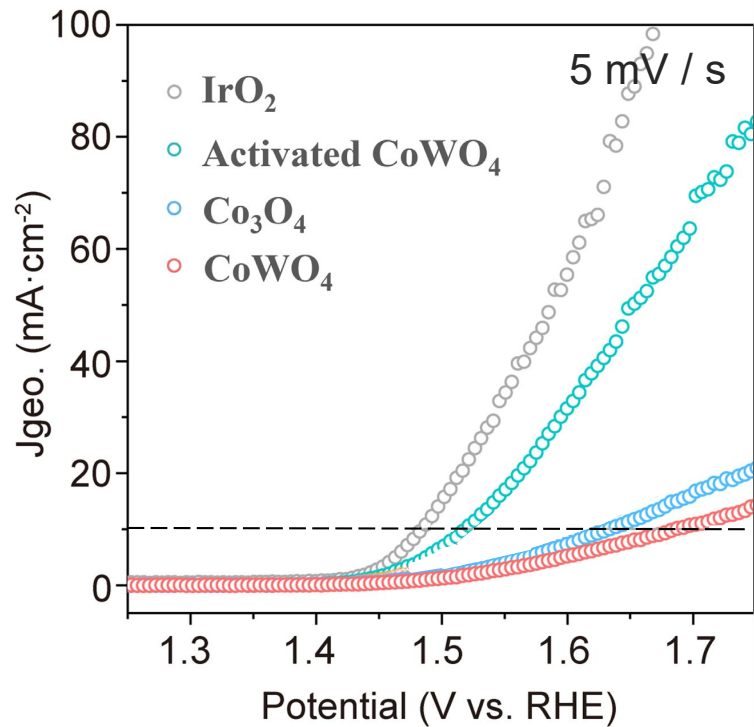
- Trapping of water and hydroxide species in the generated WO_4^{-2} vacancies
- Adsorbed-water OER mechanism enhances poor CoOx stability.
- Stable operation for >600 hour at current density of 1 A cm^{-2}

Science, **384**, 1373 (2024)



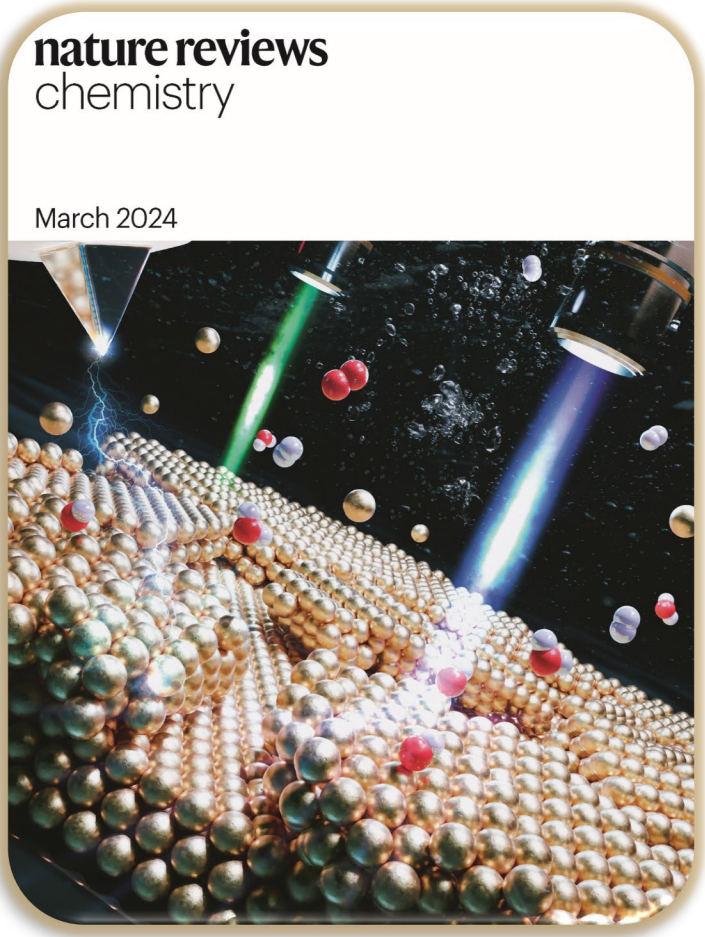
Electrochemical performance

The activated catalyst exhibited remarkable activity and stability, close to the IrO₂ benchmark



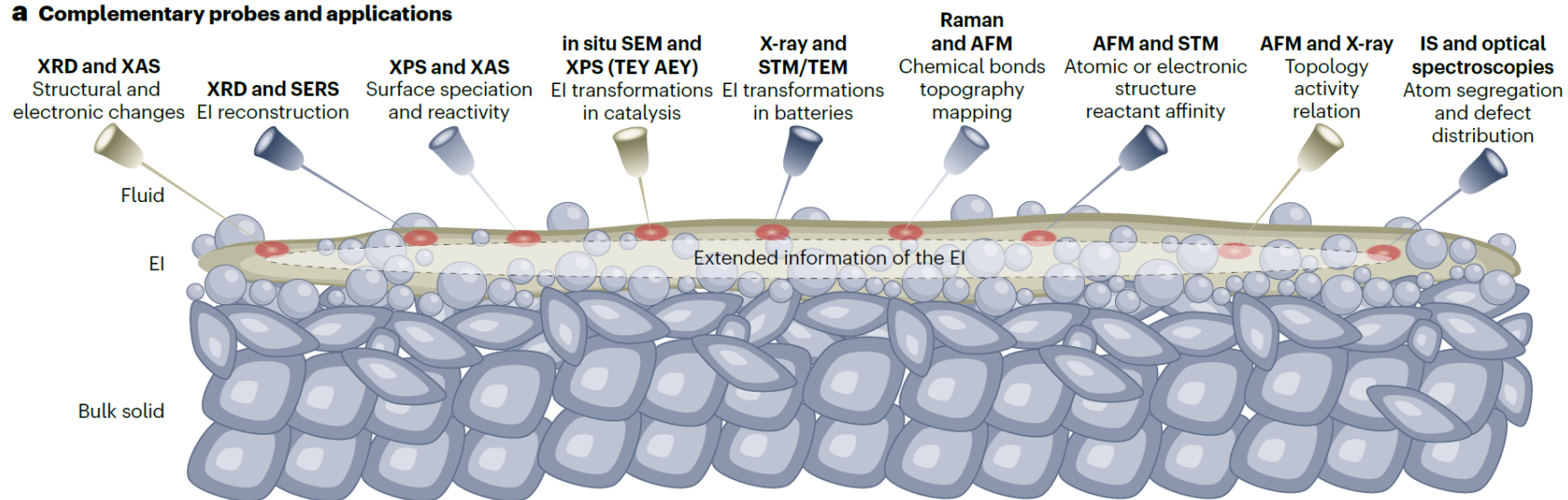
➤ Stable operation for >600 hour at current density of 1 A cm⁻²

Science, **384**, 1373 (2024)

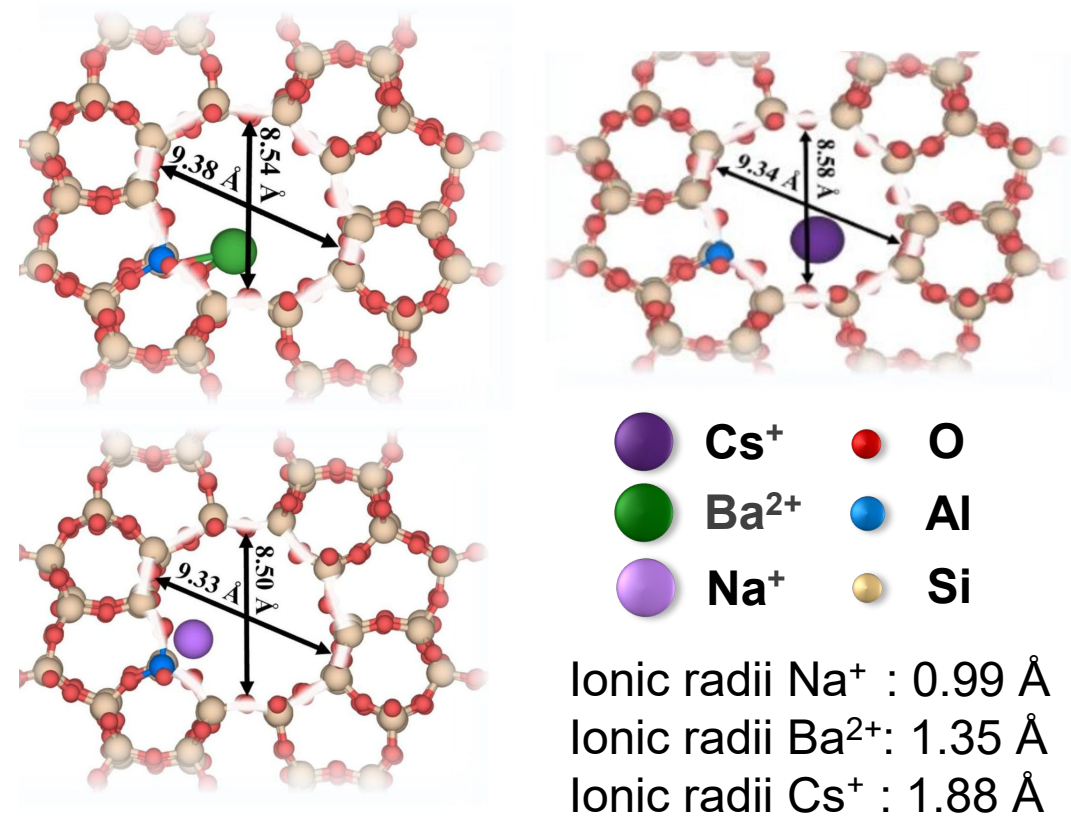


Complementary probes for the electrochemical interface.

a Complementary probes and applications



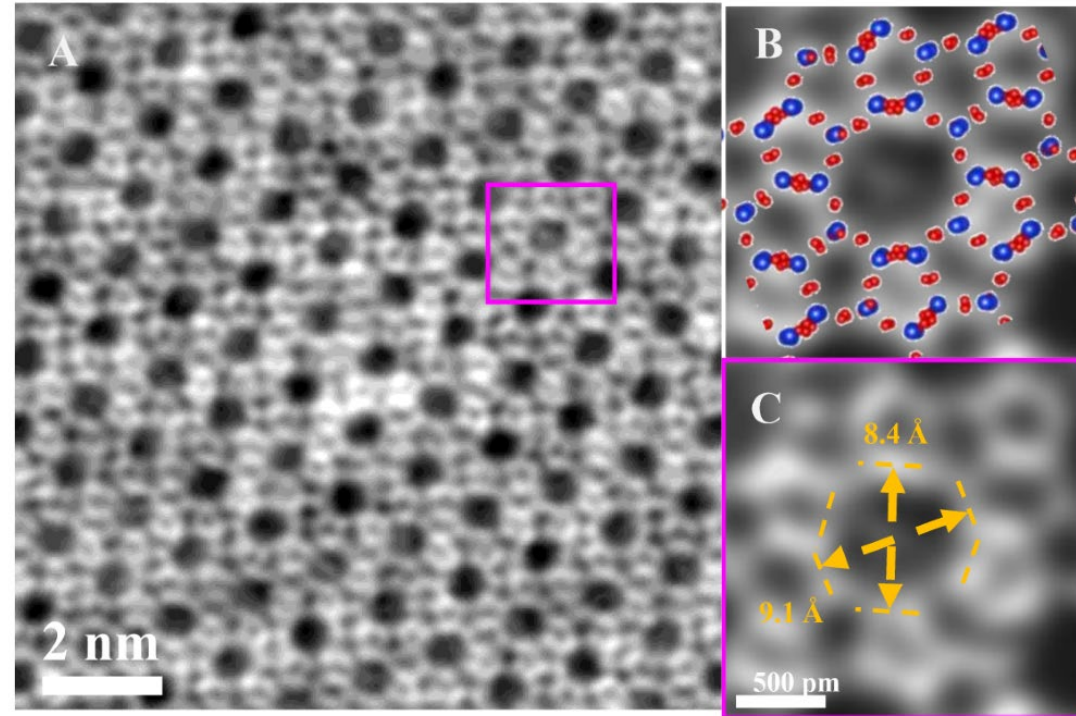
Nature Reviews Chemistry, 8, 159 (2024)



Geometric sizes:

- Unoccupied 10-MRs: 8.53 Å × 8.61 Å
- Na⁺-occupied 10-MRs: 9.33 Å × 8.50 Å
- Ba²⁺-occupied 10-MRs: 9.38 Å × 8.54 Å
- Cs⁺-occupied 10-MRs: 9.34 Å × 8.58 Å

DFT calculation of ring flexibility in ion-exchanged ZSM-5 (MFI type) zeolites for Na⁺, Cs⁺ and Ba²⁺ ions in 10-MRs

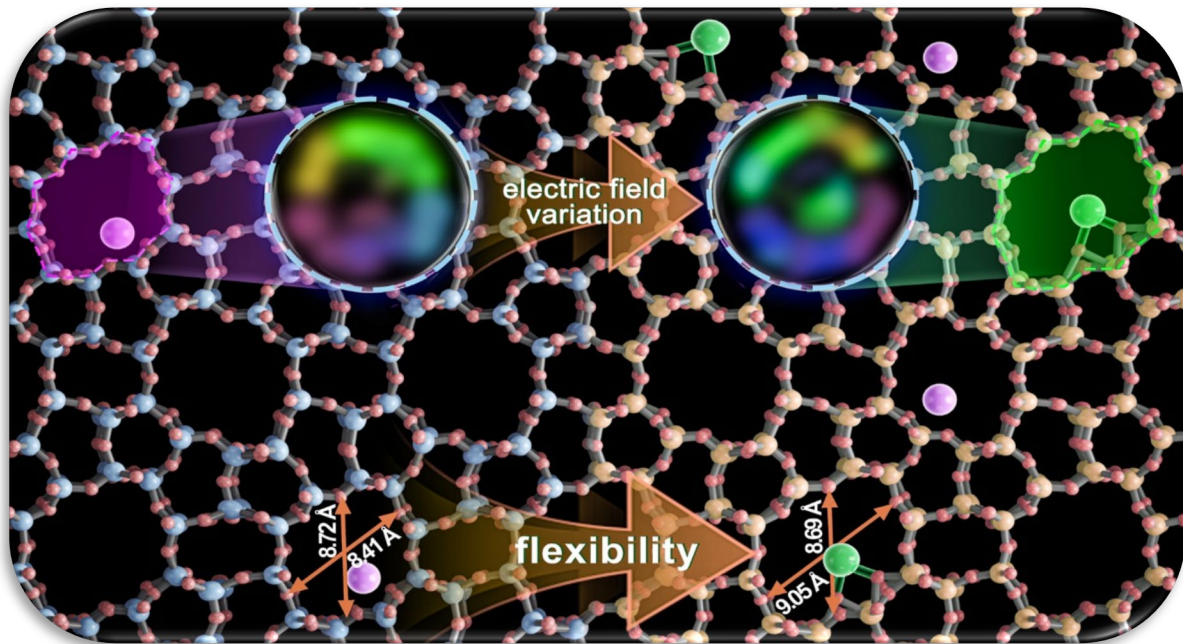


Ba²⁺ ions confined within the 10-membered rings (10-MRs) trigger a 0.5 Å channel expansion, which exceeds the 0.2 Å expansion induced by Na⁺ ions while maintaining the framework's macroscopic rigidity.

JACS, just accepted, (2026)

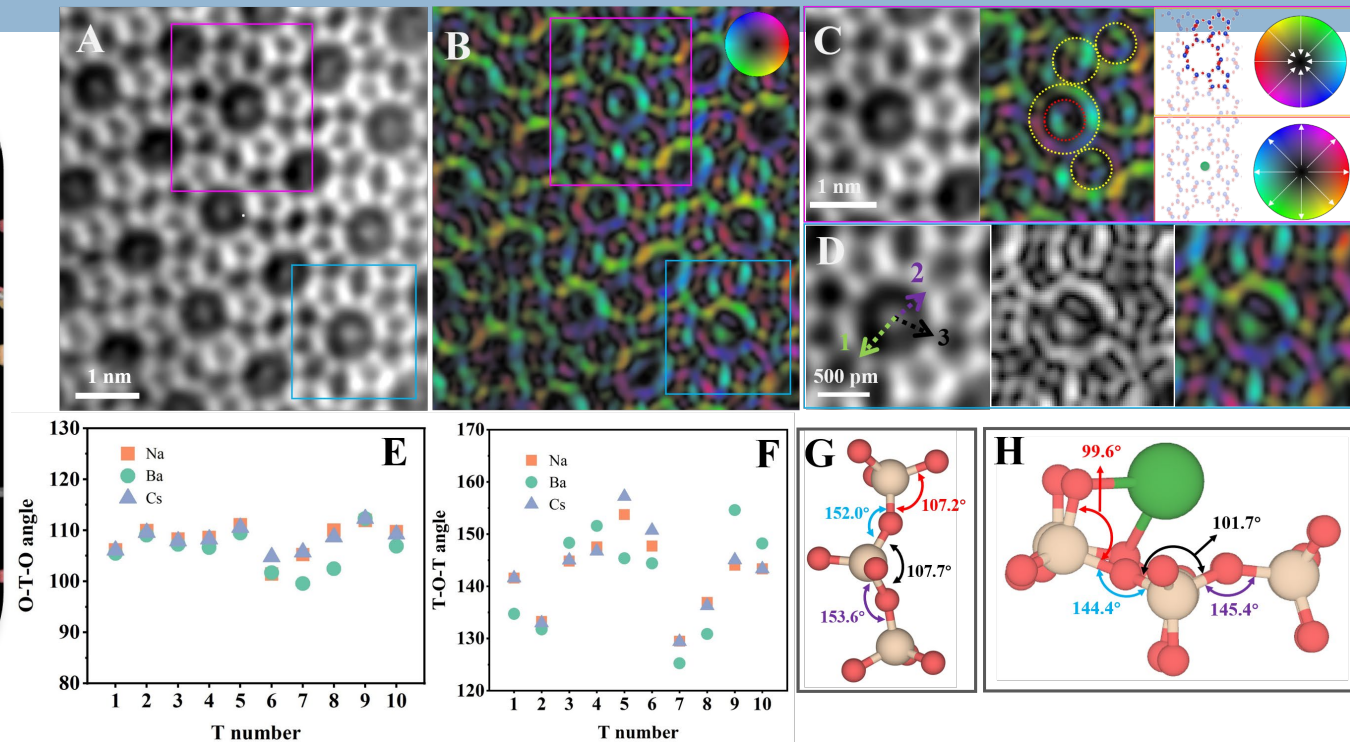
Local Electric Field induced strain in Zeolites

42



Ionic radii Na⁺ : 0.99 Å
 Ionic radii Ba²⁺: 1.35 Å
 Ionic radii Cs⁺ : 1.88 Å } Cs⁺ > Ba²⁺ > Na⁺

Ion-induced electric-field strength Ba²⁺ > Cs⁺ > Na⁺



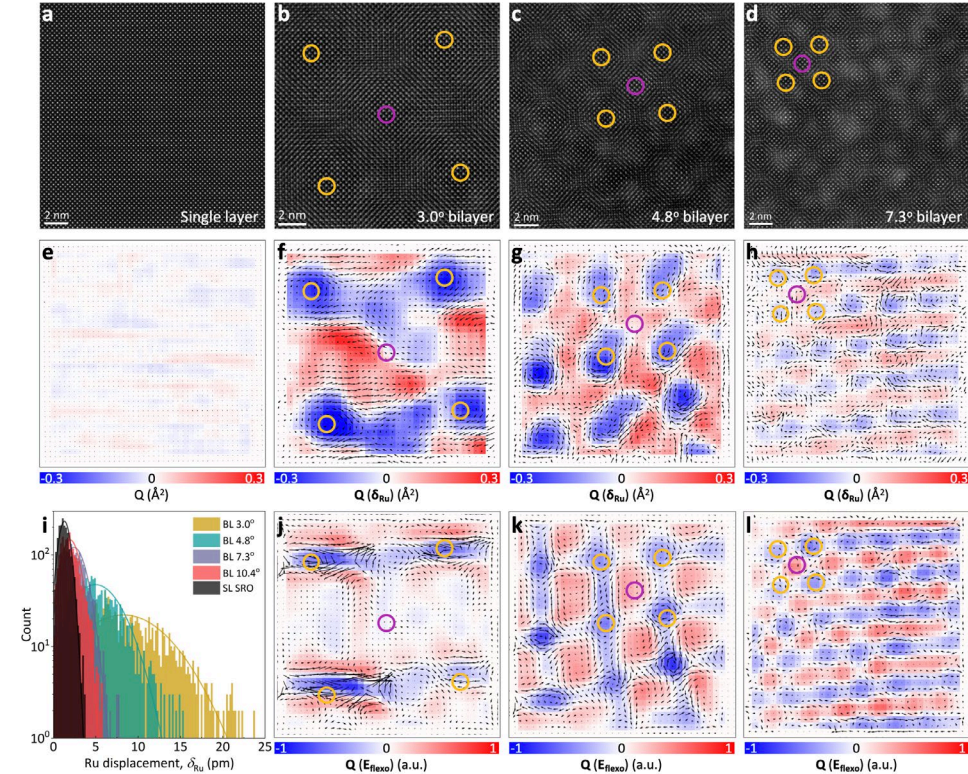
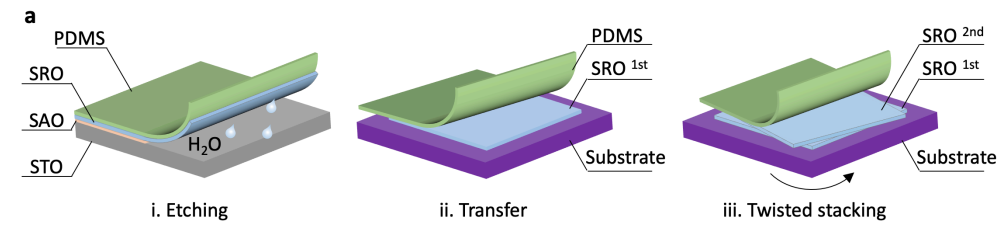
Electric field trigger mechanism for ring flexibility via DPC-STEM and DFT calculations
 For Ba²⁺ ions in 10-MRs

Atomic Imaging of Ion-Triggered Flexibility and Local Electric Field Response in Zeolite Rings

JACS, just accepted, (2026)

4D STEM Multislice Ptychography

43

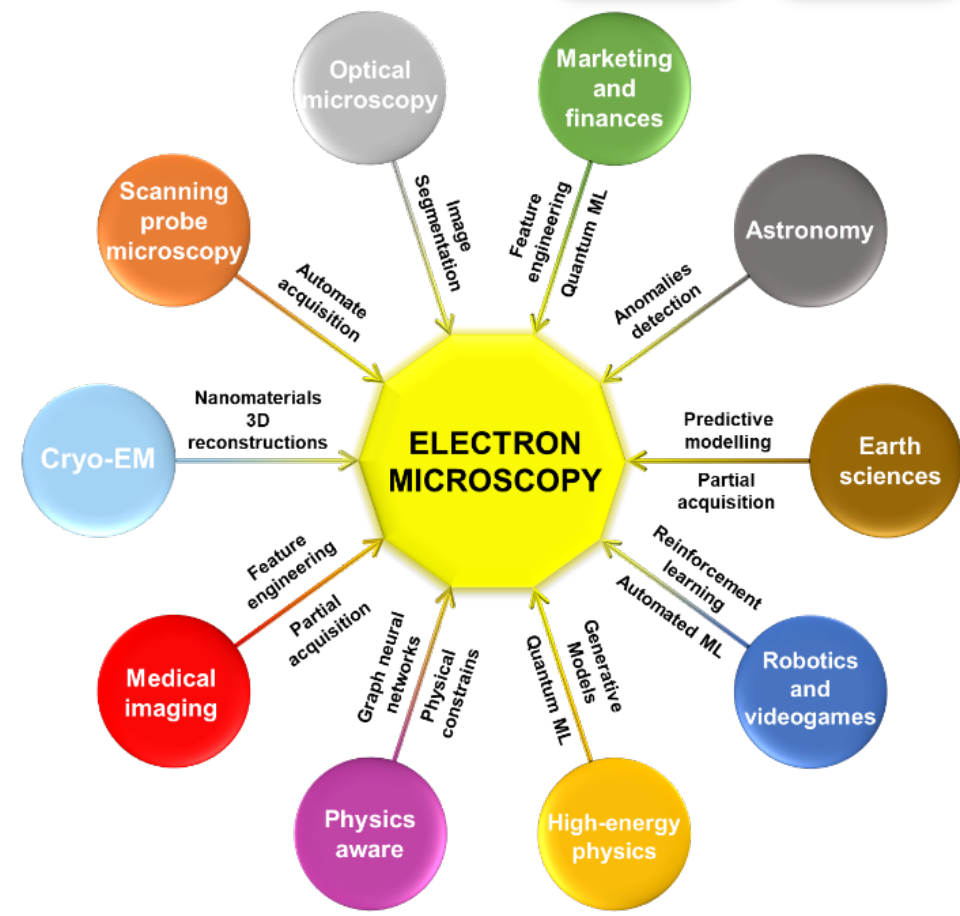
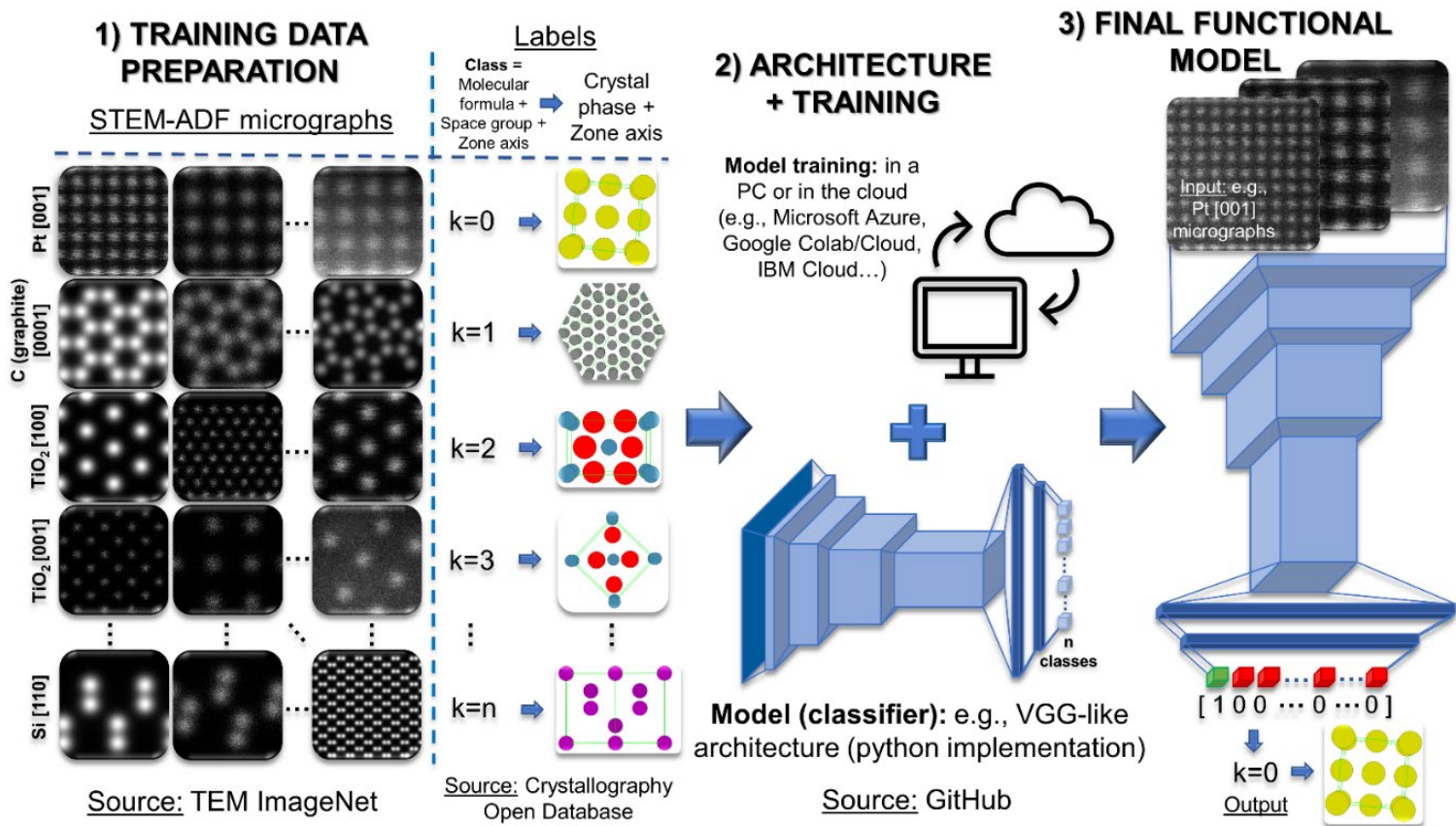


In-depth Multislice Ptychography reconstructions
Polarization Vortices in a Ferromagnetic Metal via Twistronics

Submitted, arXiv.2505.17742 (2025)



Machine learning in electron microscopy for advanced nanocharacterization: current developments, available tools and future outlook



Nanoscale Horiz. 7, 1427 (2022)

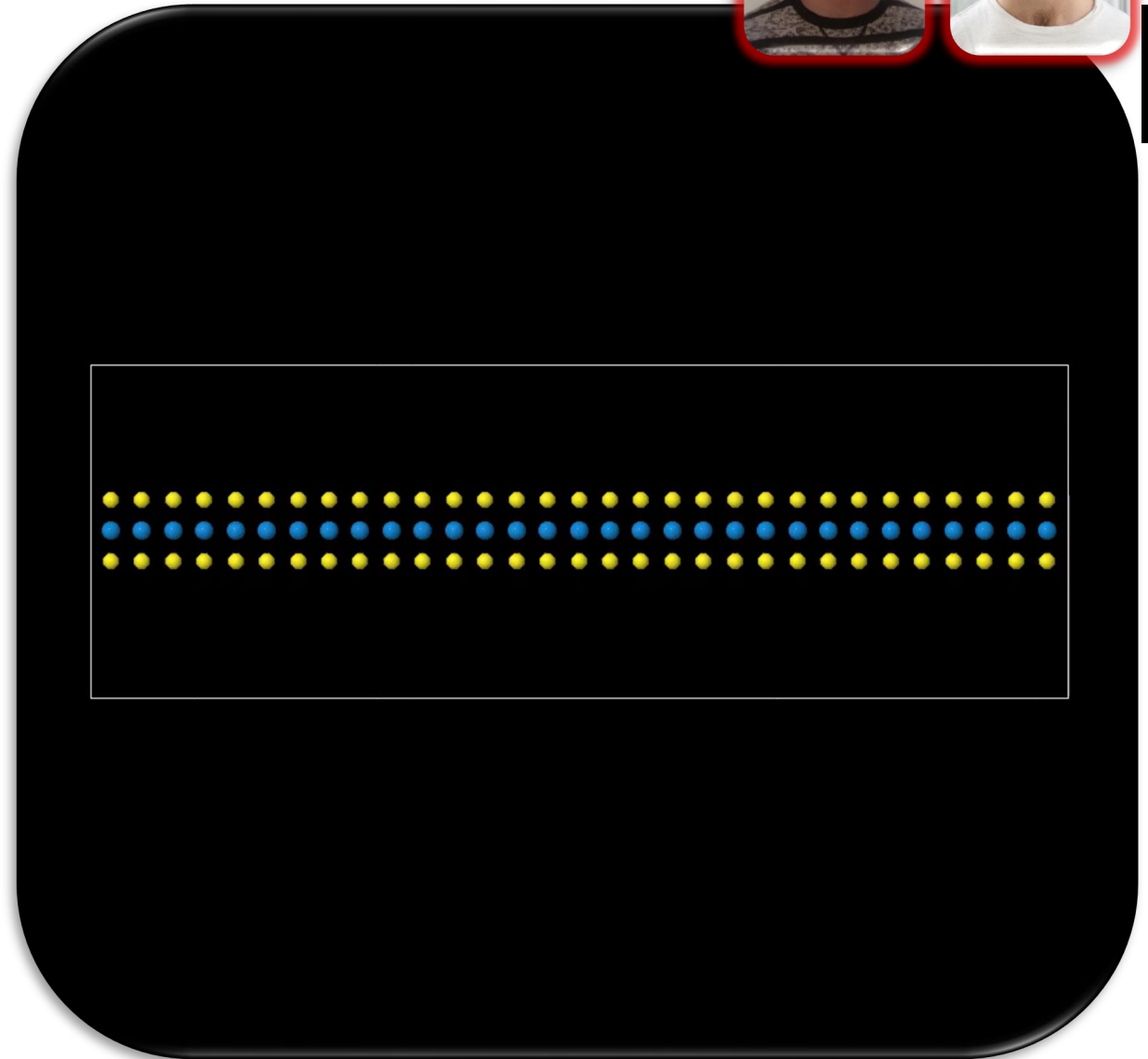
Vacancies in 2D Materials

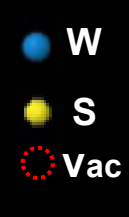


45



Presence of vacancies in 2D materials might improve their physical and chemical properties:

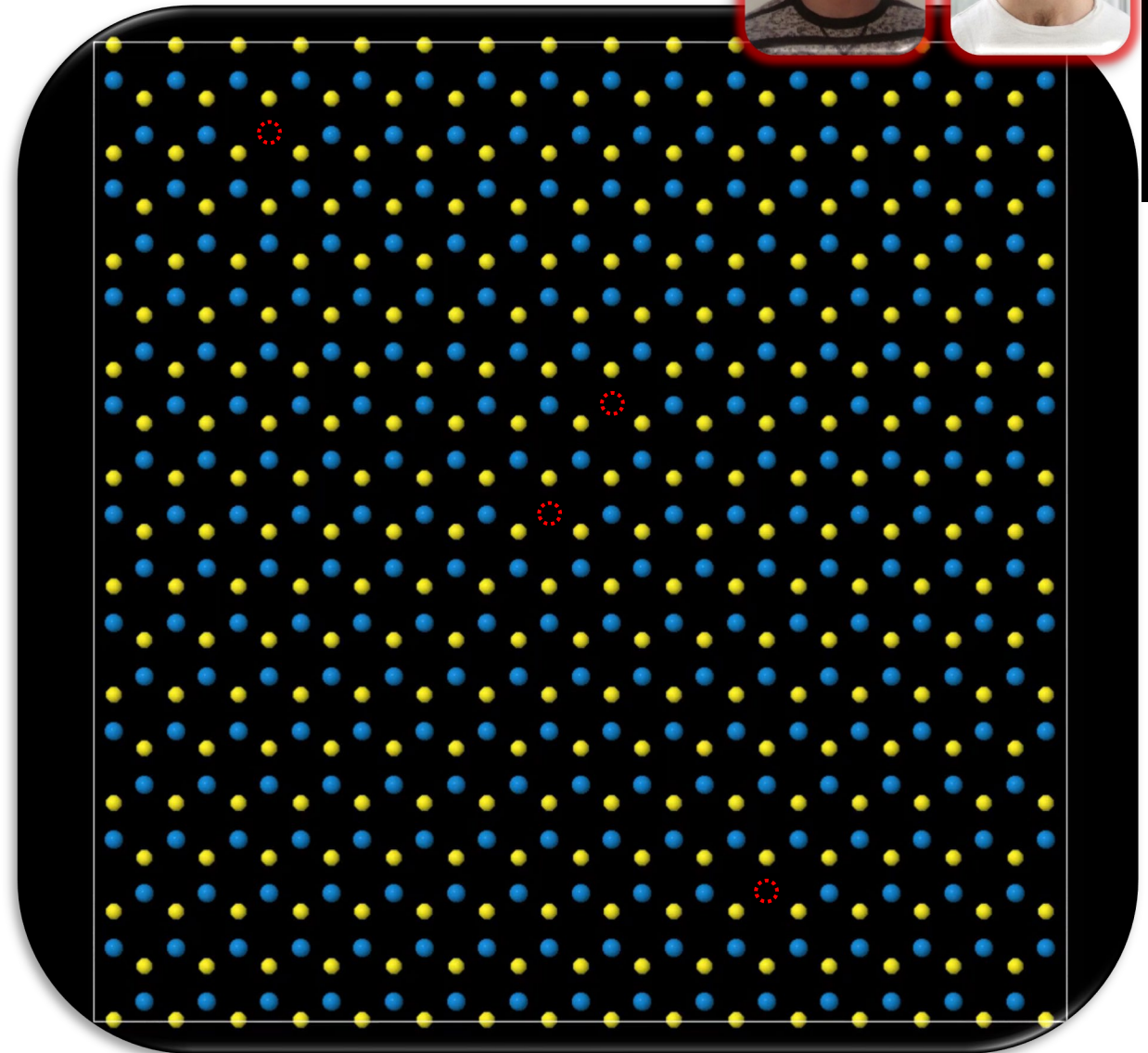




Presence of vacancies in 2D materials might improve their physical and chemical properties:

- As seen before, they can enhance the catalytic properties by modifying the local cation/metal coordination (e.g.: PtSe₂).
- In 2D material like hBN, MoSe₂ WSe₂ and WS₂, might result in single-photon emission when the material is optically or electronically excited.

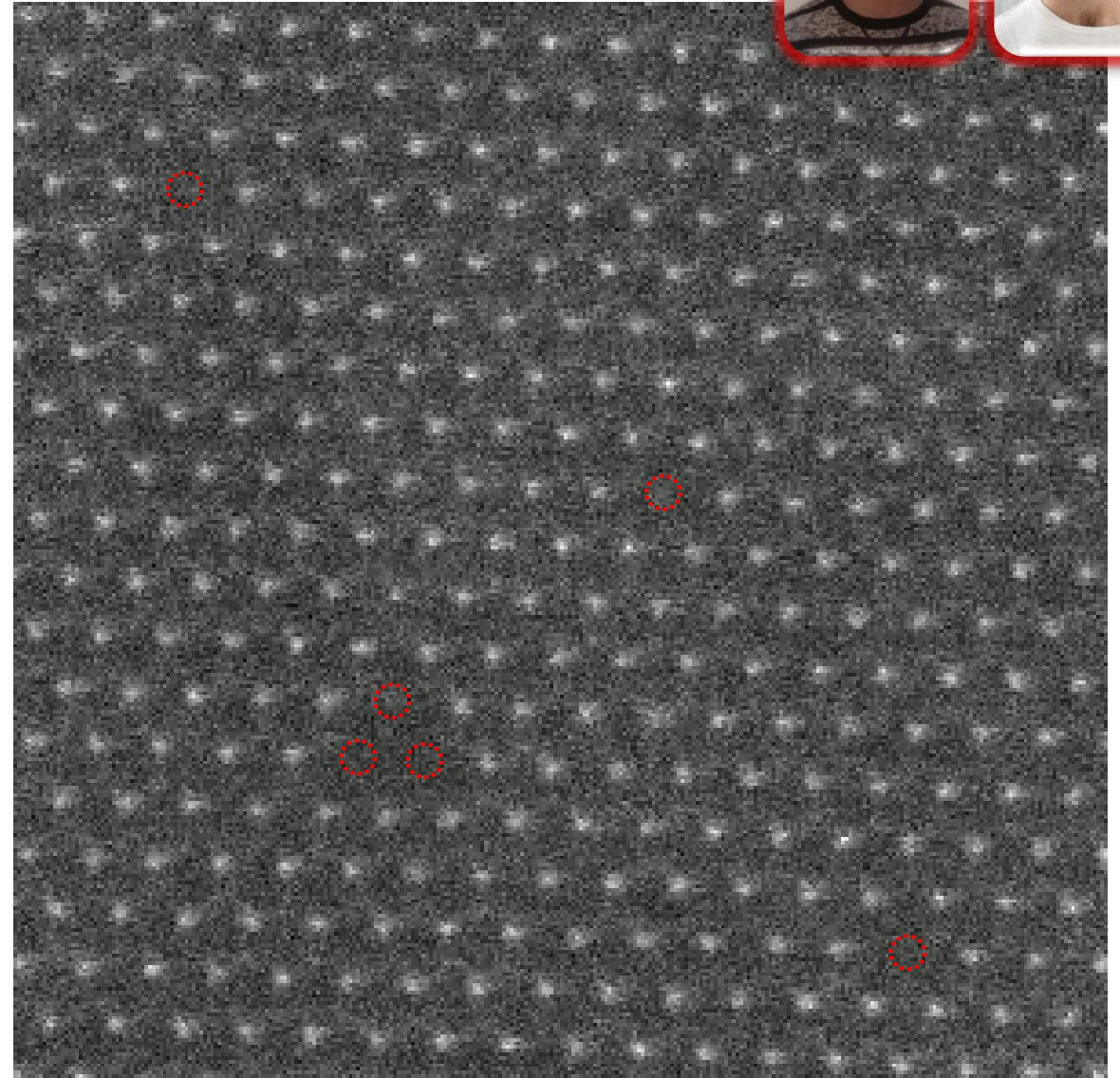
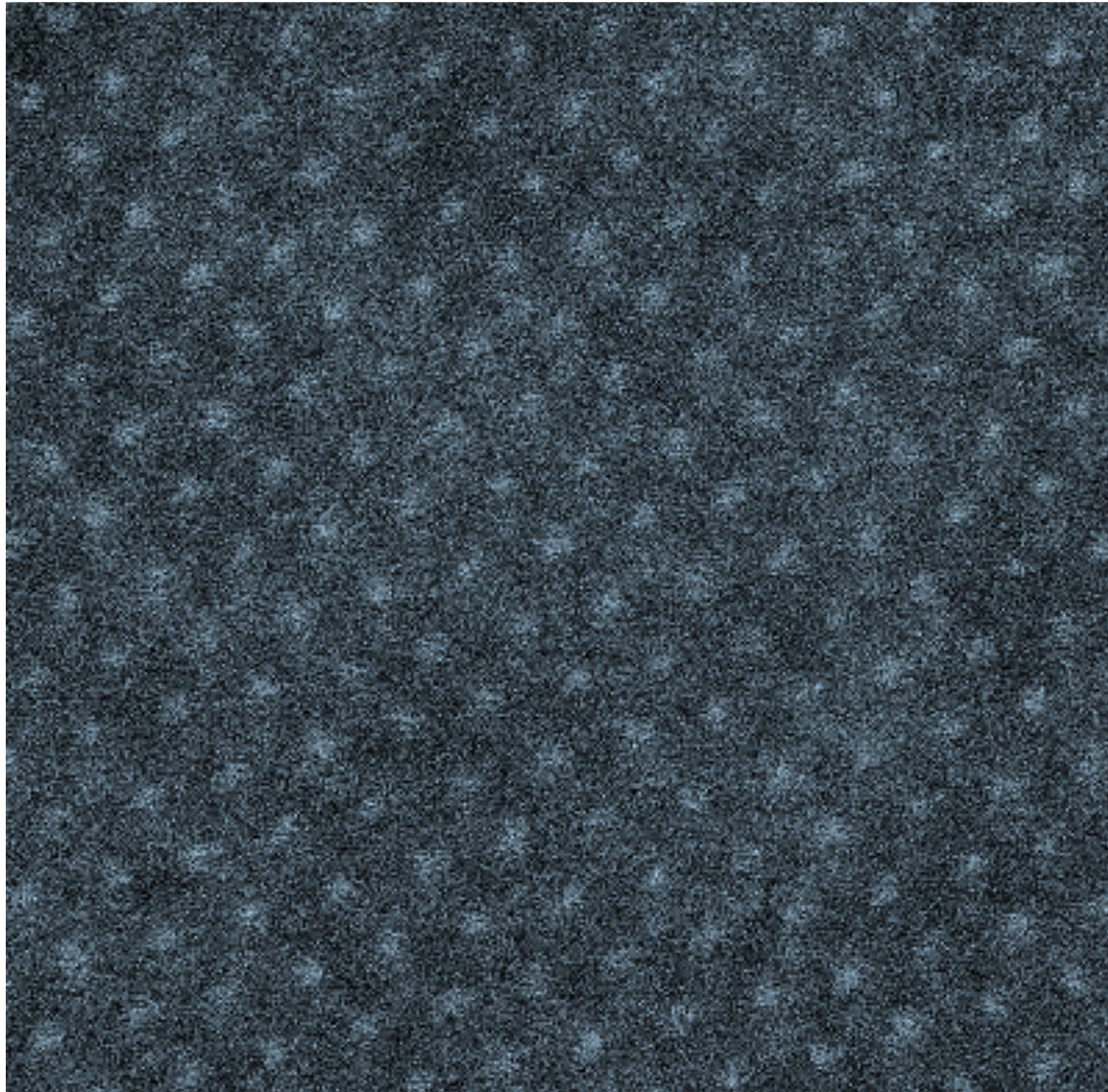
We have developed an automated AI methodology for detecting vacancies, an allow statistically significant studies



Denoising via CNN Model on FFT



47

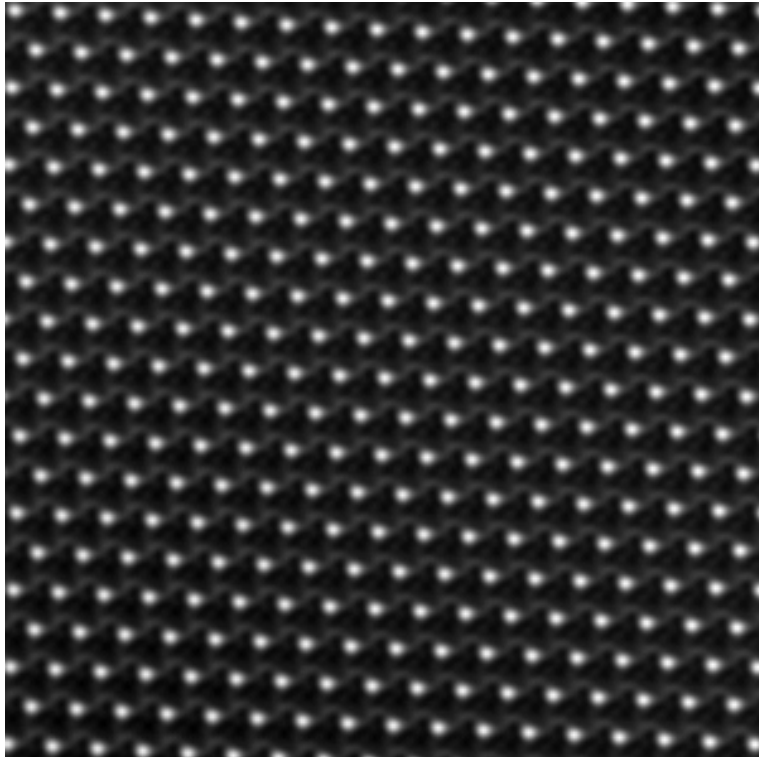


Vacancies Detection

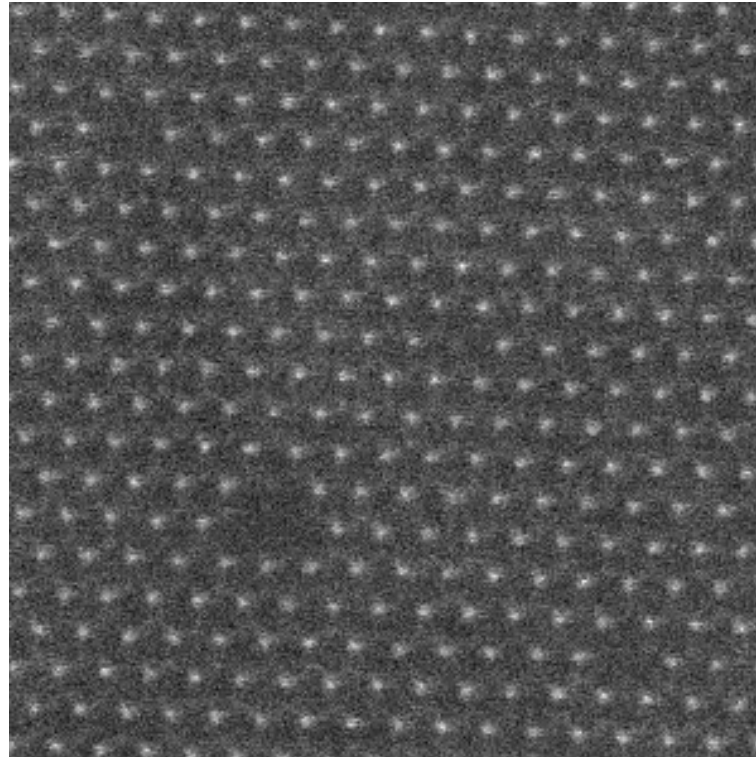


48

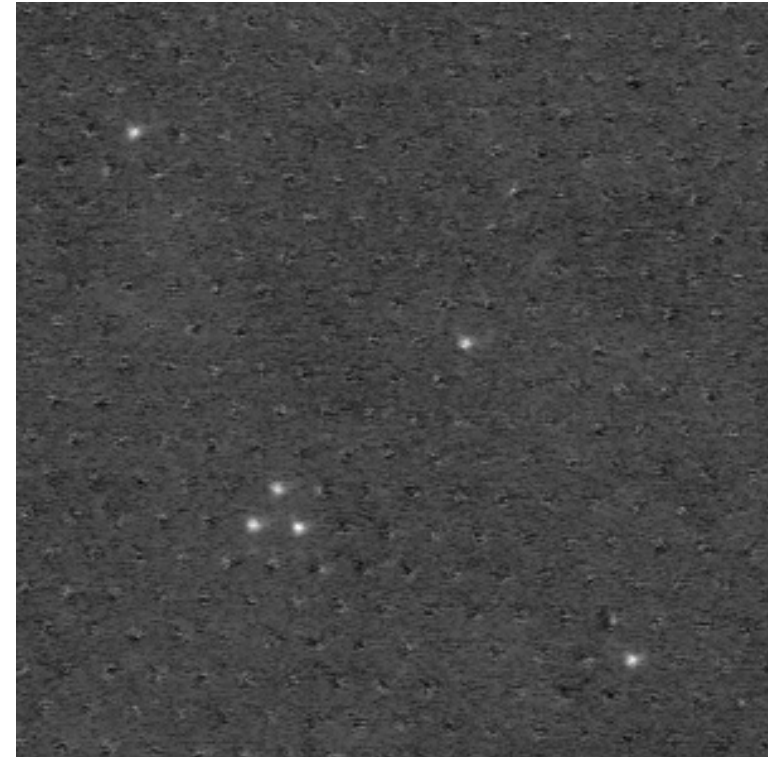
Denoised Image



Original Image



Vacancies Image

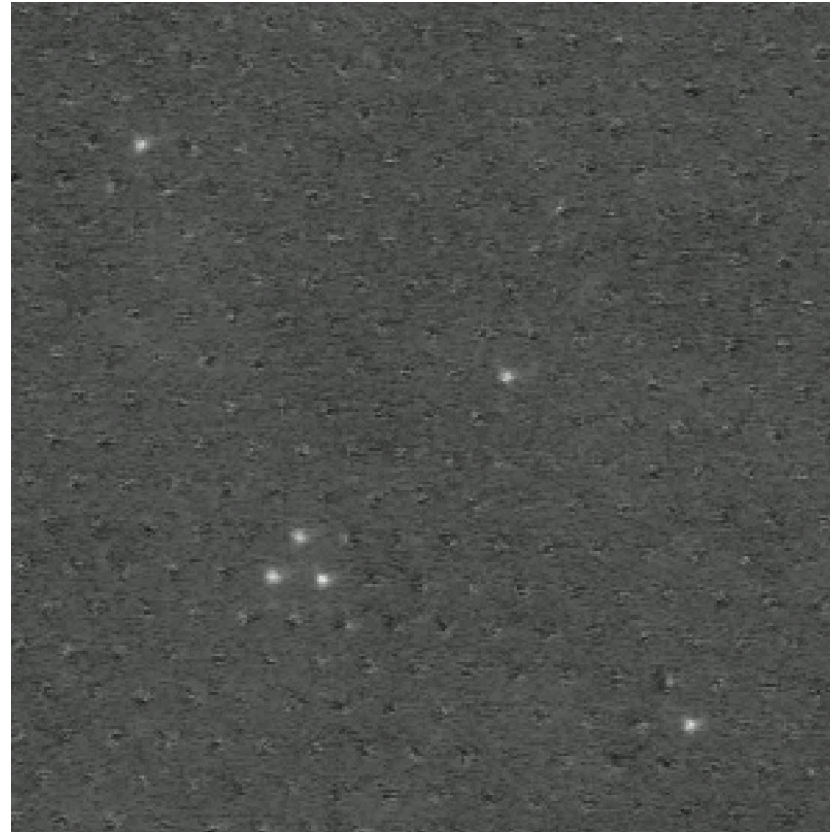


Vacancy counting: Blob Detection



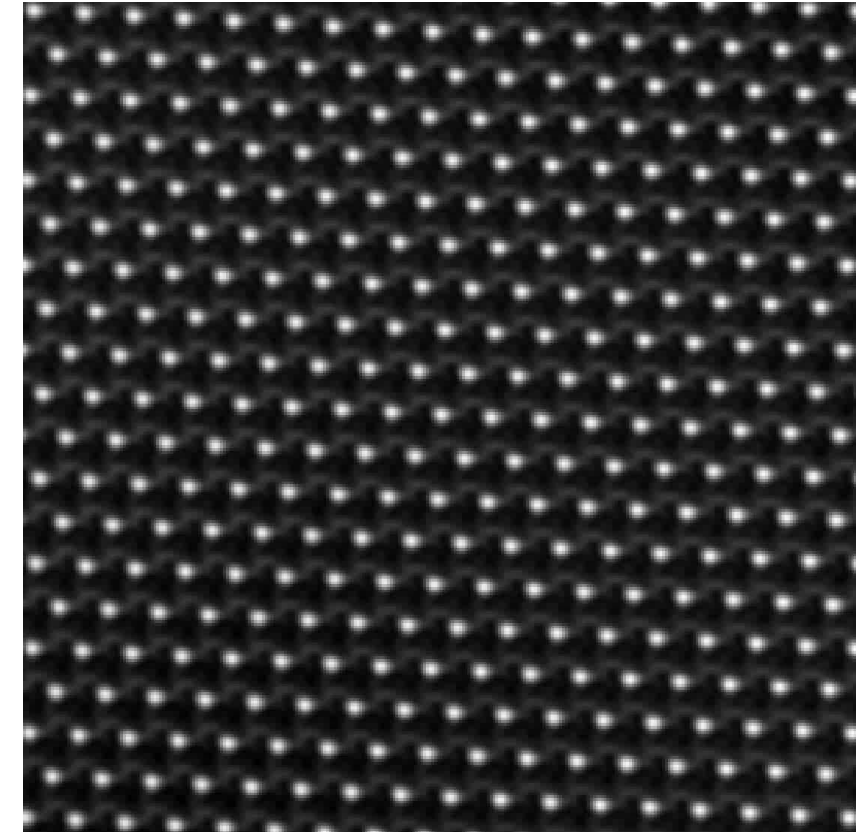
49

Vacancies Image



6 vacancies (2 %)

Denoised Image



300 atomic positions

- For vacancy detection we use a **blob detection** algorithm, in particular the one known as **Laplacian of Gaussian (LoG)**.
- We **apply this algorithm for atom detection in the denoised image**. With this complementary result **we can also provide the percentage of vacancies** in our sample.

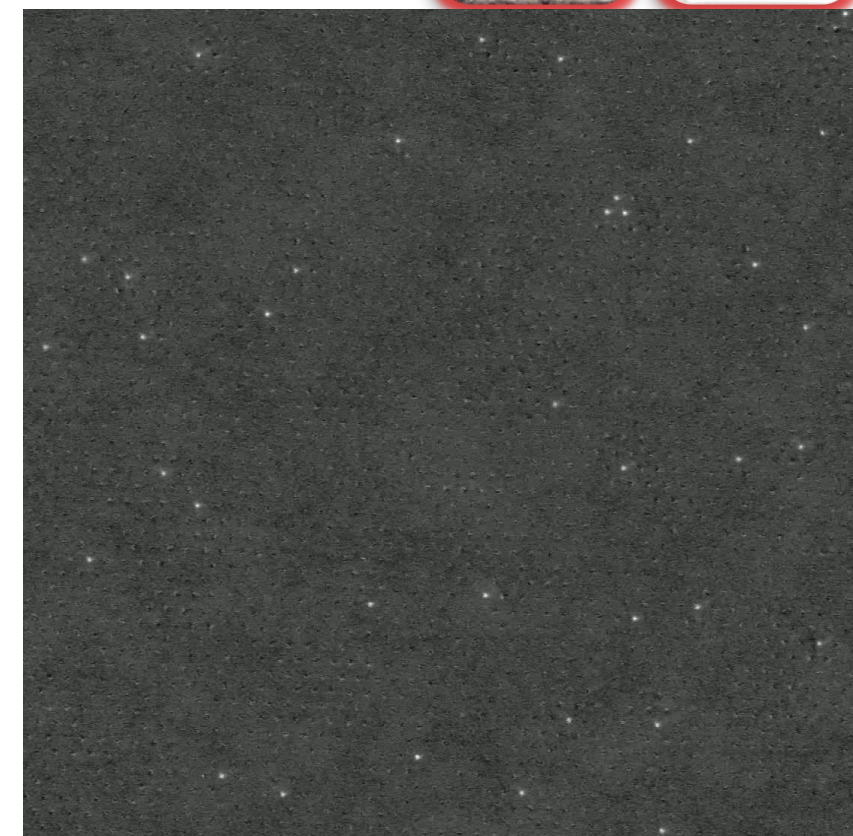
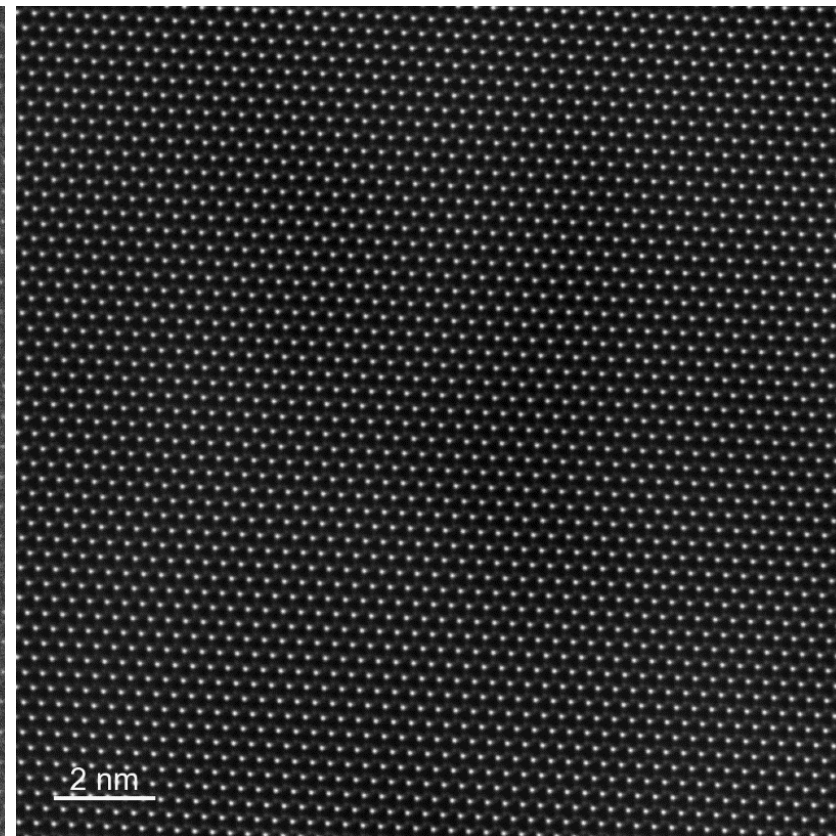
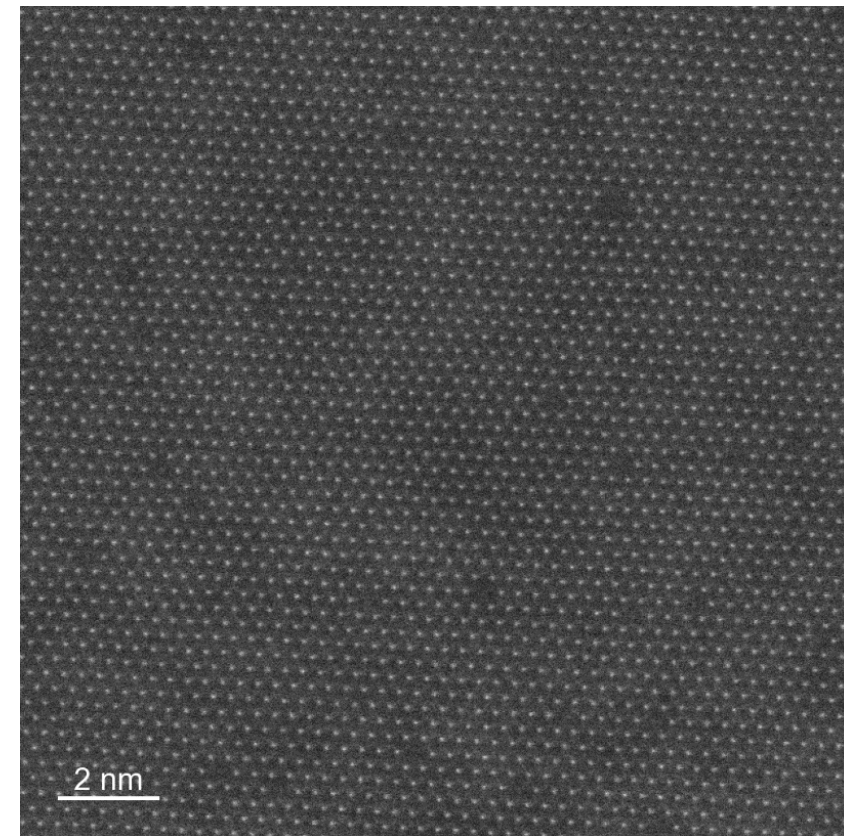


50

Original Image

Denoised Image

Vacancies Image



1.5 % of vacancies

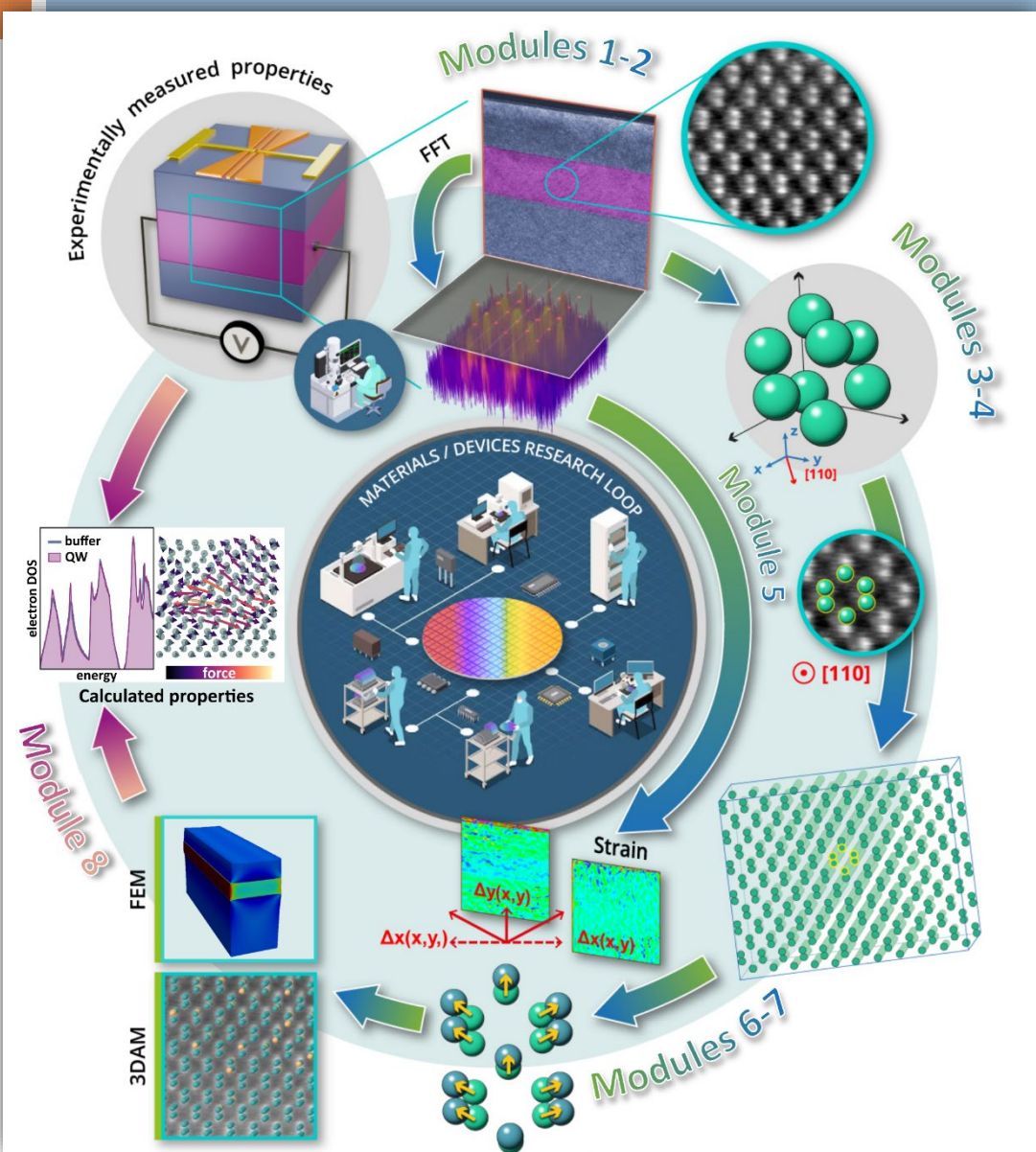
2503 atoms

37 vacancies

- We've processed **images containing over 10,000 atoms** in **less than 30 seconds**.
- Within **1 hour**, we analyze **more than 100 images**, totaling **over 1,000,000 atomic positions**.

AI-automated workflow

53



Artificial Intelligence-Assisted Workflow for Transmission Electron Microscopy: From Data Analysis Automation to Materials Knowledge Unveiling

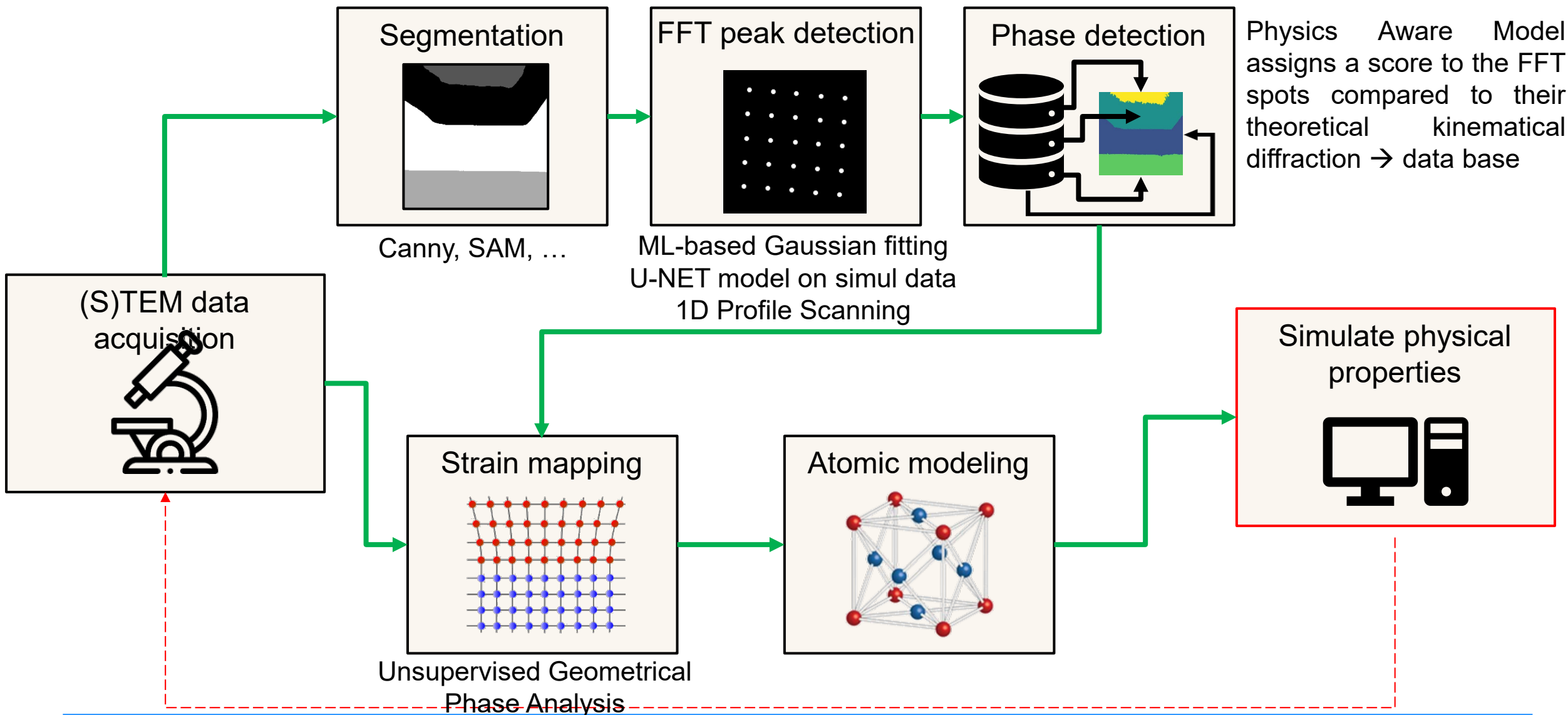
Marc Botifoll^{1,*†}, Ivan Pinto-Huguet^{1,†}, Enzo Rotunno^{2,*}, Thomas Galvani¹, Catalina Coll¹, Payam Habibzadeh Kavkani^{2,3}, Maria Chiara Spadaro^{4,5}, Yann-Michel Niquet⁶, Martin Børstad Eriksen⁷, Sara Martí-Sánchez¹, Georgios Katsaros⁸, Giordano Scappucci⁹, Peter Krogstrup¹⁰, Giovanni Isella¹¹, Andreu Cabot^{12,13}, Gonzalo Merino⁷, Pablo Ordejón¹, Stephan Roche^{1,13}, Vincenzo Grillo², and Jordi Arbiol^{1,13,*}

Transferable to any materials/technology
Enhanced characterization facilities
Self-driving labs
Fab equipment & Pilot lines

Adv. Mater. DOI: 10.1002/adma.202506785 (2026)

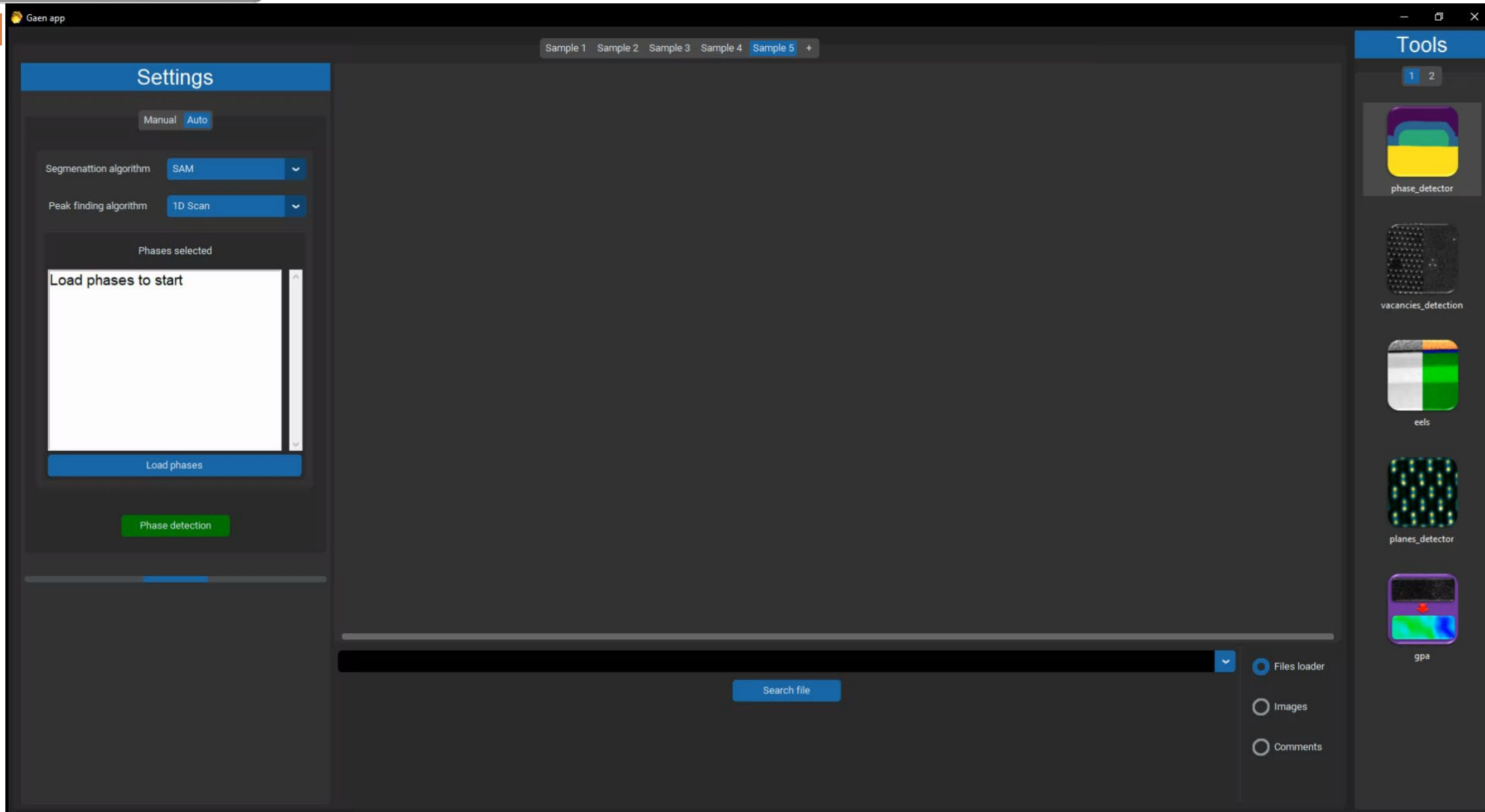
AI-automated workflow

54



Part I: Data Analysis

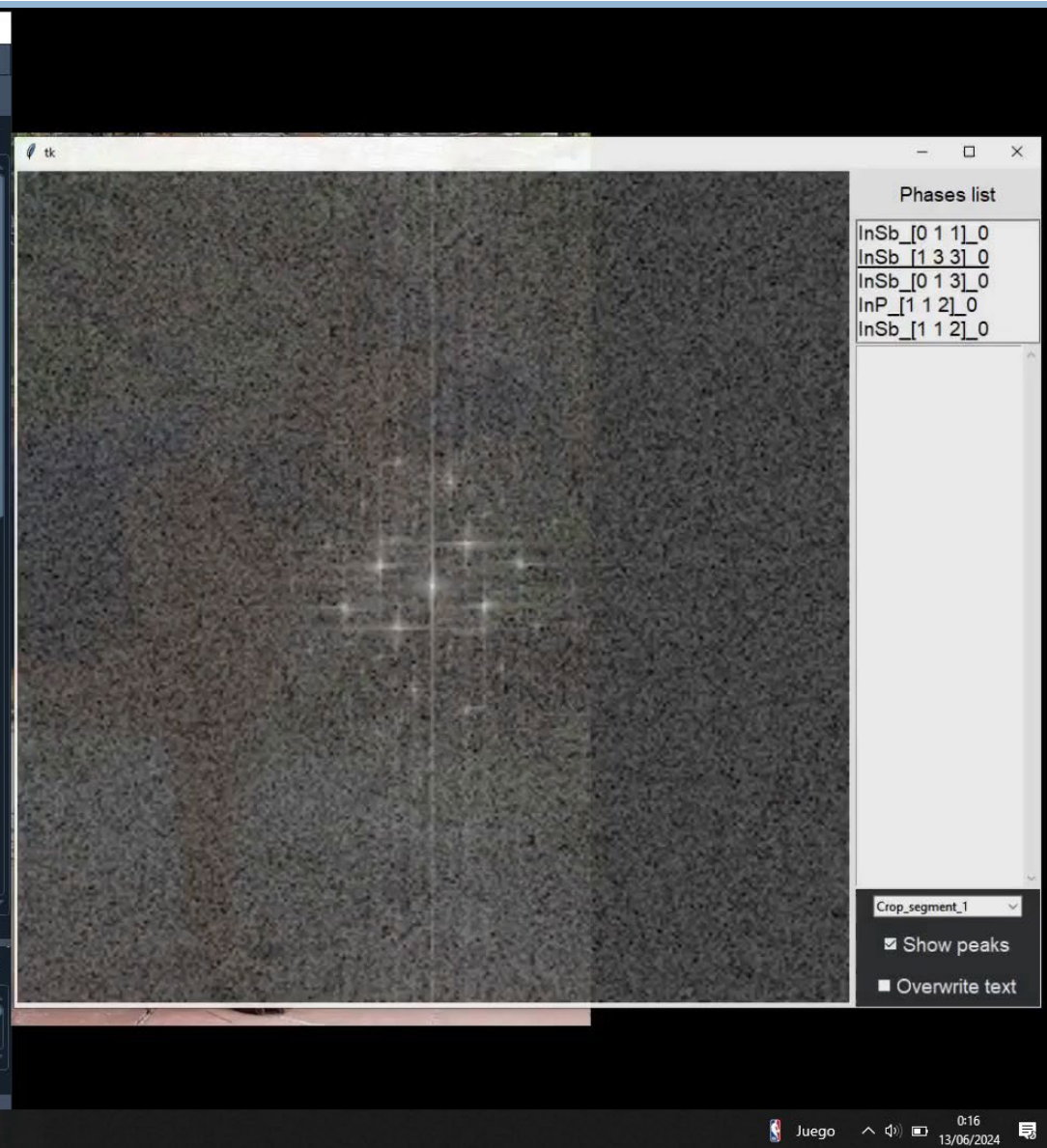
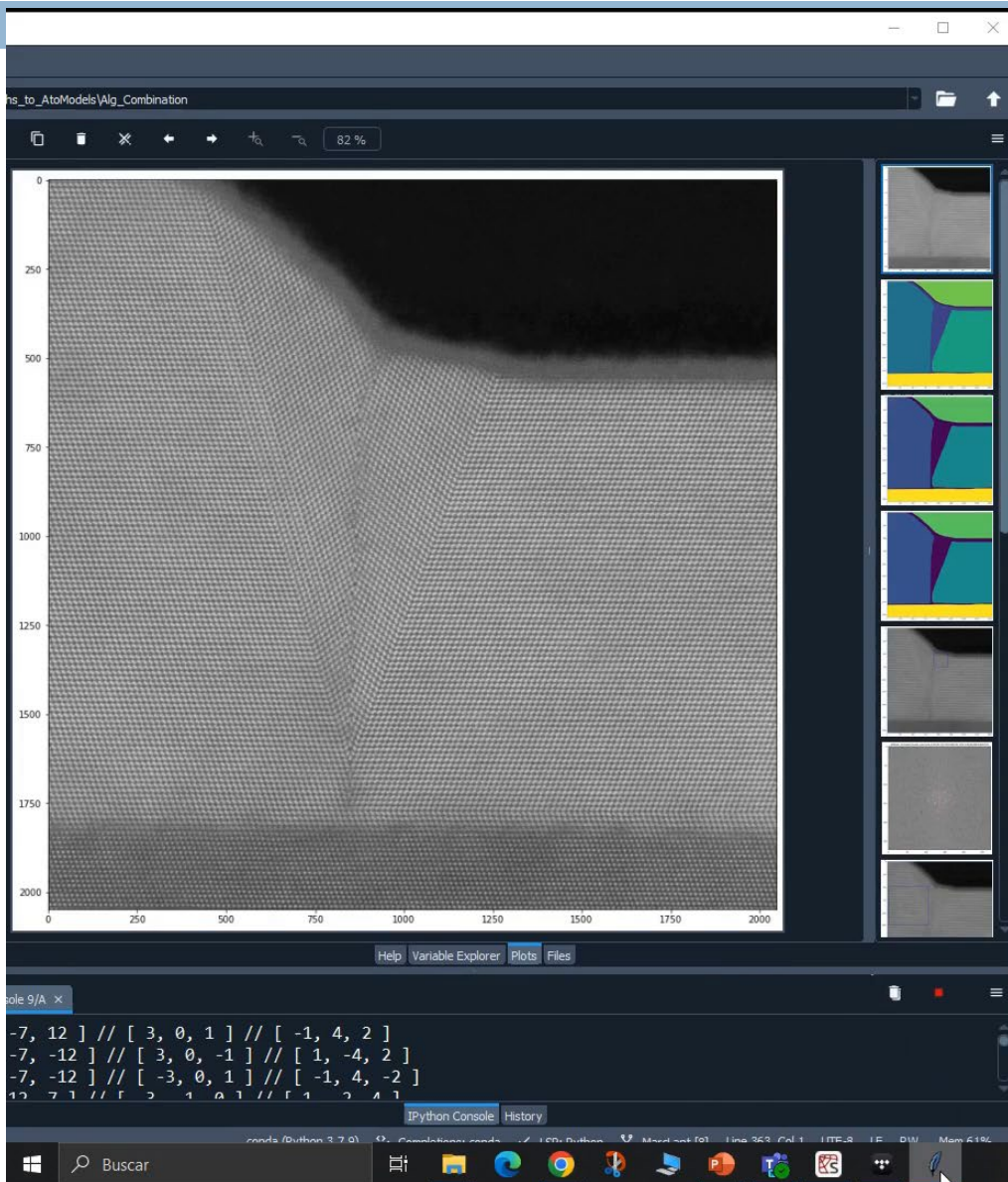
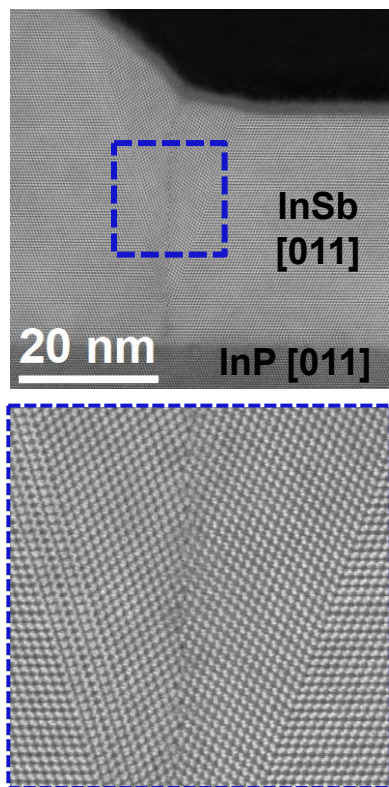
55



The screenshot displays the Gaen app interface. At the top, there are tabs for Sample 1 through Sample 5, with Sample 5 selected. On the left, a 'Settings' panel is visible, containing options for 'Manual' and 'Auto' modes. Under 'Manual', the 'Segmentation algorithm' is set to 'SAM' and the 'Peak finding algorithm' is set to '1D Scan'. Below these are 'Phases selected' and a 'Load phases to start' input field with a 'Load phases' button. A 'Phase detection' button is also present. The main area is currently empty. On the right, a 'Tools' sidebar lists several analysis tools: 'phase_detector', 'vacancies_detection', 'eels', 'planes_detector', and 'gpa'. At the bottom, there is a 'Search file' button and a list of filters: 'Files loader' (selected), 'Images', and 'Comments'.

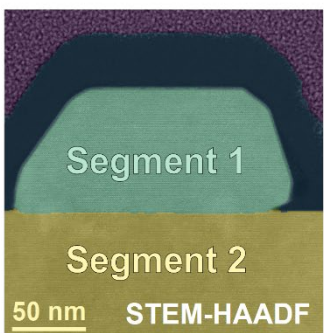
Part I: Data Analysis

56



Part I: Data Analysis

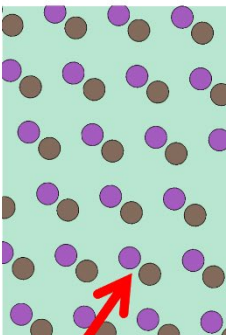
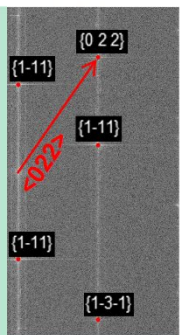
57



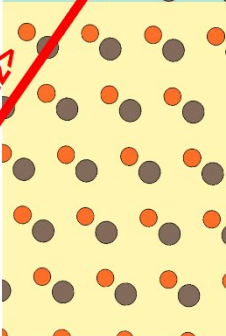
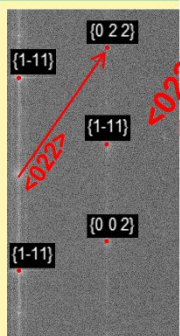
Segmentation (Canny)

Indexed FFT
Crystal phase + 3D Orientation

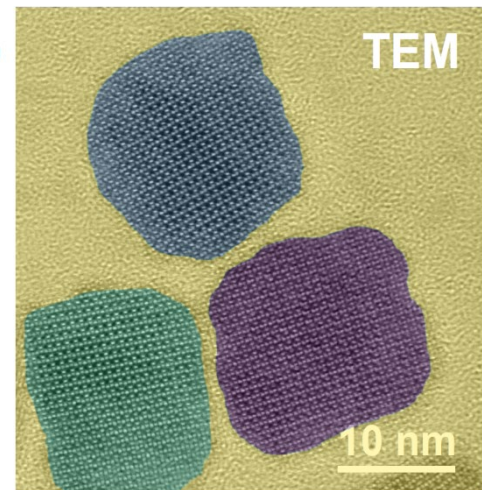
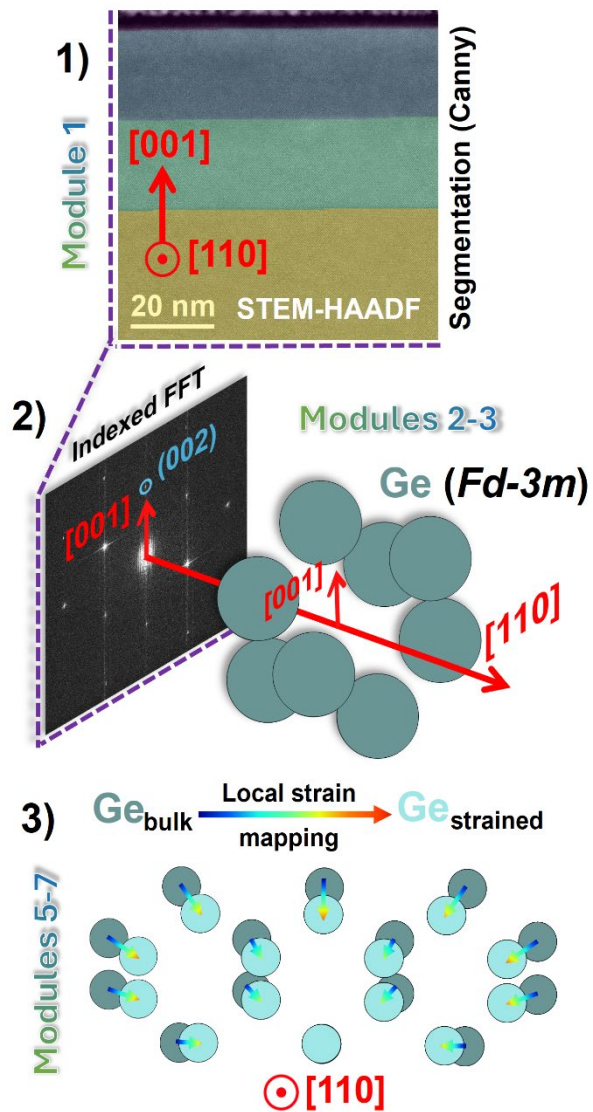
Segment 1



Segment 2

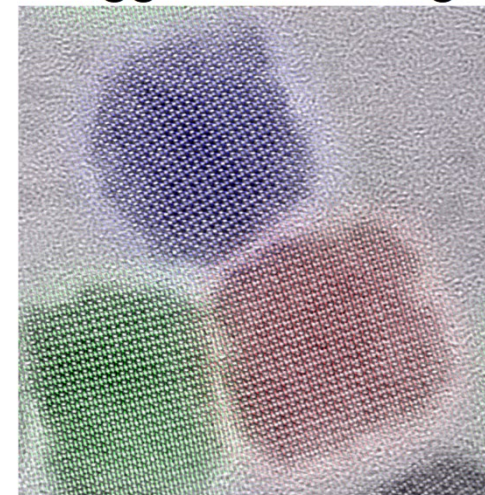


InSb (F-43m) [110] ⊙ InP (F-43m) [110] ⊙



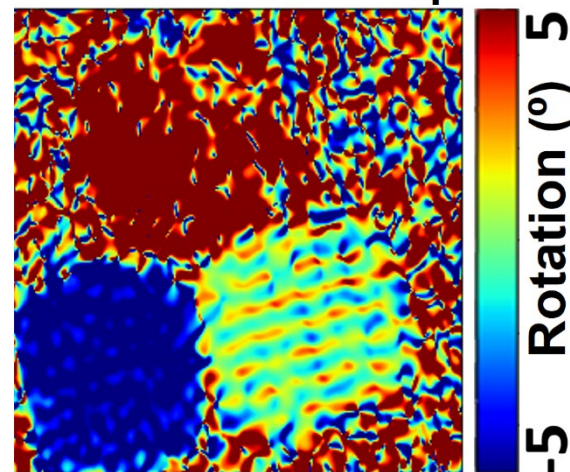
Segmentation (SAM)

Bragg-filtered image



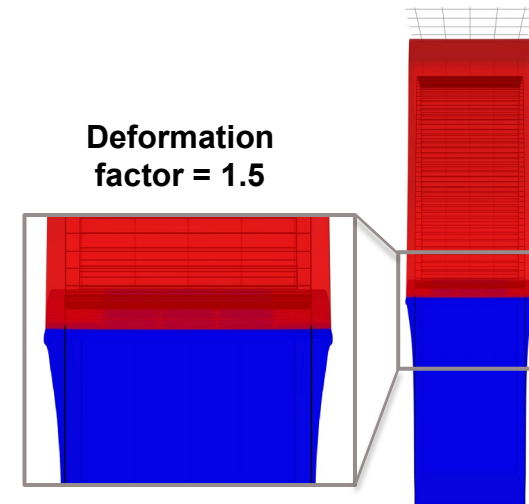
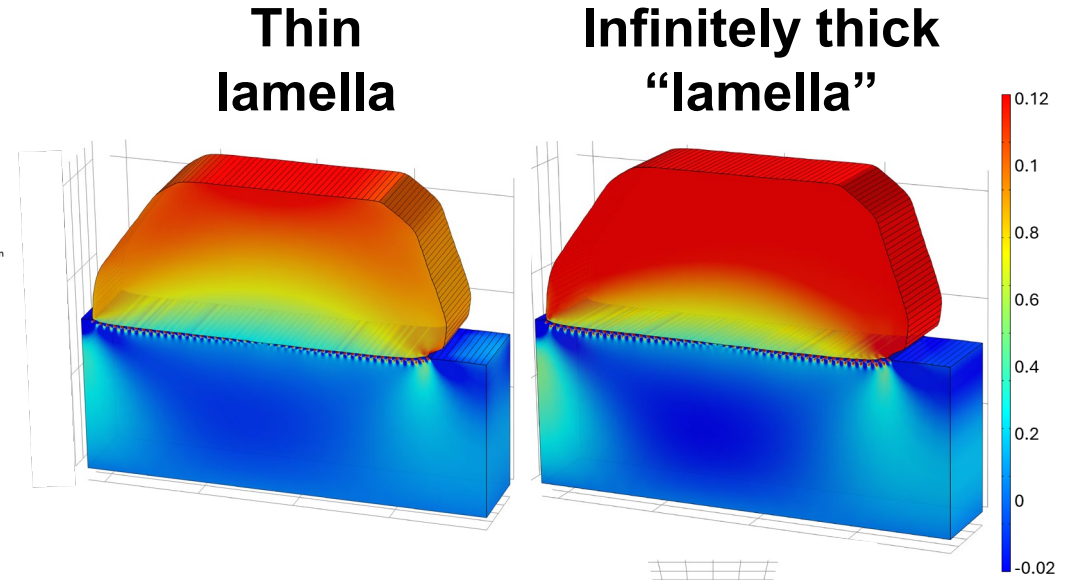
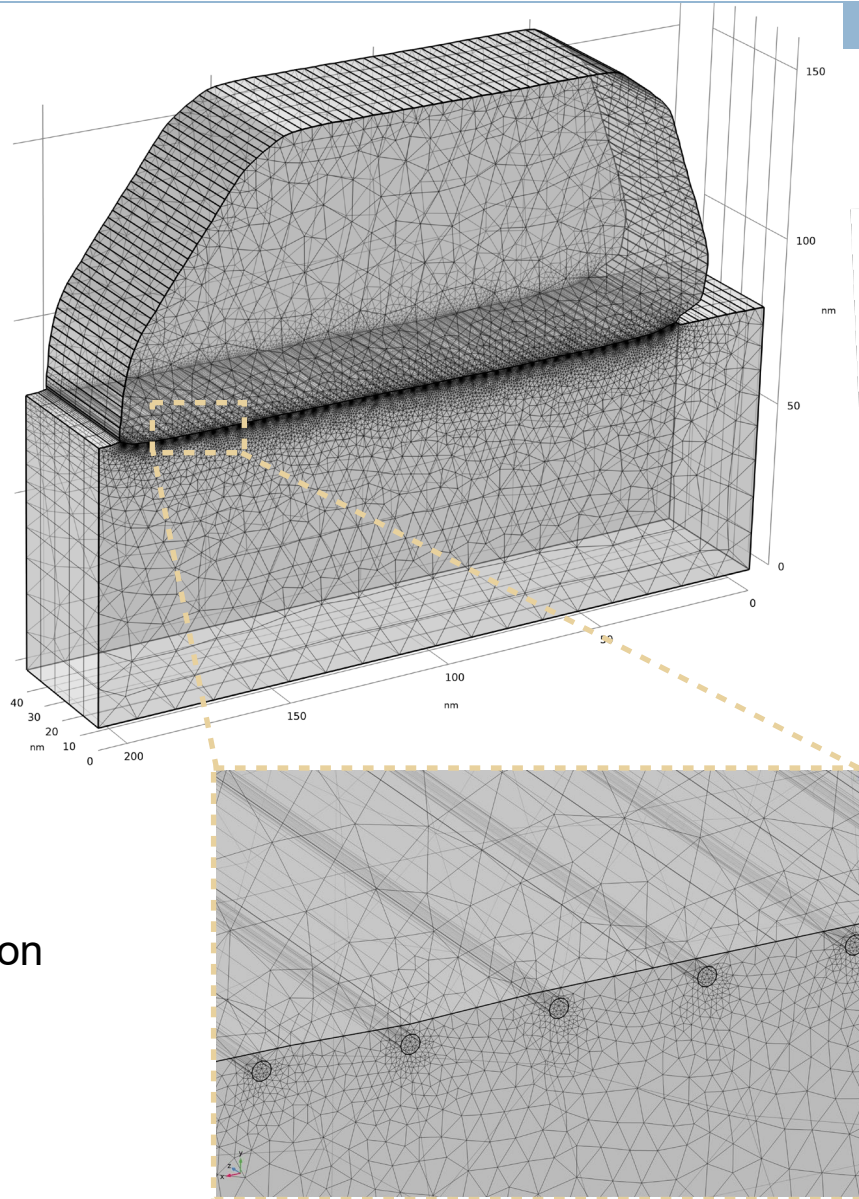
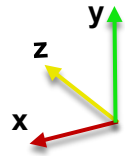
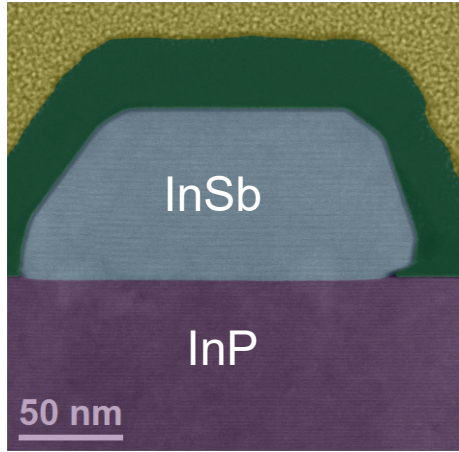
[001] ⊙ CuTe (Pm-3n)

Strain: Rotation map



Part II: Modelling and simulations

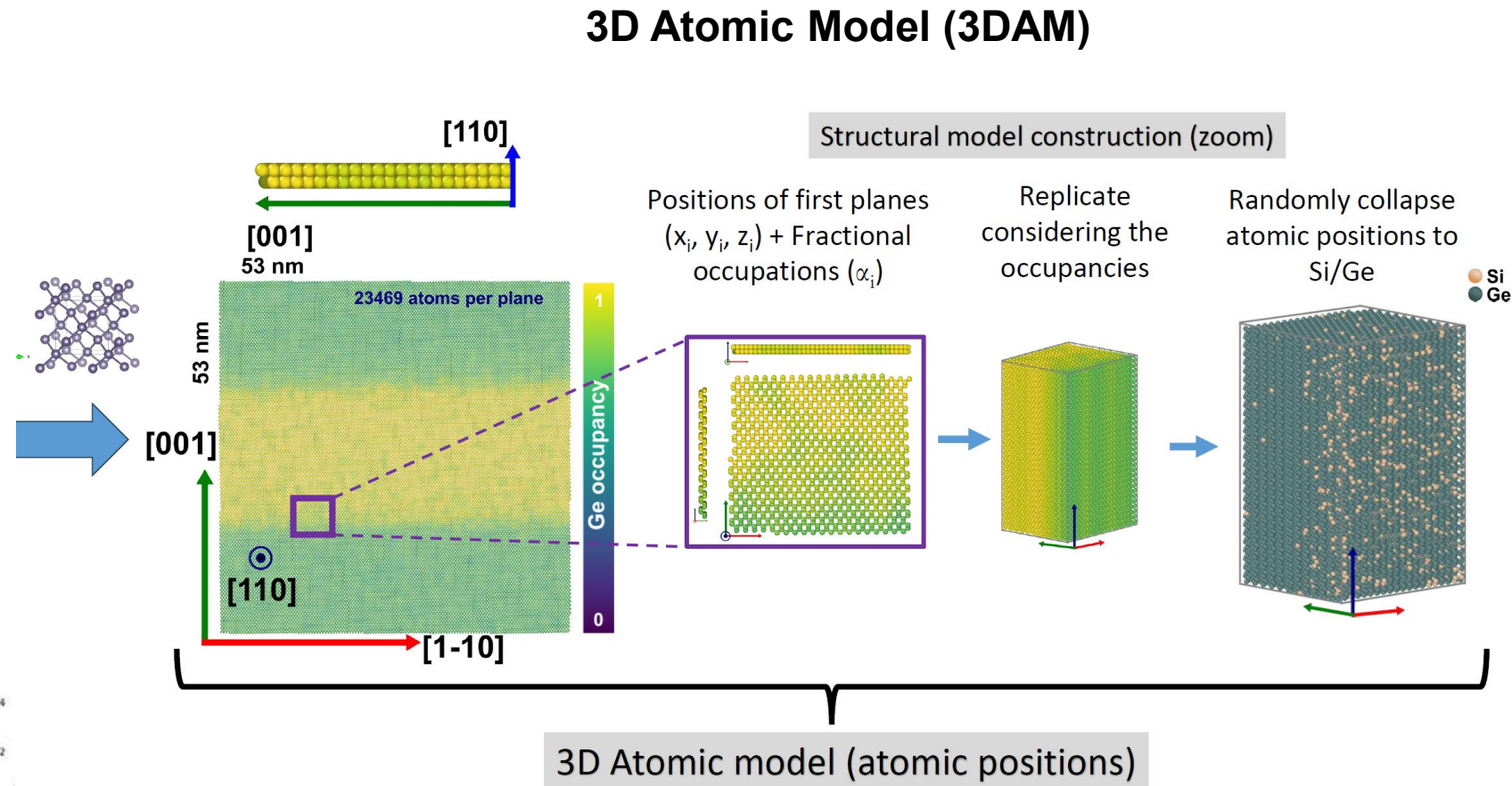
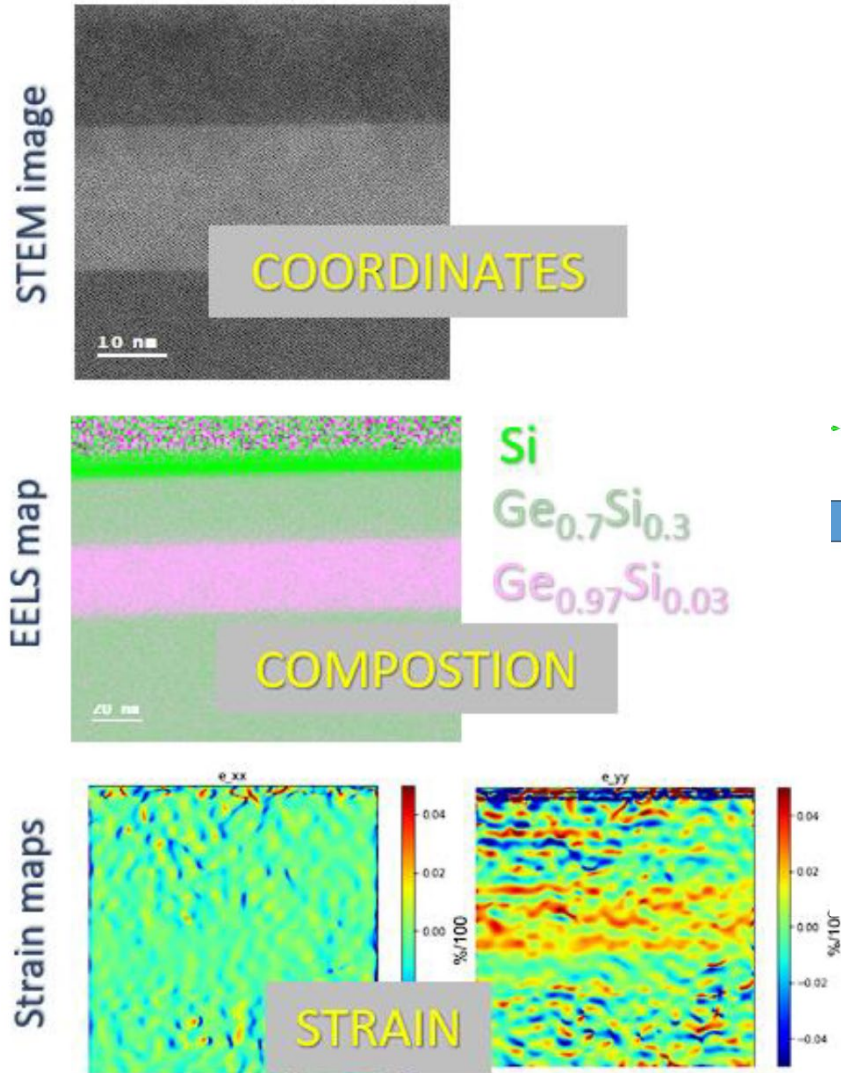
58



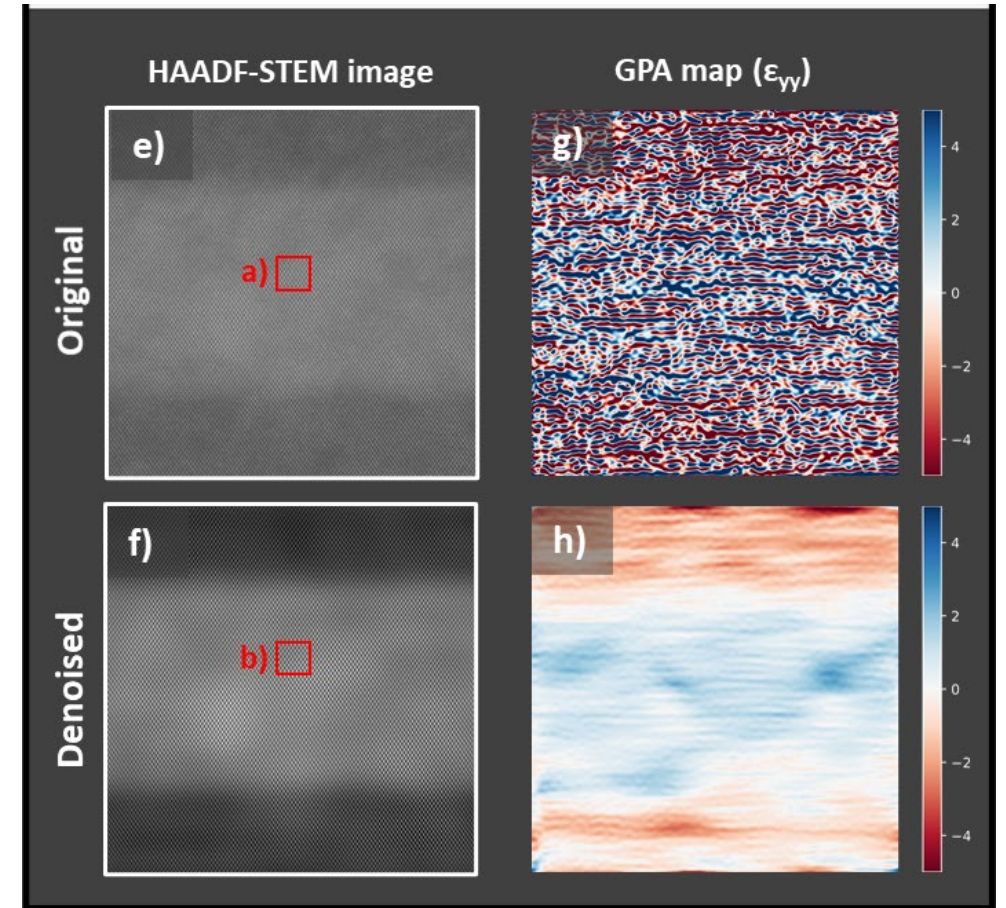
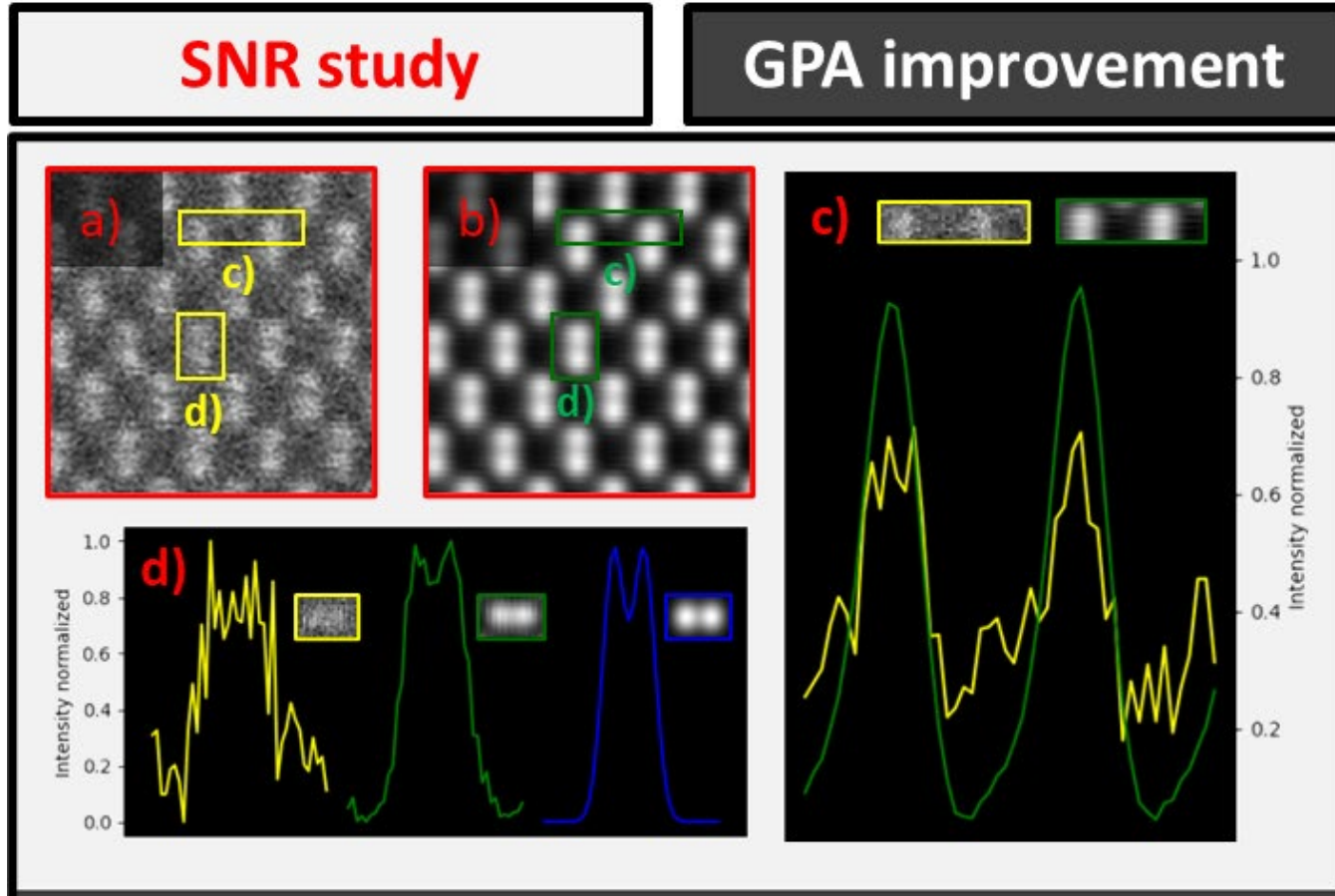
➤ Finite Elements Relaxation calculations

Adv. Mater. DOI: [10.1002/adma.202506785](https://doi.org/10.1002/adma.202506785) (2026)

Part II: Modelling and simulations



Enhancing atomic-resolution in electron microscopy: A frequency-domain deep learning denoiser

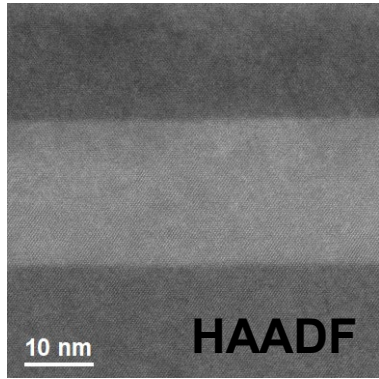


Adv. Intelligent Systems, DOI: [10.1002/aisy.202501077](https://doi.org/10.1002/aisy.202501077) (2026)

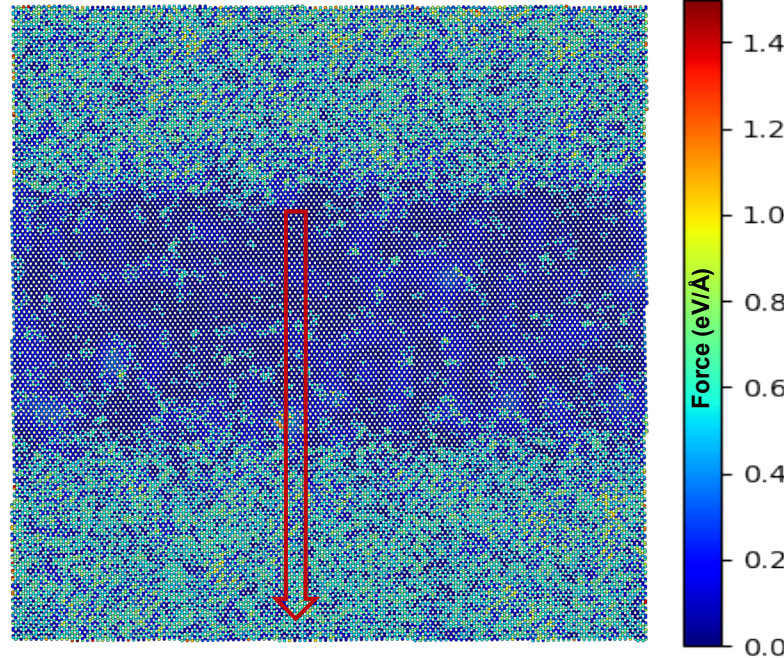
Adv. Mater. DOI: [10.1002/adma.202506785](https://doi.org/10.1002/adma.202506785) (2026)

Part II: Modelling and simulations

Atomic Keating Models → vibrational calculations

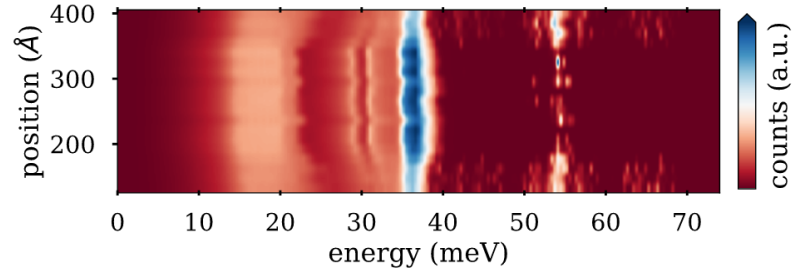
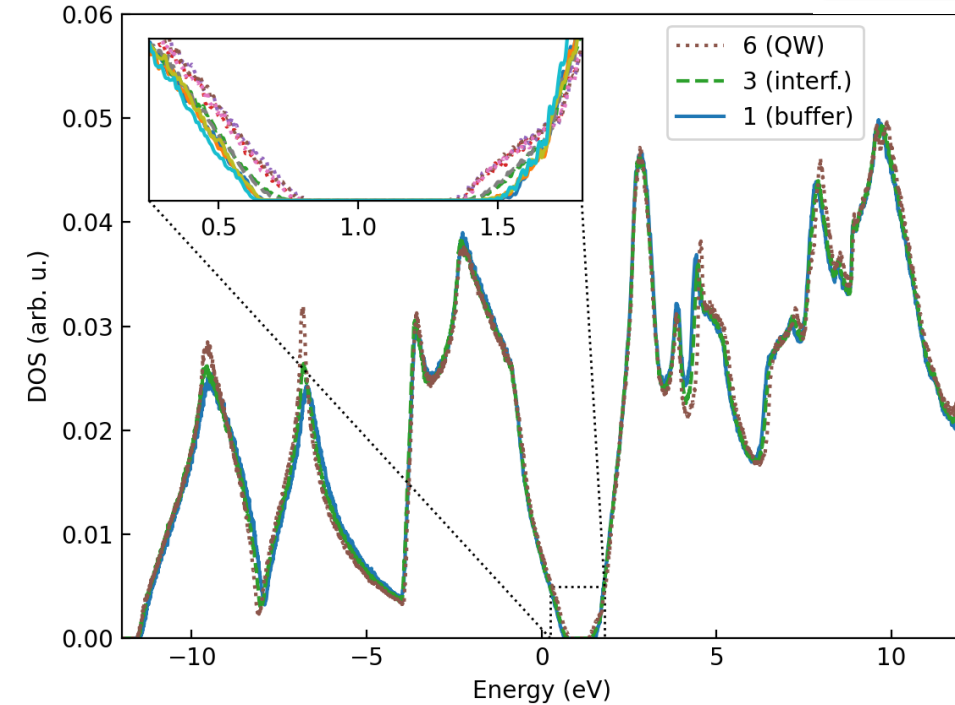
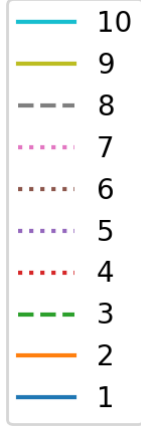


Atomic forces



Electronic LDOS from precise 3DAM-based tight binding Hamiltonians computed by using linear scaling algorithms

Local DOS



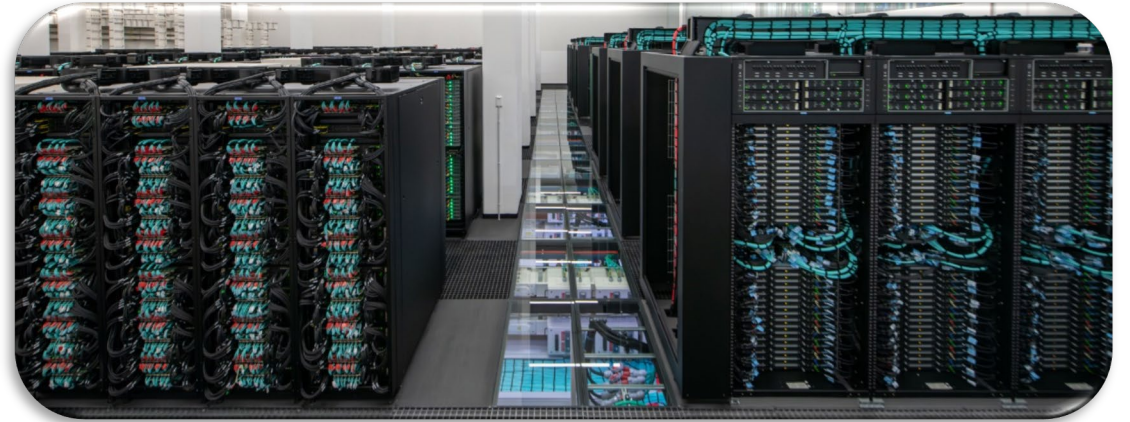
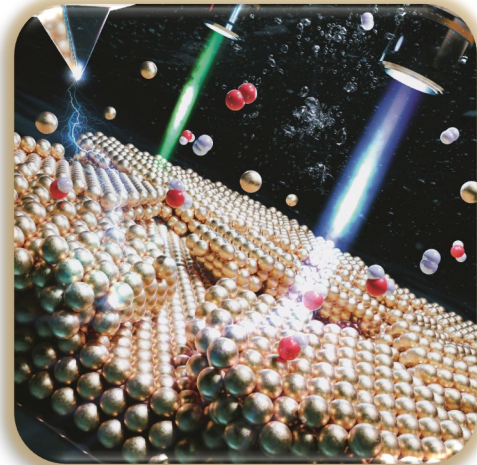
Phonon DOS

Adv. Mater. DOI: 10.1002/adma.202506785 (2026)



Future ways of integrating Multimodal, Multi length-scale and Correlative Techniques look promising: (S)TEM, Synchrotron and SPMs related imaging and spectroscopies.

AI automated data analysis combined with theoretical modeling can give statistical meaningful results on large systems (helping in-situ experiments as well)



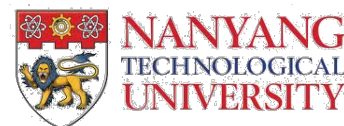
Acknowledgements



Prof. J.R. Galán-Mascarós



Prof. P. García de Arquer



Prof. Z. Liu



Dr. Y.-M. He



Shaping Energy for a Sustainable Future



Prof. A. Cabot



Prof. S. Barja



Prof. F. Fabregat



Prof. S. Giménez



Prof. H. Mas-Marzá



Institut de Recerca en Energia de Catalunya
 Catalonia Institute for Energy Research



Prof. J.R. Morante

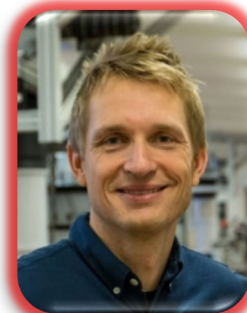
Quantum and Photonics



Prof. A. Fontcuberta i Morral



Dr. P. Caroff



Prof. P. Krogstrup



Prof. T. Jespersen



Dr. S. Khan



Prof. E. Joselevich



Prof. Q. Xiong



Prof. C. Wang



Dr. E. Alarcon-Llado



Prof. G. Katsaros



Dr. G. Scapucci

Acknowledgements



Dr. E. Rotunno



Prof. V. Grillo



Institut Català de Nanociència i Nanotecnologia



Prof. S. Roche



Dr. T. Galvani



Institut Català de Nanociència i Nanotecnologia



Prof. P. Ordejón



Dr. C. Coll



Prof. R. Dunin-Borkowski



Dr. M. Heggen



Prof. Q. Ramasse



Prof. J. García de Abajo

Acknowledgements



Prof. S. Bals



Dr. K. Jenkinson



Prof. Q. Ramasse



Prof. R. Dunin-Borkowski



Dr. M. Heggen



Prof. J. García de Abajo

Acknowledgements



Next Generation
Catalunya



Unió Europea
 Fons Europeu
 Next Generation





ICN2^R



- **EM Labs:** ICN2, CNRS (CEMES), Univ. Oxford, ER-C Jülich, EMAT Univ. Antwerp, CNR Trieste, Graz University of Technology, Norwegian University of Science and Technology



RIANA – Research Infrastructure Access in NANoscience and nanotechnology

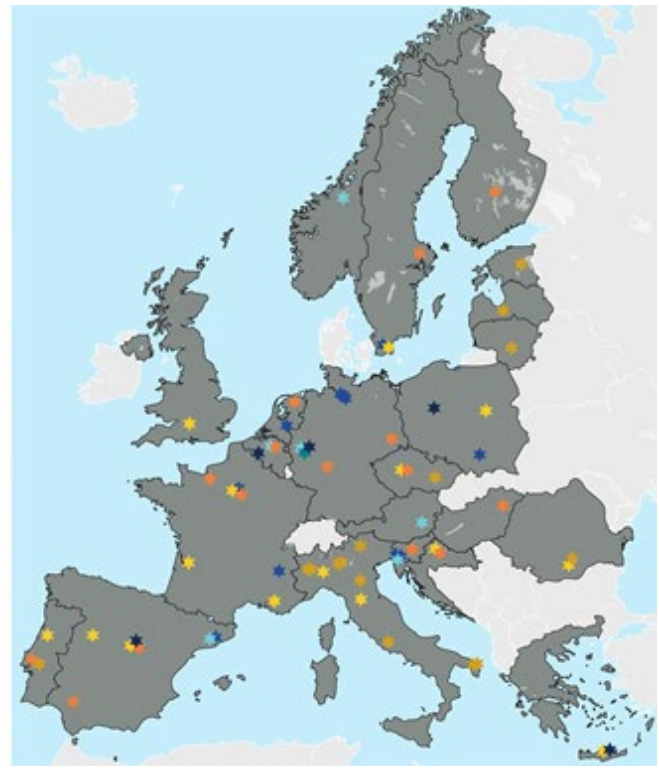


RIANA Consortium: **56 beneficiaries**
69 infrastructures
22 European countries

Duration: **48 months**
(2024-03-01 – 2028-02-29)

Budget: **14.5 M€ + in-kind**

Access offered: **35 748 h TA**
5 000 000 h_{CPU}



“e-DREAM”: European Distributed REsearch Infrastructure for Advanced Electron Microscopy



- **EM Labs:** ICN2, CNRS (CEMES), Univ. Oxford, ER-C Jülich, EMAT Univ. Antwerp, CNR Trieste, Graz University of Technology, Norwegian University of Science and Technology
- **ICN2 as Founding Member of e-DREAM**



ACS Publications
Most Trusted. Most Cited. Most Read.

Advanced electron Nanoscopy (GAe-N)

74



Alba

Francesco

Aziz

Xinxin

Jordi

David

Minggjing

Noe

Carina

Helena

Athique

Josep

Eduardo

Inas

Hui

Jinhai

Jielin



Jing



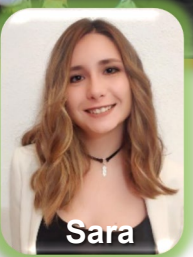
Ivan



Jovan



Chiara



Sara



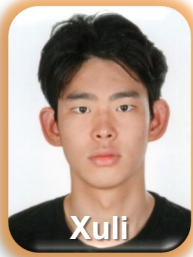
Marc



Laura



Marta



Xuli

CONTACT:
Prof. Jordi Arbiol
arbiol@icrea.cat



More about our research work, movies and models at:
<https://gaen.cat>